LOCKHEED MARTIN ENERGY RESEARCH LIBRARIES
3 4456 0451476 4

CENTRAL RESEARCH LIBRARY
DOCUMENT COLLECTION

ORNL-3691
UC-80—Reactor Technology
TID-4500 (34th ed.)

# NUCLEAR SAFETY PROGRAM
# SEMIANNUAL PROGRESS REPORT
# FOR PERIOD ENDING JUNE 30, 1964

CENTRAL RESEARCH LIBRARY
DOCUMENT COLLECTION
LIBRARY LOAN COPY
DO NOT TRANSFER TO ANOTHER PERSON
If you wish someone else to see this document, send in name with document and the library will arrange a loan.

OAK RIDGE NATIONAL LABORATORY
operated by
UNION CARBIDE CORPORATION
for the
U.S. ATOMIC ENERGY COMMISSION

Printed in USA. Price $4.00. Available from the Clearinghouse for Federal Scientific and Technical Information, National Bureau of Standards, U.S. Department of Commerce, Springfield, Virginia

LEGAL NOTICE

This report was prepared as an account of Government sponsored work. Neither the United States, nor the Commission, nor any person acting on behalf of the Commission:

A. Makes any warranty or representation, expressed or implied, with respect to the accuracy, completeness, or usefulness of the information contained in this report, or that the use of any information, apparatus, method, or process disclosed in this report may not infringe privately owned rights; or

B. Assumes any liabilities with respect to the use of, or for damages resulting from the use of any information, apparatus, method, or process disclosed in this report.

As used in the above, "person acting on behalf of the Commission" includes any employee or contractor of the Commission, or employee of such contractor, to the extent that such employee or contractor of the Commission, or employee of such contractor prepares, disseminates, or provides access to, any information pursuant to his employment or contract with the Commission, or his employment with such contractor.

ORNL-3691

Contract No. W-7405-eng-26

# NUCLEAR SAFETY PROGRAM SEMIANNUAL PROGRESS REPORT

for Period Ending June 30, 1964


Wm. B. Cottrell, Program Coordinator

Wm. B. Cottrell, Reactor Division
B. R. Fish, Health Physics Division
C. E. Guthrie, Chemical Technology Division
F. C. Maienschein, Neutron Physics Division
G. M. Watson, Reactor Chemistry Division


NOVEMBER 1964


OAK RIDGE NATIONAL LABORATORY
Oak Ridge, Tennessee
operated by
UNION CARBIDE CORPORATION
for the
U. S. ATOMIC ENERGY COMMISSION



LOCKHEED MARTIN ENERGY RESEARCH LIBRARIES

3 4456 0451476 4

# Foreword

The material covered in this report involves the work of several Laboratory divisions, each of whose activities is coordinated by the program coordinator through the division representatives. Effective May 1964, Wm. B. Cottrell replaced F. R. Bruce as program coordinator because of Mr. Bruce's increased responsibilities in Laboratory administration.

After the title of each subsection of this report, there is a list of key words which define the scope of the work included therein. These key words are included in an attempt to assist documentalists and information specialists in indexing the information and are taken from the thesaurus developed for the Nuclear Safety Information Center.

This is the fifth in a series of semiannual reports describing the Nuclear Safety Research and Development Program, which is being carried out at the Oak Ridge National Laboratory as a part of the Reactor Safety Program of the Reactor Development Division, U.S. Atomic Energy Commission. The previous reports in this series are:

For Period Ending June 30, 1962 – ORNL-3319

For Period Ending December 31, 1962 – ORNL-3401

For Period Ending June 30, 1963 – ORNL-3483

For Period Ending December 31, 1963 – ORNL-3547

# Contents


Foreword ..... iii

Introduction and Summary ..... ix

PART 1. FISSION PRODUCT RELEASE AND BEHAVIOR

1.1 Release and Transport of $UO_2$ Fission Products in the Confinement Mockup Facility ..... 3
- Modifications of the Confinement Mockup Facility ..... 3
- Fission Product Release from Melting Trace-Level-Irradiated $UO_2$ ..... 5
- Fission Product Release from Highly Irradiated $UO_2$ ..... 6
  - Comparison of Release Behavior from Tracer-Level-Irradiated $UO_2$ with That from High-Burnup-Level Fuel ..... 6
  - Total Nuclei Count in the Aerosol ..... 6
  - Fission Products Remaining Airborne as a Function of Time ..... 7
- Test of a $UO_2$-$^{131}I$ Aerosol as a Simulant for Fission Product Iodine from Fuel Meltdown ..... 8
- Adsorption and Desorption of Radioiodine in the Containment Mockup Facility ..... 9
  - Conditions of the Plate-Out Experiment in the CMF Simulating UK Experimental Conditions ..... 10
  - Results of the Simulated Experiment ..... 10
  - Velocity of Deposition of Iodine on Stainless Steel in Air ..... 12
  - Amount of Airborne Iodine in the Containment Vessel at the End of the 6-hr Aging Period ..... 12
  - CMF Gas Sampling with an Evacuated Bulb and Injection Needle Technique ..... 12
  - Rate of Uptake of Iodine by Typical Reactor Construction Materials ..... 13
  - Conclusions from Experiments in the CMF ..... 14

1.2 Release of Fission Products on In-Pile Melting of Reactor Fuels Under Transient Reactor Conditions ..... 16
  - Experimental Assembly ..... 16
  - Experimental Procedure ..... 18
- Physical Examination of Components ..... 19
- Gas Analysis ..... 22
- Radiochemical Results ..... 23
- Conclusions ..... 28

1.3 Behavior of Fission Products Released During In-Pile Destruction of Reactor Fuels ..... 29
- Effects of Atmosphere on Behavior of Released Fission Products ..... 29
  - Moist Helium ..... 30
  - Moist Air ..... 30
- Effects of Sustained Overheating in Moist Air ..... 34
- Equipment for In-Pile Melting of Stainless-Steel-Clad $UO_2$ in a High-Concentration Steam Atmosphere ..... 37
- Retention of Released Fission Products Produced by Components of the Off-Gas System ..... 40
- Analysis of Off-Gas from In-Pile Fuel Melting Experiments ..... 45

1.4 Characterization and Control of Accident-Released Fission Products ..... 46
Iodine Distribution Among Chemical Forms and Particle Sizes in Aged Aerosols ..... 46
Aerosol from 7000 Mwd/ton Burnup $UO_2$ ..... 46
Aerosol from Molten $UO_2$-Iodine Tracer (Run D) ..... 48
Aerosol from Iodine Tracer Experiment ..... 48
Identification of Chemical Forms of Iodine by a Liquid Contactor Method ..... 50
Investigation of Iodine Behavior in May Packs by Means of Composite Diffusion Tubes ..... 52
Experimental ..... 52
Results ..... 55
Discussion ..... 57
Investigation of Iodine Behavior in Composite Diffusion Tubes by Varying Their Internal Arrangement or Their Temperature ..... 58
Experimental ..... 59
Results ..... 59
Discussion ..... 60
Conclusions ..... 65
Investigation of Occurrence and Behavior of Volatile Compounds of Iodine ..... 66
In Dry Air ..... 67
In Moist Air ..... 67
Solubility Behavior of Volatile Iodine Compounds ..... 68
Innocuous Simulation of Aerosols Produced by Reactor Accidents ..... 69
Removal of Iodine and Volatile Iodine Compounds from Air Systems by Activated Charcoal ..... 70
Characterization of Radioactive Aerosols by Use of Fibrous Filters ..... 72

## PART 2. CONTAINMENT ENGINEERING

2.1 Nuclear Safety Pilot Plant ..... 77
Behavior of Particles from Molten $UO_2$ ..... 77
Development of Sampling Devices ..... 81
Plasma Torch and Furnace Development ..... 84
2.2 Reactor Containment Handbook ..... 85

## PART 3. PHYSICS

3.1 Reactivity Effects of Small Fuel Displacements for Plate-Type Reactors ..... 89
Experiment ..... 89
Diffusion-Theory Calculations ..... 92
Transport-Theory Calculations ..... 95
Results and Comparisons ..... 96
Conclusion ..... 98

## PART 4. RADIOCHEMICAL PLANT

4.1 Radiochemical-Plant Safety Studies ..... 101
Credibility of Radiochemical Plant Accidents ..... 101
Characterization of Aerosols Formed in Chemical Plants Processing Radioactive Materials ..... 101

## PART 5. NUCLEAR SAFETY INFORMATION

5.1 Nuclear Safety Information Center ..... 107
Computer Capability for Information Retrieval ..... 107
Geneva Exhibit ..... 107
Installations Visited and Meetings Attended ..... 108
Center Studies ..... 108
Evaluation of Iodine Effluent Monitoring and Area Monitoring Programs at Savannah River, Hanford, Idaho Falls, and Oak Ridge ..... 108
Behavior of Iodine in Reactor Containment Systems ..... 108
Secondary Shutdown Systems ..... 108
Reliability of Safety Systems ..... 108
Reactivity Effects of Fuel Element Bowing ..... 108
Kinetics of Large Reactor Cores ..... 108
Safety of Fast Gas-Cooled Reactors ..... 109
Review of Safety Analysis Procedures and Methods ..... 109
Nuclear Safety Contract File ..... 109
Fundamentals of Filter Testing ..... 109
Other Activities ..... 109

5.2 Technical Progress Review ..... 109

# Introduction and Summary

The Nuclear Safety Program at Oak Ridge National Laboratory is an integrated program directly involving personnel from four research divisions, as well as supporting engineering, irradiation, and analytical services. The program as currently constituted has the following objectives which change from time to time, depending on program interests:

(1) Establishing critically safe conditions for handling fissionable materials, (2) obtaining data which are needed to assess realistically the consequences of accidents in reactors and chemical plants, (3) developing and evaluating countermeasures to be employed in the event of accidents entailing radioactive materials, (4) critically evaluating and compiling, in handbook form, information on reactor containment, and (5) collecting, interpreting, and reporting data in certain key areas of reactor safety. To achieve these objectives, the activities reported in this progress report are being pursued. The significant developments which occurred during the past six months are summarized below.

## PART 1. FISSION PRODUCT RELEASE AND BEHAVIOR

### 1.1 Release and Transport of $UO_2$ Fission Products in the Confinement Mockup Facility

Two experiments were conducted in the CMF in which trace-level-irradiated stainless-steel-clad $UO_2$ specimens were melted in ambient air. In one experiment, part of the air in the component tank was unfiltered, while in the other all the air passed through an absolute filter and a charcoal bed. The fraction of released iodine in a form that can penetrate charcoal beds, possibly an organic iodine, was greater by a factor of 10 in the experiment in which some unfiltered air was present. Deposition of fission product activity in these experiments was found to be unaffected by agglomeration of particles, and a significant fraction of the released iodine remained airborne for a period of several hours. Approximately equal proportions of the airborne iodine were in particulate and molecular form.

Only one experiment on release and transport of fission products from highly irradiated $UO_2$ (7000 Mwd/ton) has been conducted to date in the CMF. Release of fission products from the melted specimen was not markedly different from results obtained with trace-level-irradiated $UO_2$ except in the case of tellurium, which increased from 12 to 55%. Release values for plutonium and strontium were about the same as the fraction of the $UO_2$ that volatilized (0.005%). Rapid deposition of fission products occurred in the confinement tank during the first few minutes after the $UO_2$ melted. The fraction of the airborne iodine inventory dropped from 0.91 to about 0.10, tellurium dropped from 0.53 to 0.07, and cesium dropped from 0.30 to 0.19. A large part of the deposited iodine was desorbed by passage of 1.5 tank volumes of argon through the confinement tank after a 3-hr aging period. Condensation nuclei in the tank dropped from a concentration of $10^7$ per $cm^3$ to $10^5$ per $cm^3$ during the period 10 to 25 min after melting and then more slowly to $10^4$ per $cm^3$, but no significant change in airborne filterable activity was noted.

An experiment was conducted in the CMF to study iodine behavior in the absence of vaporized fuel particles and other fission products for comparison with British experiments on plate-out of iodine in the Pluto and Dido reactor containment shells. Elemental $^{131}I$ with added carrier iodine was vaporized and transferred into the confinement tank filled with air at a pressure of 15 psig. Most of the airborne iodine was deposited during the

first few minutes of the 4-hr aerosol aging period. Depressurization of the tank from 15 to 2.5 psig removed only 3% of the iodine, while passage of $2\frac{3}{4}$ tank volumes of argon through the tank removed 7%; an additional 3% was removed by sweeping the tank with an equal quantity of air. In general, the iodine behavior in this experiment agreed with the results of British experiments, although there were unavoidable differences in some of the experimental conditions such as wall material and surface-to-volume ratio. It seems clear that the results of experiments on iodine behavior performed by vaporizing iodine will not accurately predict the behavior of fission product iodine released by melting irradiated $UO_2$ fuel. Desorption of iodine in the stainless steel confinement tank was much higher in the latter case for reasons that are not clear at the present.

### 1.2 Release of Fission Products on In-Pile Melting of Reactor Fuels Under Transient Reactor Conditions

Two experiments were performed in the TREAT reactor which gave data on the release of fission products and fuel material from stainless-steel-clad $UO_2$ in air-steam atmospheres. Prior to the experiments the specimens were irradiated to tracer level (about $2 \times 10^{16}$ fissions for each specimen). The transient irradiation in the TREAT reactor amounted to about $1.3 \times 10^{15}$ fissions, with a reactor integrated power of approximately 370 Mwsec and with a reactor period of approximately 75 msec. These experiments simulated transient accidents with reactors containing aged fission products in the presence of an oxidizing air-steam atmosphere. Physical examination of the transient-heated specimens revealed that the stainless steel cladding melted completely and that approximately 75% of the $UO_2$ melted. The results indicate that no large effects on fuel appearance or on fractional release and behavior of fission products can be ascribed to the presence of oxidizing steam-air mixtures in the range studied (3–50 vol %) as compared to an inert atmosphere.

### 1.3 Behavior of Fission Products Released During In-Pile Destruction of Reactor Fuels

Studies of the characteristics and behavior of fission products have been continued by melting or vaporizing miniature stainless-steel-clad $UO_2$ fuel elements in the ORR in various atmospheres. The effects of moist helium and of moist air on the behavior of released fission products were observed as well as the effects of sustained overheating in moist air. Results of an experiment using moist helium, compared with corresponding results obtained using dry helium, with environmental conditions approximately equivalent in both cases, revealed that moisture caused the stainless steel cladding to become partially oxidized; consequently, very little metallic stainless steel condensate could be found after the experiment. Otherwise the presence of moisture in the helium atmosphere seems to have had no substantial effect on the release of fission products from the fuel itself. However, the release of iodine and of tellurium from the high-temperature zone was increased in moist helium and that of ruthenium was decreased. Radiochemical results revealed that the air atmosphere had no appreciable effect on the release of nonvolatile or volatile fission products from the fuel itself but that the releases of iodine, tellurium, and cesium from the high-temperature zone appeared to be enhanced.

In the course of an experiment which was intended to study the effects of sustained overheating in moist air, it was discovered that the $UO_2$ melted at an apparently considerably lower temperature than its normal melting point. This effect was ascribed to the melting-point depression brought about by the incorporation into the $UO_2$ of oxides of the cladding material. The fuel in this experiment was not previously irradiated; so the effects of short-lived precursors on fission product behavior could be seen. The fractional release of iodine and tellurium (which have nonvolatile precursors) from the fuel was lower than the corresponding release from preirradiated specimens, while the effects of xenon and krypton precursors could be observed in the higher fractional release of cesium, strontium, and barium.

Supplementary equipment and modifications were developed for in-pile melting of stainless-steel-clad $UO_2$ in a high-concentration steam atmosphere. Modifications of the present equipment allow controlled steam injection to prevent premature condensation and provide for condensation of the steam outside the high-temperature zone. With these modifications, experiments can now be performed in air-steam mixtures up to 90% relative humidity and a total pressure of 1 atm. To date,

one in-pile experiment has been conducted in which a stainless-steel-clad fuel element was melted in a high-concentration steam atmosphere with a small amount of air.

The effectiveness of the components of the gas-cleaning system for retaining fission products was estimated by examining radiochemical data from materials plated on various portions of the in-pile system during all previous experiments. The results show that considerable amounts of iodine, tellurium, and cesium deposit in the diffusion tubes and that additional quantities of iodine deposit on the cool metal surface of the reactor furnace. Estimates of the upper limit of the amounts of fission products penetrating the filters and adsorber were also obtained.

Greater usefulness and flexibility of the off-gas analysis equipment have been obtained by recent modifications. The off-gases being studied have passed from the in-pile meltdown furnace through the filters and the charcoal trap. The modified unit permits (1) monitoring of the radioactivity of the gas during operation, (2) collection of rare gases in a refrigerated charcoal trap, (3) transfer of the collected gases into an evacuated tank by heating the charcoal trap, and (4) collection of gaseous samples in biological serum bottles.

### 1.4 Characterization and Control of Accident-Released Fission Products

Diffusion tubes were used to study the distribution of iodine in aged aerosols, in conjunction with modified May packs which consisted of an absolute filter, copper- or silver-plated copper screens, charcoal-impregnated filter paper, and a series of small charcoal beds. The unfiltered aerosol in the containment tank, produced by melting 7000 Mwd/ton irradiated $UO_2$, contained iodine which was 70% molecular and 25% associated with particles in the 20- to 30-A size range. The remaining 5% was distributed among larger particles and a charcoal-penetrating form presumed to be an organic iodine. Filtration of the aerosol by an absolute filter removed most of the particles larger than 50 A, while passage through copper screens removed molecular iodine and some that was associated with particles; of the remainder, that attached to particles in the 20- to 30-A range and the penetrating form were the principal airborne iodine species. The latter form accounted for only about 0.3% of the total iodine inventory.

Separate filter packs and diffusion tubes were used to determine the iodine distribution in the aged aerosol from the confinement tank in the absence of heated fuel at three stages in the iodine tracer experiment: during depressurization, during argon sweep, and during air sweep.

An effort was made to determine, by the liquid contactor or scrubber method, the distribution of forms of radioiodine remaining airborne after several hours in the Confinement Mockup Facility. The purpose of the test was to supplement information being obtained from the May pack filter-absorbers and from data on deposition in diffusion tubes. From the results to date it appears that this system must be thoroughly tested in order to give distribution data which can be interpreted unequivocally and that inclusion in the system of a filter having a known efficiency for very small iodine-bearing particles will aid interpretation of the data.

The efficiency of May packs as iodine samplers was investigated in two experiments by use of composite diffusion tubes connected to each section of the May pack. In the first experiment relatively dry filtered air was employed with iodine which was 99.7% elemental and 0.3% iodine compounds. As indicated by the diffusion tubes, the behavior of the volatile iodine in the May pack, in one test with fairly dry air, was observed to be generally consistent with the designed function of the May pack components. On the other hand, about 1% of the elemental iodine was apparently not retained by the copper gauze; if this is a usual occurrence, May pack measurements would incorrectly label part of the elemental iodine as nonelemental. Mislabeling to this extent could be of considerable significance in connection with the design of high-efficiency iodine removal systems.

An experiment was performed to investigate certain anomalies which have been observed in the use of composite diffusion tubes. Six diffusion tubes having various arrangements of wall material were supplied with air bearing iodine generated by the dichromate method. One of the diffusion tubes was heated to 100°C. The observations are tentatively interpreted to show the presence of at least two distinct iodine species other than $I_2$; one of the species seems to be relatively unstable. The deposition rate on rubber

tubes does not appear to be primarily dependent upon diffusion, but is probably influenced by the dissociation of an iodine compound to yield HI or $I_2$. Iodine carried by particulates is not observed in the aerosol produced by the dichromate method. A heated diffusion tube yields an altered but interpretable distribution, and the usefulness of this arrangement for characterizing radioiodine in a moist atmosphere will be investigated further.

Experiments continue to show that moisture interferes with the adsorption of volatile iodine compounds at the charcoal surface but does not have as strong an interfering effect on the sorption of elemental iodine vapor. Experiments were performed in an attempt to identify the volatile iodine compound by making use of its solubility (partition) behavior in two different solvents, such as methyl iodide and water. Results indicate that the mixture containing volatile iodine compounds includes either methyl iodide or an iodine compound of similar solubility.

The method for in-place testing of iodine adsorbers on the Nuclear Ship "Savannah" was developed further by application to the 9000-cfm building ventilation system of the ORR. Iodine vapor labeled with $^{131}I$ is released into the ventilation duct and is measured before and after the iodine adsorber. Satisfactory efficiencies were observed. Plans are being considered to establish a routine in-place testing procedure.

Experiments have shown that while activated charcoal is highly efficient for removal of volatile iodine compounds from dry air at room temperature, its efficiency drops off sharply with increasing humidity; it is also a function of the nature of the iodine compounds present. The removal efficiency of the charcoal was shown to increase when the temperature of the adsorber was increased to about 100°C. It was also shown that coconut charcoal is the most effective of the three types of charcoal studied for the removal of the volatile (penetrating) iodine fraction. Elemental iodine was removed from air by charcoal with high efficiency for all conditions tested.

Fibrous filters are being employed for the characterization of radioactive aerosols. By this method the distribution of radioactive particles in a series of uniform fiber filters is interpreted in terms of three main filtration mechanisms – diffusion, interception, and inertial impaction. Several experiments were performed in order to compare filters of 72 and 94% porosity. Streams of air, flowing at linear velocities from 0.4 to 88 fpm and carrying particles labeled with $^{65}Zn$, which ranged in diameter from 20 to 300 A, were passed through successive layers of identical filters. The filtration curves obtained were resolved into three straight lines indicating three different particle-size groups. The results also showed that decreasing the porosity reduced the amount of penetration. Decreasing the porosity seems to improve filter efficiency, particularly at intermediate flow rates (40 fpm), less so at lower (10 fpm) and higher (80 fpm) velocities, and negligibly at very low flow rates (2.5 fpm).

## PART 2. CONTAINMENT ENGINEERING

### 2.1 Nuclear Safety Pilot Plant

Construction of the Nuclear Safety Pilot Plant (NSPP) was completed, and two experimental runs in which unirradiated $UO_2$ was melted were carried out during the report period. A number of plasma torch runs were made in connection with development of plasma flame melting of ceramic fuel elements under some of the operating conditions proposed for the NSPP. Three new sampling devices have been added: May-pack sampler for taking time-dependent aerosol samples and differentiating the chemical form of the iodine in these, a device for investigating how the diffusion behavior of the aerosol is changed by removal of some of its components by elements of the May pack, and a device for collecting time-dependent fallout samples.

### 2.2 Reactor Containment Handbook

Technical revision of the Reactor Containment Handbook based upon the reviews received by June 1, 1964, is now completed, and the Handbook is being indexed and edited for preliminary release this fall.

## PART 3. PHYSICS

### 3.1 Reactivity Effects of Small Fuel Displacements on Plate-Type Reactors

A slab-geometry plate-type critical experiment was constructed to measure the reactivity effects

of small perturbations introduced by fuel-element displacements. These perturbations were calculated by both diffusion-theory and transport-theory codes, with careful attention to sources of error in the calculation model, in order to test the relative abilities of the two calculation methods to predict the magnitude of such perturbations. The transport-theory results were in rather good agreement with the experiment, whereas the diffusion theory was far less accurate in its predictions.

## PART 4. RADIOCHEMICAL PLANT

### 4.1 Radiochemical-Plant Safety Studies

The hazards associated with a large radiochemical plant were evaluated in a published report. One of the critical assumptions in this report was the characterization of aerosols formed by fires and explosions. Since little experimental work has been done in this area, an experimental program involving the combustion of organic solvents has been initiated.

## PART 5. NUCLEAR SAFETY INFORMATION

### 5.1. Nuclear Safety Information Center

The Nuclear Safety Information Center has collected, evaluated, and stored over 2500 sources of information in its first year of operation. Those sources pertaining to the containment of nuclear facilities, over 1300, were selected to form a miniature information center exhibit for the Third International Conference on the Peaceful Uses of Atomic Energy at Geneva, Switzerland, August 31 through September 9, 1964. During the report period, the Center received and answered 31 specific requests for information and consulted with 16 visitors.

### 5.2 Technical Progress Review

During the past six months, two issues of the technical progress review *Nuclear Safety* were prepared.

# Part 1
# Fission Product Release and Behavior

Reactor Chemistry Division

W. R. Grimes, Division Director
G. M. Watson, Coordinator

Key Words[a]

accident, loss of coolant, loss of flow
adsorption
aerosol
air cleaning
barium
behavior of fission products
cesium
charcoal
condensation
containment
deposition
filter
filter efficiency
filter systems
fission gas (release)
fission product (release)
fission product transport
fuel meltdown
halogens
impaction
in-pile
in-pile release
iodine
loss of coolant
loss of flow
meltdown
particulate
rare earth
reactor transient
ruthenium
silver
stainless steel
strontium
tellurium
uranium oxide
vapor
water
zirconium

[a]See Foreword.

# 1.1 Release and Transport of $UO_2$ Fission Products in the Confinement Mockup Facility

G. W. Parker
R. A. Lorenz
G. E. Creek
J. G. Wilhelm
W. J. Martin
C. J. Barton

The ORNL Hot-Cell Confinement Mockup Facility (CMF) has been described in previous reports.[1] The advantages of an integrated release experimental device, of which the CMF is the first of a series,[2] are mainly associated with the study of post-release fission product transport and deposition. It appears that after most of the parameters of the $UO_2$ fission product release have been somewhat roughly evaluated, the remaining uncertainties of greatest significance are in the parameters controlling the transport process, especially those of iodine. The fact that the CMF tank is constructed of stainless steel suggests that it might simulate the primary reactor or pressure vessel; in fact, it merely represents a compromise between what is experimentally expedient and what would be more realistic. Suitable provisions have been made to evaluate the probable differences between this small stainless steel system and a large heterogeneous confinement building; however, extrapolation of the transport and deposition data to actual reactor environment will be more easily accomplished in the 1350-$ft^3$ Nuclear Safety Pilot Plant facility at ORNL and in the 33,000-$ft^3$ Containment Systems Experiment at the Hanford laboratories. The flexibility of the CMF will permit the substitution of several alternate confinement vessel types and materials, including a simulant of a primary vessel.

## MODIFICATIONS OF THE CONFINEMENT MOCKUP FACILITY

Recent modifications of the CMF are indicated in Fig. 1.1. Significant changes include the provision for operating with air or steam pressures up to 30 psig. Besides having to improve the seal quality at all connections and entry points, this provision required double valving for safety reasons and the installation of pressure-type letdown valves for releasing gas streams to test equipment. Operation with steam pressure is simplified by deferring sample removal until the temperature of the tank (and its contents) has dropped significantly and most of the water vapor which would complicate sampling has condensed. Added to the facility are: (1) a more elaborate filter pack (May pack), (2) a condensation nuclei counter, (3) a heated catalytic burner to convert organic forms of iodine to free iodine, and (4) an aerodynamic particle separator, commercially known as an Andersen sampler. New arrangements for measuring deposition rates in the confinement tank and for sampling the tank aerosol are discussed elsewhere in this report.

In the following sections, five experiments performed in air in the CMF are discussed. These represent four different sets of conditions; runs A and B are duplicates. These two runs (A and B) were conducted with tracer-level-irradiated $UO_2$. Run C was the first of the high-burnup $UO_2$ melts, and run D was an $^{131}I$-tracer simulation run using

[1] G. W. Parker *et al.*, *Nucl. Safety Program Semiann. Progr. Rept. June 30, 1963*, ORNL-3483, p. 33; *Nucl. Safety Program Semiann. Progr. Rept. Dec. 31, 1963*, ORNL-3547, p. 3.

[2] W. B. Cottrell *et al.*, "U.S. Experience on the Release and Transport of Fission Products Within Containment System Under Simulated and Actual Reactor Accident Conditions," paper to be presented at the Third International Conference on Peaceful Uses of Atomic Energy, Geneva, 1964.

UNCLASSIFIED
ORNL-DWG. 64-4999

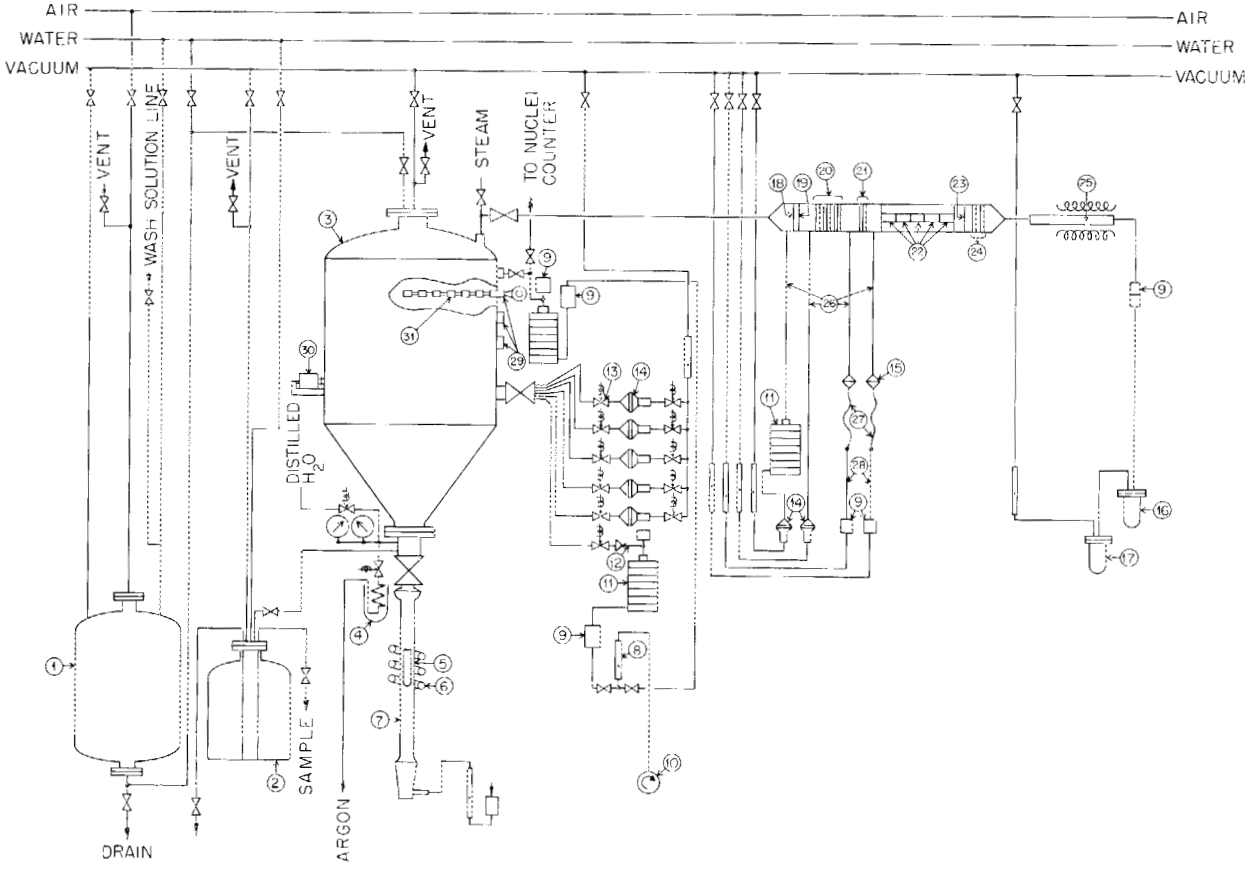


① WASH TANK
② 20 LITER CARBOY
③ 50 GAL. S.S. HOLD-UP TANK
④ COOLING BATH
⑤ CRUCIBLE AND SAMPLE
⑥ INDUCTION HEATER COIL
⑦ QUARTZ TUBE
⑧ ROTAMETER
⑨ CHARCOAL TRAP
⑩ VACUUM PUMP
⑪ ANDERSON "IMPACTOR" SAMPLER
⑫ ORIFICE
⑬ SOLENOID VALVE
⑭ MILLIPORE FILTER AND CHARCOAL
⑮ MILLIPORE FILTER
⑯ RASHIG RING TRAP
⑰ CHARCOAL TRAP
⑱ ROUGHING FILTER
⑲ ABSOLUTE FILTER
⑳ COPPER SCREENS (8)
㉑ CHARCOAL PAPER (3)
㉒ CHARCOAL CARTRIDGES
㉓ ABSOLUTE FILTER
㉔ COPPER SCREENS (4)
㉕ PLATINIZED ALUMINA
㉖ DIFFUSION TUBE (Ag lined Cu tubing)
㉗ DIFFUSION TUBE (rubber tubing)
㉘ DIFFUSION TUBE (charcoal-lined S.S. tube)
㉙ SAMPLER HOLES
㉚ FAN
㉛ CUTAWAY, SHOWING PLATE OUT SAMPLER

Fig. 1.1. Schematic Diagram of Modified Confinement Mockup Facility.

unirradiated $UO_2$. Run E was a straight $^{131}I$-tracer run under 15 psig air pressure.

## FISSION PRODUCT RELEASE FROM MELTING TRACE-LEVEL-IRRADIATED $UO_2$

Two experiments on melting trace-level-irradiated stainless-steel-clad $UO_2$ in the CMF have been completed. The $UO_2$ was melted over a period of several minutes while a stream of air flowing at 3 liters/min was passed over the crucible to transport the smoke and volatile fission products into the stainless steel confinement tank. The two experiments differed only in that one had a portion of unfiltered cell air, approximately 25% of the tank volume, accidentally added to the tank after melting of the fuel was completed. This difference in the conditions of the two experiments had a significant effect on the chemical form of the released radioiodine. The proportion of penetrating forms (possibly organic iodine compounds) was increased by a factor of approximately 10. This was the ratio between the amounts of iodine found to penetrate a $1\frac{1}{2}$-in. charcoal bed (ORR specifications) in these tests. Data on iodine behavior, total fission product release from the $UO_2$, and the amount of each fission product deposited during a 3-hr aging period in the confinement tank are summarized in Table 1.1.

It is interesting that the rate of removal of radioactivity from the aerosol was low in these experiments, which suggests that the particles remained too small to deposit rapidly. Analyses of the diffusion tube, of the absolute filter, and of the charcoal bed showed that approximately equal parts of particulate and molecular iodine were present in the confinement tank at the end of the 3-hr period. The amount of iodine in a penetrating (organic) form was only a fraction of either form and varied between the runs.

Table 1.1. Distribution of $UO_2$ Aerosol and Fission Products from $UO_2$[a] Melted in Air[b]

| | Distribution (% of inventory) | | | | | | | | | |
|---|---|---|---|---|---|---|---|---|---|---|
| | Iodine | | | Tellurium | | | Cesium | | | Plutonium |
| | A | B | C | A | B | C | A | B | C | C |
| Total release | 84 | 64 | 91 | 12 | 12 | 55 | 29 | 37 | 37 | 0.005 |
| Hot-zone deposition[c] | 6.3 | 11 | 0.4 | 3.3 | 1.9 | 2.5 | 3.2 | 16 | 6.2 | 0.0005 |
| Total in aerosol tank | 47 | 24 | 25 | 3.1 | 3.4 | 46 | 20 | 9.3 | 14 | 0.004 |
| Activity remaining airborne after 3 hr | 31 | 30 | 62 | 3.3 | 6.5 | 6.2 | 5.7 | 13 | 16 | 0.0001 |
| Amount of iodine in penetrating form | 3.7 | 0.4 | 0.3 | | | | | | | |
| Iodine loss through 1.5 in. of charcoal | 1.3 | 0.1 | 0.01 | | | | | | | |

[a]Runs A and B were made with tracer-level-irradiated $UO_2$. Run C was made with 20 g of stainless-steel-clad $UO_2$ irradiated to 7000 Mwd/ton.

[b]Run A was performed with filtered air diluted by ~25% with unfiltered air. Runs B and C were performed with air entirely filtered by absolute filters and a charcoal bed.

[c]Temperature in the "hot zone" varied from an undetermined value close to that of the fuel to approximately room temperature.

## FISSION PRODUCT RELEASE FROM HIGHLY IRRADIATED $UO_2$

### Comparison of Release Behavior from Tracer-Level-Irradiated $UO_2$ with That from High-Burnup-Level Fuel

The initial meltdown of highly irradiated (7000 Mwd/ton) $UO_2$ was performed in ambient air in the CMF. This experiment was of special interest since it provided the first opportunity to compare fission product release values from fuel irradiated to a realistic level with the results of tracer-level experiments. Total release values, as expected, were not markedly different except in the case of tellurium, which increased from about 12 to 55%. The total release data are summarized for this experiment in Table 1.1, and more detailed data are given in Table 1.2.

The release of plutonium was in good agreement with previous estimates that its volatility would correspond to that of $UO_2$. Under the conditions of melting (20 g of stainless-steel-clad $UO_2$ in a zirconia crucible with air flowing at 18 fpm), only $5 \times 10^{-3}$% of both Pu and $UO_2$ vaporized; most of this vaporized fraction deposited rapidly in the confinement tank.

Data obtained by sampling the confined aerosol at intervals showed a rapid reduction from the calculated initial concentration of fission products in the tank to that in the first sample, which was drawn 10 min after melting. Iodine concentration dropped from 91 to 10%; cesium dropped from 35 to 19%; and tellurium dropped from 53 to 7%. Evidence of probable deposition of all three fission products in the sampling tubes was observed. In addition, it was found that about 75% of the iodine that deposited on the walls of the confinement tank was desorbed by passing 1.5 tank volumes of argon (270 liters) through the tank.

### Total Nuclei Count in the Aerosol

A condensation nuclei counter (supplied by Gardner Instrument Co.), which is a light-scattering

Table 1.2. Distribution of Fission Products Released from High-Burnup (7000 Mwd/ton) $UO_2$ (Run C)

| Location | Release as Percent of Total in Sample | | | | | | |
|---|---|---|---|---|---|---|---|
| | Iodine | Cesium | Tellurium | Ruthenium | Plutonium | Strontium | Gross Gamma |
| Furnace tube | 0.4 | 6.2 | 2.5 | 0.0006 | 0.0006 | 0.001 | 0.03 |
| Aerosol tank | 25.2 | 13.9 | 46.3 | 0.001 | 0.004 | 0.007 | 0.5 |
| Filter pack: | | | | | | | |
| Roughing filter | 3.4 | 16.5 | 6.2 | 0.0008 | 0.0001 | 0.002 | 0.004 |
| Absolute filter | 0.5 | 0.04 | 0.008 | 0.00003 | | | |
| Copper screens | 52.7 | $10^{-6}$ | | | | | |
| Charcoal paper | 4.1 | | | | | | |
| 1st charcoal | 4.4 | | | | | | |
| 2d charcoal | 0.07 | | | | | | |
| 3d charcoal | 0.01 | | | | | | |
| 4th charcoal | 0.002 | | | | | | |
| 5th charcoal | 0.0005 | | | | | | |
| 2d absolute | 0.00003 | | | | | | |
| 2d copper screens | 0.000005 | | | | | | |
| Misc backup | 0.002 | | | | | | |

ion-chamber device with a maximum scale reading of $10^7$ nuclei/cm$^3$, was employed to follow the rapid change in the total nuclei concentration released in the preceding test. Agglomeration of small particles is one of the processes expected to influence the deposition of activity from the tank aerosol. In Fig. 1.2, a comparison of the number of particles is given, as well as the relative quantity of filterable activity in the aerosol. The rapid agglomeration rate (which can be extrapolated to approximately $10^{10}$ nuclei/cm$^3$ at release time) dropped from about $10^7$ to $10^5$ in 15 min and then decreased slowly to $10^4$ nuclei/cm$^3$. The total amount of filterable activity in the gas samples removed during this period (with the fan operating 1 min before each sample) did not change appreciably over the first 3-hr period. This suggests that while the nuclei did increase in size, growth was terminated by a reduction in concentration of particles so that deposition was not appreciably enhanced.

## Fission Products Remaining Airborne as a Function of Time

Radiochemical data obtained from samples of the aerosol in the confinement tank during the preceding test with the 7000-Mwd/ton $UO_2$ were supplemented by data at two additional calculated points: activity at the initial (zero) time and activity at final (300 min) time. The initial value is based on knowledge of the total amount released (all of which was initially airborne), and the final value is based on knowledge of the amount displaced by the argon gas sweep. Some unexplained variations are noted in the data shown in Fig. 1.3, such as a peak in the iodine curve at the third point and an apparent increase in the concentration of cesium and tellurium at the calculated end point. This latter condition is very likely due to deposition of the aerosol activities (cesium and tellurium) in the sample lines. The most pleasing aspect of the data in Table 1.3 and in Fig. 1.3 is

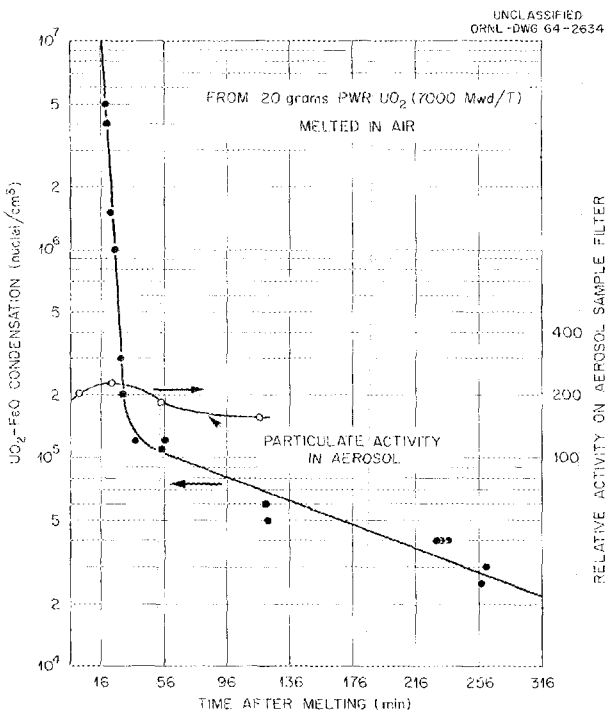


Fig. 1.2. Comparison of Nuclei Concentration and Particulate Aerosol Activity from High-Burnup $UO_2$.

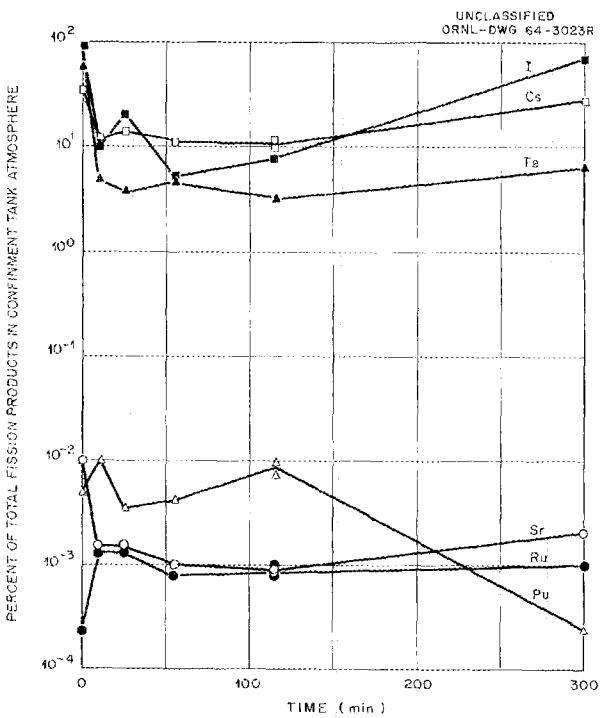


Fig. 1.3. Concentration of Airborne Fission Products as a Function of Time After Melting.

Table 1.3. Percent of Total Fission Product Inventory in the Aerosol as a Function of Time After Melting

| Time After Melting (min) | Iodine | Cesium | Tellurium | Ruthenium | Plutonium | Strontium |
|---|---|---|---|---|---|---|
| 0[a] | 91 | 30 | 53 | 0.002 | 0.005 | 0.01 |
| 10 | 11 | 12 | 5 | 0.001 | 0.010 | 0.001 |
| 25 | 21 | 15 | 4 | 0.001 | 0.004 | 0.002 |
| 55 | 5 | 12 | 5 | 0.0008 | 0.004 | 0.001 |
| 115 | 6 | 10 | 3 | 0.0008 | 0.008 | 0.001 |
| 118 | 11 | 11 | 3 | 0.001 | 0.010 | 0.0008 |
| 300[b] | 72 | 19 | 7 | 0.001 | 0.0003 | 0.002 |

[a]Calculated from total amount released to the confinement vessel.
[b]Calculated from total amount airborne to collecting filter-absorber system.

the very low release ($10^{-3}$%) of strontium, plutonium, and ruthenium.

## TEST OF A $UO_2$-$^{131}I$ AEROSOL AS A SIMULANT FOR FISSION PRODUCT IODINE FROM FUEL MELTDOWN

The cost of testing large confinement test facilities with real fission product mixtures released by melting highly irradiated fuel is very high; therefore development of a well-characterized $^{131}I$ simulant which gives realistic behavior is one of the present objectives of the CMF program.

In one experiment (run D) an attempt was made to produce a realistic $UO_2$ aerosol with added tracer $^{131}I$. A sample of carefully prepared molecular iodine having a known quantity of carrier iodine, in addition to several millicuries of $^{131}I$, was sealed in a $\frac{1}{2}$-in. length of a $\frac{1}{16}$-in.-diam quartz ampul. The ampul was placed in the melting crucible under a layer of insulating $ZrO_2$ powder, in an effort to delay the heating of the quartz until after some $UO_2$ had melted and until some $UO_2$ vapor was entering the tank. However, premature release of iodine occurred in this experiment, so that melting of the specimen cladding and of the $UO_2$ occurred after the iodine vapor had entered the containment tank.

Comparison of results of three experiments using irradiated fuel with data obtained in run D (Table 1.4) indicates that the $UO_2$ meltdown with simulated fission product iodine was reasonably successful in duplicating the aerosol from the irradiated (7000 Mwd/ton) fuel but that the iodine behavior here differed from that in the low iodine concentration experiments. The amount of iodine penetrating the $1\frac{1}{2}$-in.-thick charcoal bed (first two charcoal traps) was lower in the higher iodine concentration runs, C and D. The proportion of iodine in one particle-size range (18 to 22 A) was low in the simulation run; it possibly would have been higher if vaporization of the iodine and $UO_2$ had occurred simultaneously as planned. Desorption data obtained in these experiments and information on distribution of iodine among different forms are discussed later in this report. An interesting observation made in this run was that the copper screens apparently were deactivated by some foreign material and thus permitted most of the iodine to pass through them to the charcoal paper and beds. Diffusion tube data (Figs. 1.34 1.35) indicate clearly that the iodine form and proportions were quite similar to those shown in Figs. 1.29, 1.30, and 1.31 for run C.

Table 1.4. Deposition and Transport of Iodine in $UO_2$ Fuel Meltdown Tests[a]

| Location of Iodine | Inventory in Each Location (% of iodine) | | | |
|---|---|---|---|---|
| | A | B | C | D |
| Total release | 83.8 | 63.8 | 90.9 | 92.1 |
| Hot zone | 6.3 | 10.6 | 0.4 | 0.4 |
| Aerosol tank | 47.5 | 23.8 | 25.2 | 34.2 |
| Filter pack | | | | |
| Roughing filter | 15.7 | 15.1 | 3.4 | 0.84 |
| Absolute filter | 0.3 | 0.3 | 0.5 | 0.24 |
| Silver-copper screens | 4.8[b] | 8.1 | 49.4 | 2.0 |
| Charcoal paper | | | 4.1 | 14.7 |
| 1st charcoal | 5.5 | 3.0 | 4.4 | 39.2 |
| 2d charcoal | 2.3 | 0.2 | 0.07 | 0.18 |
| 3d charcoal | 0.6 | 0.02 | 0.01 | 0.02 |
| 4th charcoal | 0.3 | 0.003 | 0.002 | 0.005 |
| 5th charcoal | | | 0.0005 | 0.002 |
| 2d absolute filter | 0.00005 | 0 | 0.00003 | 0.00003 |
| 2d copper screens | 0.0002 | 0 | 0.000005 | 0.0002 |
| Cold trap backup | 0.26 | 0.04 | 0.0002 | 0.0001 |

[a]Runs A and B were with trace-irradiated $UO_2$.
Run C was performed with irradiated (7000 Mwd/ton) $UO_2$.
Run D was a $^{131}I$ tracer simulant released by melting unirradiated $UO_2$.

[b]In run A, bronze screens were used. They were later found to be less efficient than copper screens, which were used in subsequent runs.

## ADSORPTION AND DESORPTION OF RADIOIODINE IN THE CONTAINMENT MOCKUP FACILITY

The significance of the reported[3] high degree of desorption or resuspension of radioiodine adsorbed on the stainless steel walls of the Containment Mockup Facility (CMF) could not be determined from the results obtained in the first tests. Other experiments have been conducted or planned in an effort to determine the fraction of fission product iodine (adsorbed on metal surfaces) that might become airborne under realistic reactor accident conditions.

In reported studies conducted in the United Kingdom[4] on the behavior of iodine in containment vessels, the concentration of airborne iodine was reduced by about two orders of magnitude with a wide range of iodine concentrations. There were, however, several important differences between the UK experiments and those at ORNL, besides the large scale of the former which involved the containment facilities of the Dido and Pluto reactors. These differences included use of wall

[3]G. W. Parker *et al.*, "Properties of Aerosols Released from Overheated Reactor Fuels," *Oak Ridge National Laboratory Status and Progress Report, April 1964*, ORNL-3628, pp. 15–16.

[4]W. J. Megaw and F. G. May, *J. Nucl. Energy: Pt. A & B* **16**, 427–36 (1962).

materials such as polyvinyl chloride sheet, paint, and concrete in the UK experiments in contrast to clean stainless steel used in the CMF. The UK method of iodine release involved only oxidized radioiodine tracer with the desired amount of carrier, while in the ORNL experiments an attempt was made to present a more realistic system by releasing iodine only in the presence of simultaneously melted $UO_2$. Therefore, there was always an accompanying aerosol of fuel element components in the CMF tank atmosphere. This factor may have contributed to iodine desorption. The experiment described in the following section was performed in an effort to evaluate the effect of the $UO_2$ aerosol on iodine behavior.

## Conditions of the Plate-Out Experiment in the CMF Simulating UK Experimental Conditions

In order to observe the behavior of iodine in the CMF under conditions similar to those that prevailed in the Dido and Pluto experiments, except for the unavoidable difference in tank wall material mentioned above, an experiment was conducted in the CMF using oxidized $^{131}I$ with carrier iodine (2 mg/m$^3$ level). The containment tank was also pressurized to 15 psig, in order to provide a means of removing a fraction of the gas content of the tank which would more nearly represent accident conditions than was possible in the previous experiments.

The conditions and sampling sequences described in the following paragraphs were employed in this experiment.

**Source.** – The source was 50 mc of $^{131}I$ as $I_2$, with 350 $\mu$g of $^{127}I$ carrier.

**Method of Introduction.** – A liquid-nitrogen-cooled ampul containing the source was broken open and dropped into a quartz furnace tube. Volatilization was accomplished in less than 1 min by use of a gas torch to heat the quartz tube and ampul while air flowed through the tube to carry the iodine into the containment tank.

**Atmosphere.** – Air at ambient relative humidity (~60%) and at 15 psig was used. Half of the air was filtered; the other half was unfiltered.

**Mixing.** – The tank fan was operated for only about 2 min at the time of addition of the iodine to the containment tank. This was apparently sufficient to produce a homogeneous system, as was indicated by the ionization chamber adjacent to the tank.

**Plate-Out Cycle.** – Approximately 4 hr was allowed for plate-out deposition.

**Deposition Samples.** – A new technique was employed in this experiment to obtain plate-out samples. Cylindrical specimens $^3/_8$ in. by 0.8 in. long were inserted horizontally in the tank and removed at the following intervals after transfer of iodine to the tank: 6, 14, 34, 74, 134, and 214 min.

**Gas Sampling.** – *1. Plate-Out Cycle.* – Six gas samples were removed from the tank at the same time that the deposition samples were taken. These were taken by inserting a hollow needle through a rubber membrane and filtering a measured volume of tank air through an absolute filter and a charcoal trap.

*2. Pressure Release.* – Starting at 15 psig, the tank air was released through a stainless steel control valve and a filter pack at a rate of 3 liters/min for 1 hr. At the end of this period a residual positive pressure of $2^1/_2$ psi remained.

*3. Wet Contactor Sampling.* – A final sampling of the remaining gas at a pressure of $2^1/_2$ psi was conducted by use of a wet scrubber or contactor method described in another section of this report.

*4. Argon Sweeping.* – After the air in the containment tank reached atmospheric pressure, a new filter pack and a diffusion tube were installed, and $2^3/_4$ tank volumes of argon were passed through the tank to displace most of the remaining airborne iodine and to remove easily desorbed iodine from the wall of the tank.

*5. Air Sweeping.* – Finally, $2^1/_2$ tank volumes of air were passed through the tank and through a separate filter pack and diffusion tube.

**Instrumentation.** – The iodine activity in the containment tank ($^{131}I$ gamma) was observed and recorded continuously. Each of the three filter packs was monitored separately, and the total activity was also recorded continuously.

## Results of the Simulated Experiment

The complete record of the experiment is shown in Fig. 1.4. From this series of graphs it is apparent that most of the iodine deposited during the 4-hr period and that release of air pressure of 12.5 psi removed only a small fraction of the iodine (2.8%). The argon sweep removed a somewhat larger fraction (7.0%), and the air sweep removed an additional 2.9%. About 7% was removed in various plate-out samples. Including the latter amount, 86% of the iodine remained adsorbed on

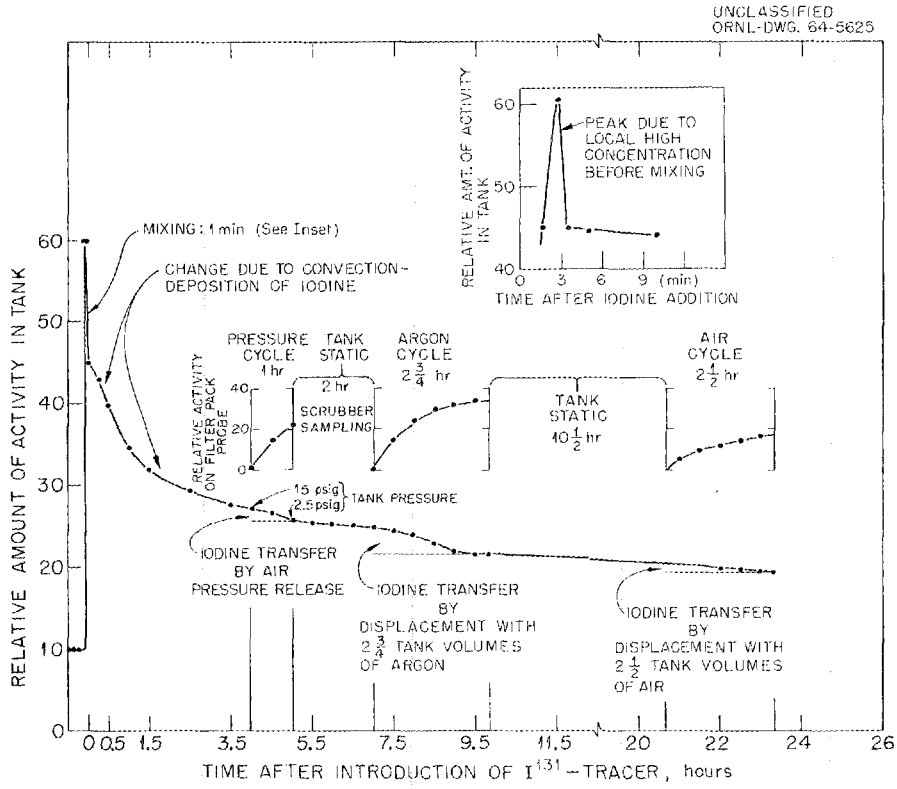


**Fig. 1.4. Rate of Iodine Deposition and Transfer to Filter Packs During Release of Air Pressure and Sweeping with Argon and Air.**

**Table 1.5. Comparison of the Behavior of Iodine from $UO_2$ Fuel Meltdown Tests[a] with That of Tracer Iodine in the Absence of Vaporized $UO_2$**

| Iodine Disposition | Percentage of Iodine Inventory | | | | |
|---|---|---|---|---|---|
| | Low Iodine Concentration | | High Iodine Concentration | | |
| | A | B | C | D | E |
| Total release from fuel | 83.8 | 63.8 | 90.9 | 91.6 | 100 |
| Amount deposited in furnace chimney | 6.3 | 10.6 | 0.4 | 0.4 | 0 |
| Total on aerosol tank wall after 2-hr aging and 2.5-hr gas sweep period | 46.5 | 23.8 | 25.2 | 34.2 | 86 |
| Amount airborne and desorbed from tank wall during 2.5-hr gas sweep period | 31.0 | 29.6 | 60.4 | 57.0 | 13 |
| Amount in penetrating form[b] | 3.7 | 0.4 | 0.3 | 0.5 | 0.3 |
| Loss through 1.5-in. charcoal bed[c] | 1.3 | 0.14 | 0.03 | 0.03 | 0.003 |

[a]Run A – trace-irradiated $UO_2$ (approx 1 $\mu$g I) with 20% unfiltered air (~5 $\mu$g I per $m^3$).
Run B – trace-irradiated $UO_2$ (approx 1 $\mu$g I) with 100% filtered air (~5 $\mu$g I per $m^3$).
Run C – 7000-Mwd/ton $UO_2$ (20 g $UO_2$, approx 400 $\mu$g I) with filtered air (~3 mg I per $m^3$).
Run D – tracer $^{131}I$ simulation with approx 200 $\mu$g I and with filtered air (~1.5 mg I per $m^3$).
Run E – tracer $^{131}I$ in filtered air without vaporized $UO_2$.

[b]Determined from distribution of iodine activity in charcoal beds after removal of elemental iodine.

[c]This is a part of the penetrating iodine activity.

the tank walls after more than 20 hr. Iodine behavior in this experiment is compared in Table 1.5 with that observed in experiments in which $UO_2$ was vaporized.

### Velocity of Deposition of Iodine on Stainless Steel in Air

The rate of deposition on the tank wall was determined from the change in iodine concentration in the tank air as a function of time, according to the analysis of the six gas samples. A plot (Fig. 1.5) of these six points and the initial "zero time" point, which was calculated from the total iodine displaced, as well as that adsorbed in the tank, showed that very rapid plate-out of 60% of the iodine apparently occurred before the first sample was removed (6 min after addition of iodine to the tank). The deposition velocity (the ratio of surface deposition rate to the aerosol concentration) calculated for this interval was $1.9 \times 10^{-2}$ cm/sec which is equivalent to a half-time of about 5 min. After 6 min the data show a change to a slower process and to a constant rate of deposition for the next 2 hr that was almost a factor of 10 lower ($2.2 \times 10^{-3}$ cm/sec) than the initial rate. This corresponds to a half-time of nearly 45 min. The final sample in the series indicated a further reduction in deposition velocity to $5.5 \times 10^{-4}$ cm/sec and a half-time of several hours.

In a previous experiment approximately half of the iodine deposited in the sampling lines, but in this experiment the lines were considerably shortened in order to reduce this effect.

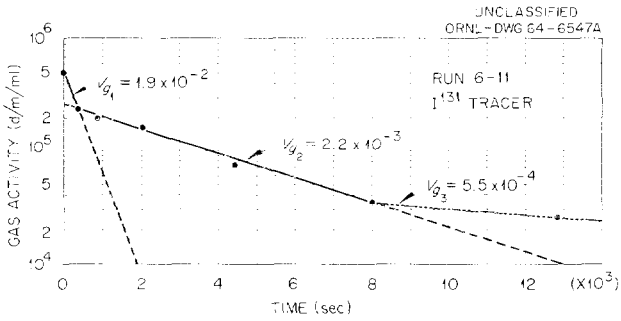


Fig. 1.5. Rate of Deposition of Iodine in the CMF Confinement Tank (Run E).

The initial very short half-time for iodine deposition (5 min) is in agreement with that observed in the Pluto experiment (20 to 30 min) when allowance is made for the difference in surface-to-volume ratio in the two experiments (2.8 $ft^2/ft^3$ in the CMF and 0.12 $ft^2/ft^3$ in Pluto). Since the rapid deposition process stopped at the end of 6 min, it brings to attention the question of the importance of the use of the fan and leads to speculation as to whether the plate-out process was initially enhanced by turbulence produced by the fan.

### Amount of Airborne Iodine in the Containment Vessel at the End of the 6-hr Aging Period

A comparison of the amounts of iodine removed by each of the pressure release and sweep cycles is shown in Table 1.6. It is possible to estimate from these values the proportion that was left airborne as well as the amount adsorbed.

The amount displaced in reducing the pressure from 15 to 2.5 psi was 2.8%. Correcting this value to 0 psig and multiplying by 2 gives a value of 6.8% for airborne iodine. Subtracting this figure from that for the total displaced iodine, 12.7%, leaves 5.9% as the amount desorbed. An adequate explanation for the small amount of iodine desorbed in this experiment as compared to the large fraction of iodine desorbed in previous experiments (Table 1.1) cannot be offered at the present time. However, as was mentioned elsewhere in this report, the principal difference in experimental conditions seems to be the absence of small particles from vaporized $UO_2$ in the present experiment.

### CMF Gas Sampling with an Evacuated Bulb and Injection Needle Technique

One problem encountered in previous attempts to sample gas in the CMF tank was the difficulty of obtaining representative samples through connecting tubes without an uncertain or indeterminate amount of deposition in the tubes and valves. A gas bulb, a filter pack, and a needle holder were arranged as shown in Fig. 1.6 to test a vacuum-bulb, injection-needle technique. The needle socket was cemented to the aluminum filter housing,

Table 1.6. Summary of Iodine Displaced and Desorbed from Containment Tank in Iodine Tracer Experiment (Run E)

| Collection Point and Time | Percent of Total |
|---|---|
| Adsorbed on tank wall during entire experiment | 79.5 |
| 1st filter compact during release of air pressure | 2.8 |
| Associated diffusion tubes | 0.1 |
| 2d filter compact during argon sweep | 7.0 |
| Associated diffusion tube | 0.4 |
| 3d filter compact during air sweep | 2.8 |
| Associated diffusion tube | 0.08 |
| Gas samples Nos. 1 through 6 — 1st 4-hr aging period | 0.1 |
| Scrubber system during release of last 2.5 psi of air pressure | 0.2 |
| Plate-out samples — 1st 4-hr aging period | |
| Stainless | 0.1 |
| Mild steel | 3.6 |
| Painted steel | 2.4 |
| Backup charcoal traps (entire experiment) | 0.00004 |
| Letdown valve — 1st 4-hr aging period | 0.8 |

and it was made vacuum-tight by the addition of a Teflon gasket.

To obtain a gas sample, the bulb was connected to a filter pack and attached needle with heavy pressure tubing. A gas manometer was attached to a side tee, the needle was pushed through a special rubber diaphragm, and the bulb was then evacuated. After closing a stopcock between the bulb and the vacuum system, a small stainless steel valve on the tank was opened to allow the pressurized gas in the tank to flow into the bulb until the pressure reached 1 atm. The needle was then withdrawn, and the total iodine in the sample was determined by measuring the gamma activity of the needle, the filter, and the charcoal with a gamma spectrometer. It was noted that the amount of iodine that was held up in the needle was quite variable, ranging from less than 1% of the total sample to a maximum of 16%. The sampling was apparently much more consistent than had been obtained previously, and the amount deposited in the needle was not considered excessive.

### Rate of Uptake of Iodine by Typical Reactor Construction Materials

Several investigations have established the importance of surface composition on rates of deposition of iodine in reactor containment buildings. Since the tank of the CMF is made of stainless steel, which is typical only of reactor pressure-vessel material, it was of interest to develop and test a method of comparing some materials with stainless steel in the CMF. Deposition samplers employing pressure-tight Teflon and neoprene O-ring seals, shown in Fig. 1.7, were designed and installed in the containment tank of the CMF. Small cylindrical specimens $\frac{3}{8}$ in. in diameter and 0.8 in. long connected by $\frac{1}{2}$-in.-diam segmented rods can be

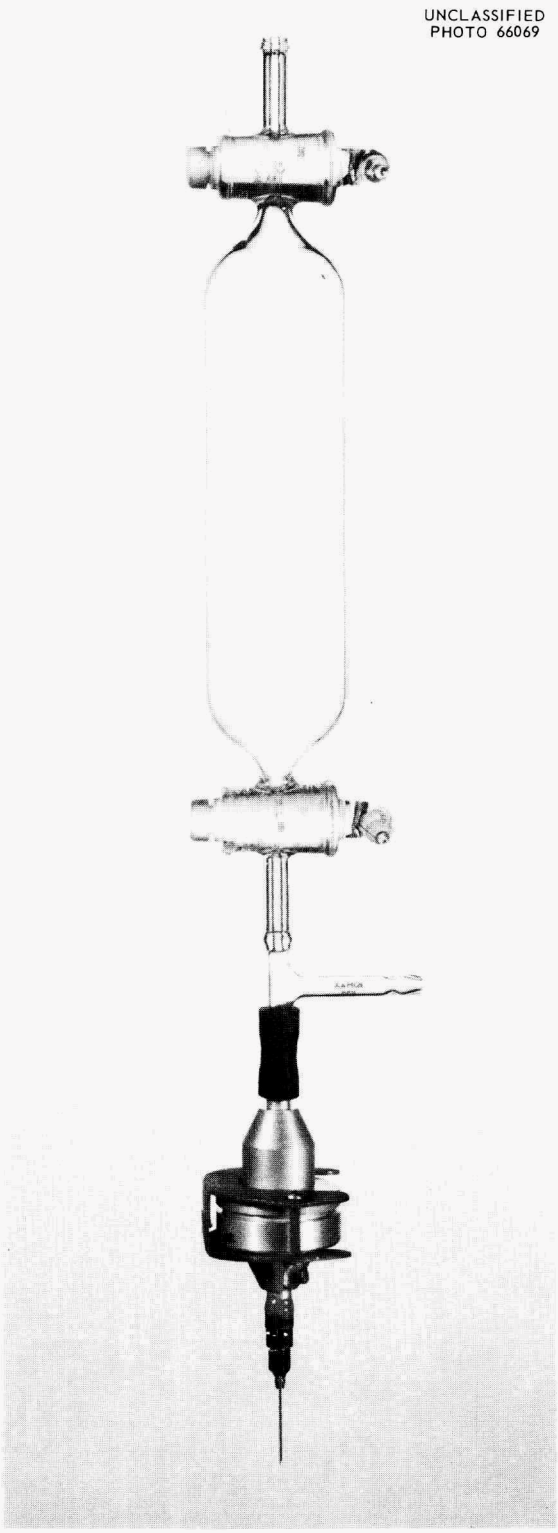


Fig. 1.6. Injection-Needle Gas Sampler.

withdrawn from the tank atmosphere after desired intervals of exposure.

Three samplers of this type were used in the tracer $^{131}I$ plate-out study described above with samples of slightly rusted mild steel, alkyd-enamel-painted steel, and polished stainless steel. The samples were tested once to measure uniformity of exposure under typical operating conditions and were found to be satisfactory in this respect.

The three sample rods were completely inserted into the tank at the start of the experiment, and one sample of each type was withdrawn at selected sampling intervals, starting 6 min after introduction of iodine.

The deposition results plotted in Fig. 1.8 show a striking difference between stainless steel and the other two materials. The rusty steel was slightly more reactive to iodine than the fresh alkyd paint, and both were almost 20 times as adsorptive as the polished stainless steel. The amount of iodine adsorbed by the small amount of surface exposed (Table 1.2) for the reactive materials suggests that a far faster process for plate-out should be experienced with containment building materials than was observed with the stainless steel vessel.

## Conclusions from Experiments in the CMF

This series of iodine release tests has not completely clarified the anomalous iodine behavior which results in 30 to 60% desorption by an inert-gas displacement of air from the CMF.

After duplicating more closely the iodine release conditions used in the UK in experiments involving no $UO_2$ vapor, the rapid deposition rate characteristic of the former experiments was observed. The iodine desorption process was minimized, and relatively modest desorption of only a few percent of the iodine occurred. No reason for the different behavior in the presence of $UO_2$ aerosol is suggested. Experiments are continuing to aid in interpreting this behavior.

The striking difference in plate-out of more than 20 to 30 times as much iodine on test samples of mild steel and of painted steel over that on stainless steel confirms the importance of the materials of construction. Major differences (30% desorption) are shown between trace level (6 $\mu$g of

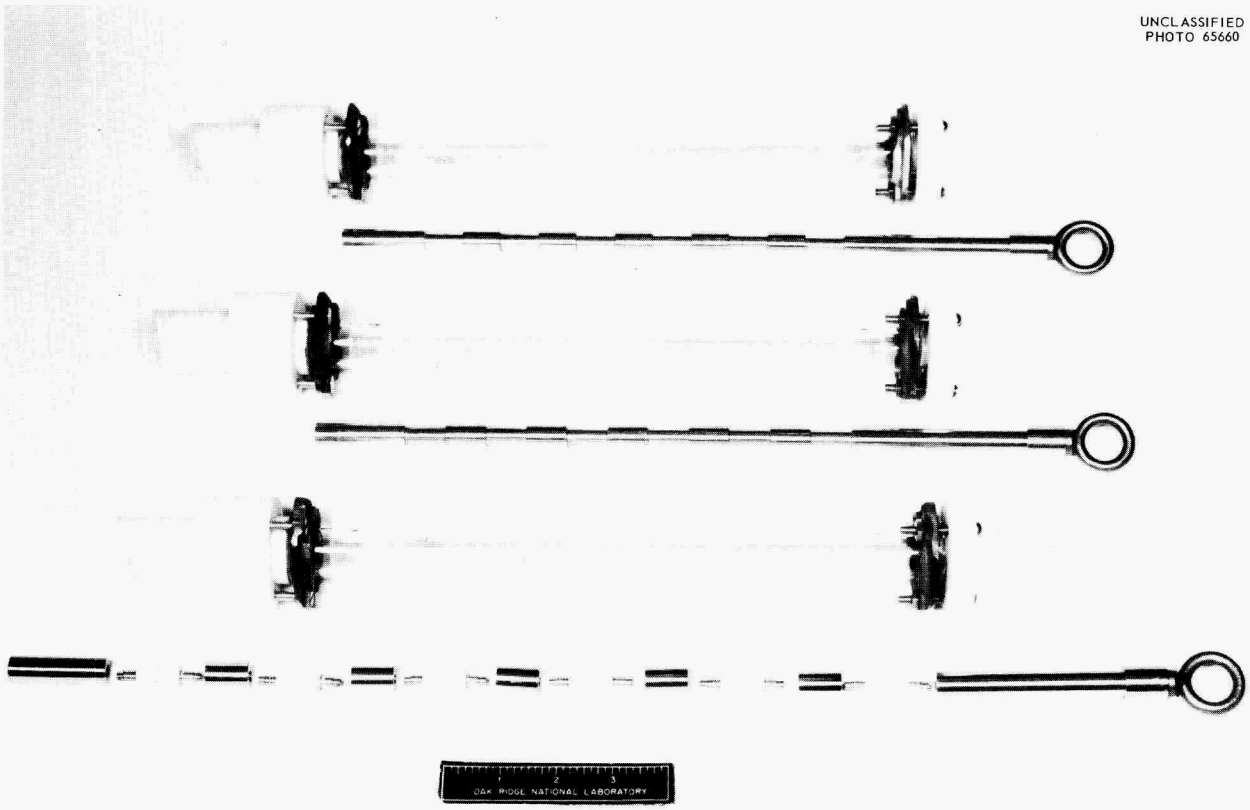


Fig. 1.7. Segmented Deposition Samplers Employed in the CMF.

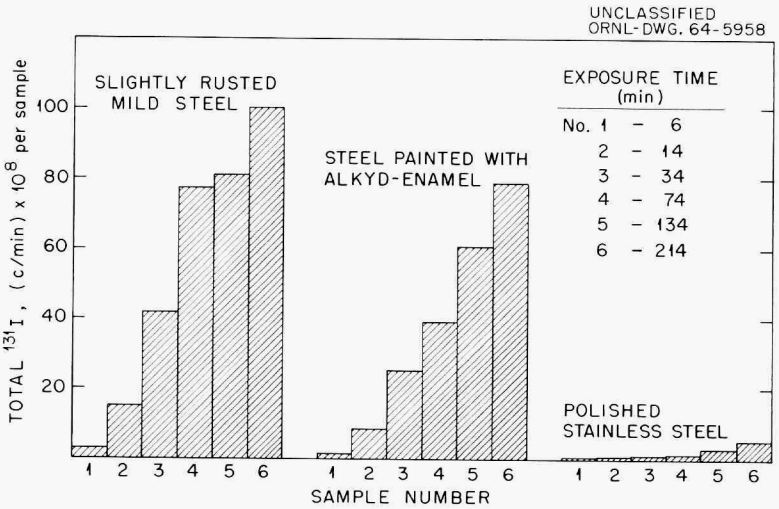


Fig. 1.8. Rates of Deposition of Iodine on Metal and Painted Surfaces.

I per $m^3$) (60% desorption) and at high-burnup level (2 $mg/m^3$). More than twice the total gas sweeping in the nonmeltdown experiment desorbed only 13% of the injected iodine. A pressure release simulating an actual accidental overpressurization and leakage to atmosphere released only 3% of the total iodine from the containment vessel.

# 1.2 Release of Fission Products on In-Pile Melting of Reactor Fuels Under Transient Reactor Conditions

G. W. Parker
C. E. Miller, Jr.
R. A. Lorenz
J. G. Wilhelm

The purpose of the ORNL fission-product-release experiments in the ANL TREAT facility is to study the release of fission products from fuel during a reactor transient in which the fuel melts rapidly as the result of a reactor transient. The objectives of this program are to measure and interpret the release of fission products as a function of fuel type, cladding, atmosphere, burnup, and transient characteristics.

In the first two experiments,[5] previously unirradiated stainless-steel-clad uranium dioxide specimens were heated in an argon atmosphere. These experiments simulated the type of transient accident that could occur with a clean reactor core where the only fission products available for release are those formed during the transient.

Two additional experiments were performed in this series that employed similar specimens and procedures, except that the specimens received a preliminary tracer-level irradiation to build up an inventory of fission products and the atmosphere in both cases was a mixture of air and steam. These experiments simulated transient accidents with reactors containing aged fission products in the presence of an oxidizing air-steam atmosphere.

### Experimental Assembly

The experimental equipment used for the third and fourth experiments was identical to that used with the first two experiments, except for elimination of the vacuum testing gage and minor structural changes inside the fuel autoclave for withstanding the oxidizing atmosphere. A diagram of the experimental assembly is shown in Fig. 1.9. The apparatus was composed of three interconnected parts: a fuel autoclave, a diffusion system that included a flow regulator, and a second autoclave, initially evacuated, to collect filtered gas

**Table 1.7. Fuel Specimen Characteristics**

| | |
|---|---|
| Cladding | |
| Material | Type 347 stainless steel |
| Wall thickness | 0.035 in. |
| Inside diameter | 0.407 in. |
| Pellet end clearance | 1/16 in. total |
| $UO_2$ Fuel | |
| Specimen weight | 30.4 g (two pellets, 15.2 g each) |
| Density | 10.39 $g/cm^3$ (94.7% of theoretical) |
| Diameter | 0.405 in. |
| U | 86.2 wt % |
| $^{235}U$ | 10.1 wt % |
| O/U ratio | <2.001 |
| N | 50 ppm |
| C | 500 ppm |
| Fe + Zr + Ni + Cr | 800 ppm |
| W[a] | 2.1% |

[a]Impurity introduced during fabrication.

[5]G. W. Parker *et al.*, *Nucl. Safety Program Semiann. Progr. Rept. Dec. 31, 1963*, ORNL-3547, pp. 25–42.

UNCLASSIFIED
ORNL-DWG 63-14458R3

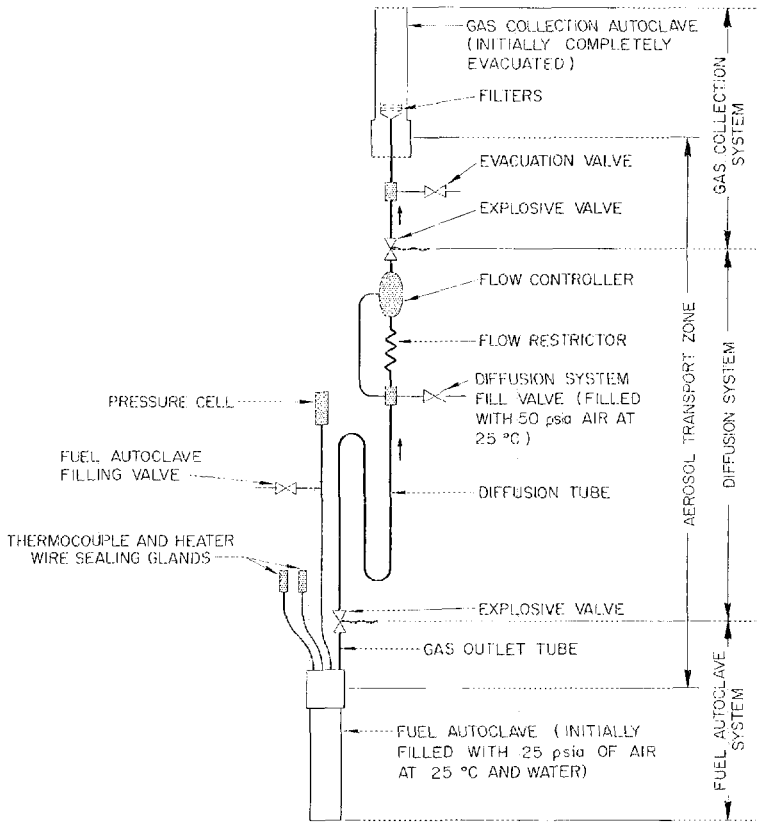


**1.9. Flow Diagram for Experiments on Release of Fission Products on In-Pile Melting of Reactor Fuels Under Transient Reactor Conditions.**

from the fuel autoclave. The fuel autoclave contained an electric heater to preheat the fuel specimen and to vaporize the water to form a steam-air atmosphere for the transient.

The revised fuel autoclave is shown in Fig. 1.10. An evacuated stainless steel Dewar flask was used to line the autoclave to serve as thermal insulation in place of the reflective tungsten sheet used in the first two experiments. The $UO_2$ fuel, cladding, and thermocouples were identical to those used in experiments 1 and 2, except that 10-mil-diam wires of tungsten and tantalum only were used in grooves between the two pellets to provide evidence of the maximum temperature reached during the transient. More space was left between the pellets and end caps for longitudinal expansion. Fuel specimen characteristics are given in Table 1.7.

The diffusion system was identical to that used previously in experiments 1 and 2. The filter assembly for experiments 3 and 4 consisted of five membrane-type filters in series. The first was a 1.2-$\mu$ pore size filter, and the last four were 0.45-$\mu$ nylon-reinforced membrane filters. These membrane filters should effectively collect particles as small as 0.01 $\mu$.

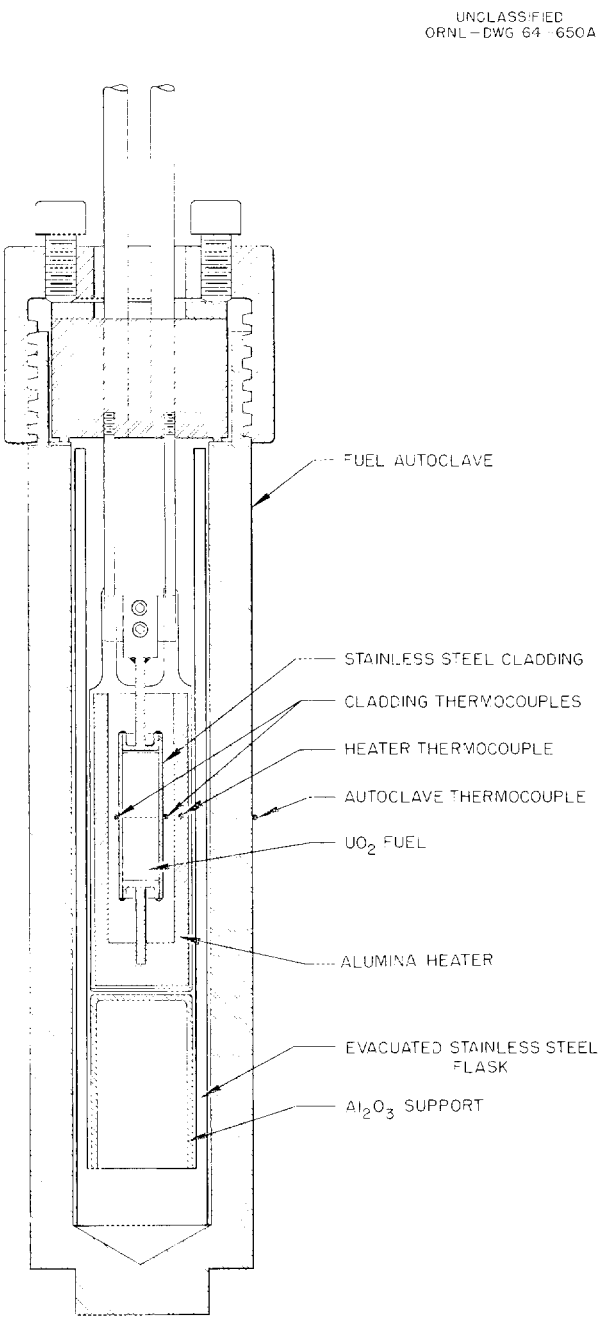


**Fig. 1.10. Diagram of Fuel Autoclave for In-Pile Melting of Reactor Fuels Under Transient Reactor Conditions.**

## Experimental Procedure

Preliminary experimentation was performed with various amounts of air and water heated in assembled fuel autoclaves. The temperature distribution, air and steam partial pressures, diffusion of steam to low-temperature areas, and change in atmosphere composition were determined. The assembled autoclaves were pretreated by flowing air through the heated autoclaves. Subsequently, heating tests 30 to 70 min long were made with air and water sealed in the autoclaves. Loss of steam to low-temperature regions such as the pressure cell was negligible during the time required for the experiments. The consumption of oxygen ranged from 10 to 50 $cm^3$ (STP). The generation of $CO_2$ ranged from 2 to 17 $cm^3$, $H_2$ from 0.1 to 1 $cm^3$, and $CH_4$ from 0 to 2 $cm^3$. Refilling and reheating the autoclaves resulted in the smaller changes.

After these preliminary heating tests, the clad fuel specimens were given a trace irradiation, were allowed to decay two weeks, and were reinstalled in the fuel autoclaves. The fuel autoclave of experiment 3 was filled to 25 psia with air saturated with water at 24°C. The fuel autoclave of experiment 4 was filled with 0.21 ml of $H_2O$ and 25 psia of air at 25°C. The diffusion tubes were filled with air at 50 psia, and the gas-collection autoclaves were evacuated. The fuel autoclaves were not heated after the irradiated fuel specimens were installed until the experiments were performed in the TREAT reactor.

After each experiment was installed in the reactor, the specimen was preheated electrically to 800°C, in order to simulate realistic reactor conditions, to vaporize excess water (experiment 4), and to help reduce fuel fragmentation during the transient. The reactor transient was performed with the reactor integrated power approximately 10% greater than that used in experiment 2, wherein 65% of the $UO_2$ fuel melted. Similar transients were used in experiments 3 and 4, so that the only difference would be the amount of water available for reaction with the fuel and cladding. Twelve seconds after the transient, the explosive valves were opened, and the aerosol from the fuel autoclave flowed through the diffusion system and filters into the gas-collection autoclave until the pressure was equalized throughout the assembly.

A summary of the reactor transient data and calculated specimen fission energy is given in Table 1.8.

A comparison of the heating of fuel and cladding in both experiments is shown in Fig. 1.11. The time scale was arbitrarily selected to be zero at a reactor integrated power of 23 Mwsec. The stainless steel temperatures were recorded with

Table 1.8. Summary of Operating Conditions

| | Experiment 3 | Experiment 4 |
|---|---|---|
| Reactor integrated power, Mwsec | 378 | 363 |
| Reactor period, msec | 74 | 77 |
| Estimated $UO_2$ temperature range, °C | 800 to mp | 800 to mp |
| Stainless steel cladding temperature, °C | 800 to mp | 800 to mp |
| Alumina heater temperature, °C | 710 to 1020 | 780 to 1140 |
| Autoclave wall temperature, °C | 108 to 138 | 162 to 195 |
| Fission energy input, cal per g of $UO_2$[a] | 291 | 280 |
| Initial fuel autoclave fill: | | |
| Air at 25°C, psia | 25 | 25 |
| Water, g | 0.05 | 0.21 |
| Volume percent steam (assuming complete vaporization) | 3 | 50 |
| Fuel autoclave pressure at start of transient: | | |
| Total pressure, psia | 43 | 53–58 |
| Air partial pressure, psi | 42 | 48 |
| Water partial pressure, psia | 1.2 | 5–10 |

[a]Calculated using a value of 0.77 cal per g of $UO_2$ per Mwsec determined from experiments 1 and 2.

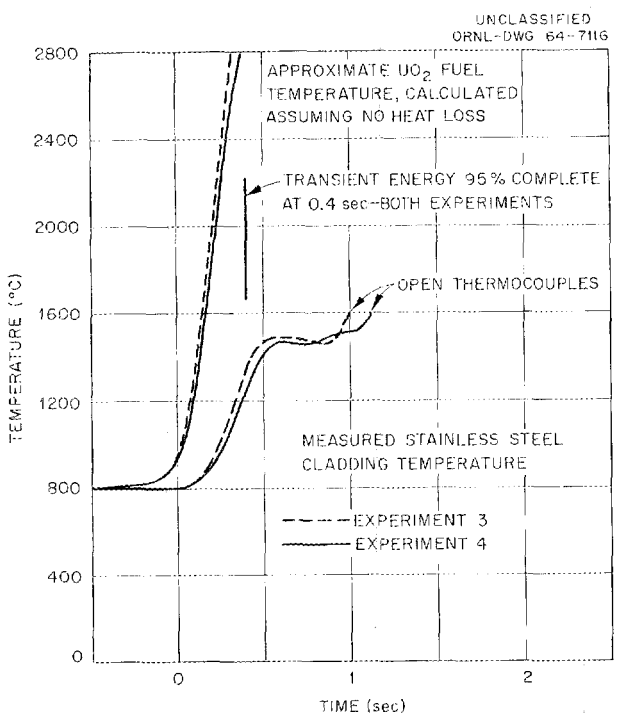


Fig. 1.11. Comparison of Transient Heating Rates of $UO_2$ Fuel and Stainless Steel Cladding in Experiments Containing Moist Air Atmosphere Showing that the $UO_2$ Fuel Reached Maximum Temperature While Cladding Was Intact.

high-speed equipment. The $UO_2$ fuel temperature was calculated assuming that no heat was lost from the fuel and that 320 Mwsec heated the fuel from 800 to 2800°C. The figure shows that the $UO_2$ fuel reached its maximum temperature while the stainless steel cladding remained intact.

## PHYSICAL EXAMINATION OF COMPONENTS

All components of experiment 3 appeared similar to those of experiment 4. Figure 1.12 illustrates the postexperimental specimen distribution observed in experiment 4. Most of the melted stainless steel formed a puddle at one side of the bottom, while $UO_2$ that melted and expanded to a porous or foamy condition ran mainly out the side of the lower pellet opposite the stainless steel puddle. The stainless steel entrained approximately 1% of the total $UO_2$, while the $UO_2$ that ran out of the pellet shells entrained a greater fraction of stainless steel. Figures 1.13 and 1.14 show the fuel specimen and heater from experiment 3, while the fuel specimen and heater from experiment 4 are shown in Fig. 1.15. The puddle of melted stainless steel is visible in the bottom

of the heater. Some small pieces of melted $UO_2$ broke off during disassembly of both experiments. There was no evidence of fracturing or shattering of the specimen. The fuel in experiment 3 appeared to have been hotter than that in experiment 4, since the upper pellet drained more completely of $UO_2$ and a thinner shell remained. The lower pellet of experiment 3 contained some large voids. Approximately 75% of the $UO_2$ melted in each experiment. The upper pellets swelled less than 5%, but the diameter of the lower pellets of experiments 3 and 4 increased a maximum of 10 and 15% respectively. Approximately 50% of the $UO_2$ ran out of the pellet shell in experiment 3 and 30% in experiment 4. The bulk density of $UO_2$ which ran out of the pellets was measured by displacement of water. Immersion of dry pieces in water showed a density of 6.4. When the large open pores were filled by prewetting with water, the measured bulk density was 4.1. The lower pellets from both experiments contained surface cracks which apparently resulted from stretching of the pellet skin. The tungsten and tantalum wires originally placed between the pellets were not recovered, and no metallographic work was done. The oxidizing steam-air atmosphere used in these experiments produced no observable effects.

Deposits on the filters of experiments 3 and 4 were similar to those in experiment 2. A light film of gray material was deposited on the first filter in each experiment, with no visible deposits on other filters. Figure 1.16 shows the size distribution of particles from the first filters in experiments 1 to 4. Experiments 3 and 4 showed identical particle-size distribution, and the reported mean particle size was much less than that of experiments 1 and 2. This difference in mean particle size may not be significant, since both the electron microscope and the particle-size analyzer used in experiments 3 and 4 had better resolving power than that used in the earlier experiments. The size distribution is that of the individual particles which were either separate or formed the agglomerates. Since most of the particles were agglomerated, the behavior of the solids in the aerosol (diffusion coefficients, e.g.) will be determined by the size or other properties of the agglomerates rather than the properties of the individual particles. Adequate methods for relating microscopic observations of agglomerates to settling or diffusion rates do not seem to be presently available.

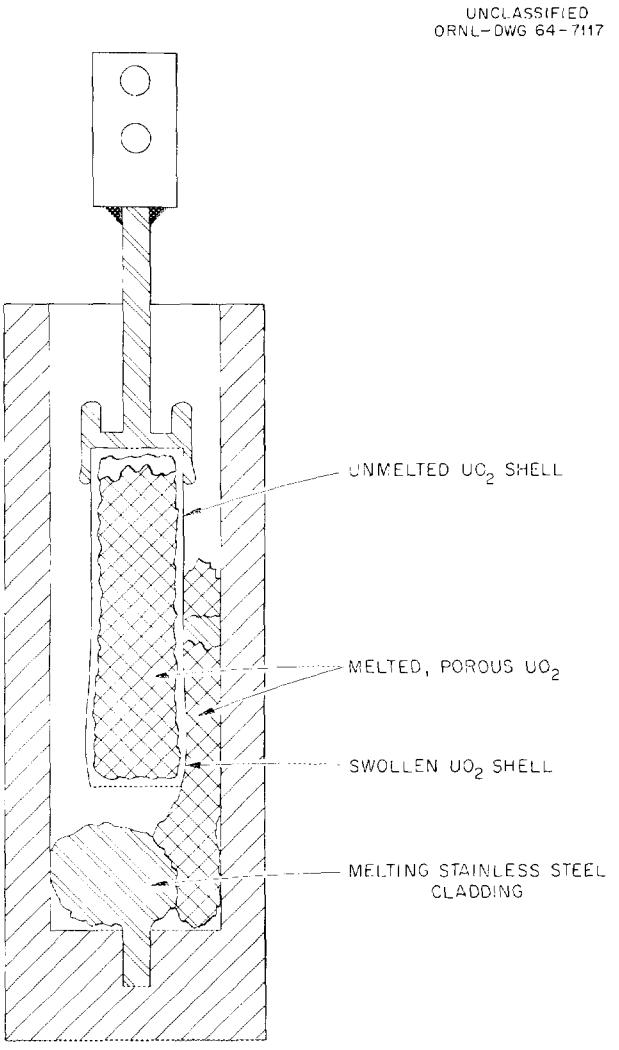


Fig. 1.12. Diagram Showing Distribution of $UO_2$ Fuel and Stainless Steel Cladding in Fuel Autoclave After In-Pile Melting Under Transient Reactor Conditions (Experiment 4).

Fig. 1.13. Melted Fuel Assembly and Heater After In-Pile Melting in a Moist Air Atmosphere Under Transient Reactor Conditions (Experiment 3).

Fig. 1.14. Lower Portion of Fuel Assembly Showing Hollowed $UO_2$ Pellet, Melted $UO_2$, Melted Stainless Steel Cladding, and Part of Ceramic Heater After In-Pile Melting in Moist Air Atmosphere Under Transient Reactor Conditions (Experiment 3).

UNCLASSIFIED
R-20112

Fig. 1.15. Melted Fuel Assembly and Heater After In-Pile Melting in a Steam-Air Atmosphere Under Transient Reactor Conditions (Experiment 4).

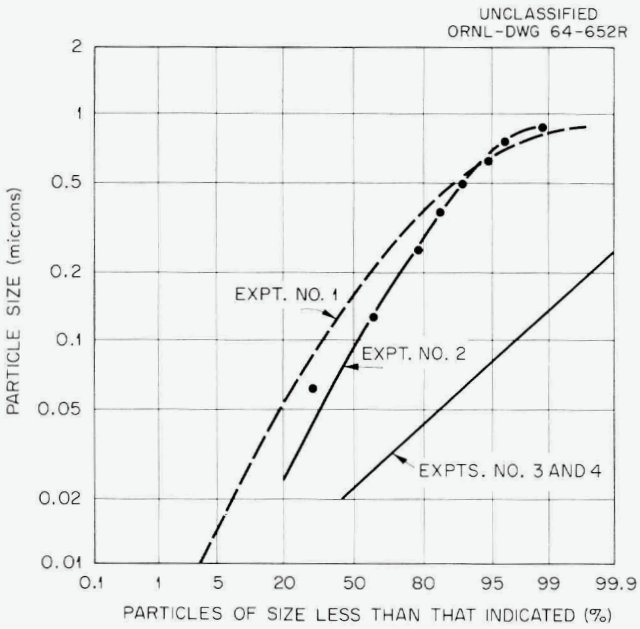


Fig. 1.16. Sizes of Particles Collected on Filters During In-Pile Melting of Stainless-Steel-Clad $UO_2$ in Steam-Air Atmospheres Under Transient Reactor Conditions.

## GAS ANALYSIS

The gas was removed from each experimental assembly and analyzed by mass spectrometry. Table 1.9 lists the results and shows that the two experiments were essentially identical with respect to gas composition. The greatest changes were loss of $O_2$ and formation of $CO_2$ and $H_2$. The method of sampling and analysis does not give the total amount of $H_2O$. The oxygen consumed was approximately 75% of that originally in the fuel autoclave and suggests that more might have been consumed if it had been available to the heated fuel specimen. The $CO_2$ may have been formed by oxidation of organic material introduced when the irradiated fuel specimen was installed. The amount of hydrogen found in the system cannot be used as a measure of metal-water reaction, since the reaction of $H_2$ with $O_2$ to form $H_2O$ can occur at the high-temperature conditions in these experiments.

Table 1.9. Composition of Gas in the Fuel Autoclave and Diffusion System[a] After Experiments and Observed Changes

| | Experiment 3 | | Experiment 4 | |
|---|---|---|---|---|
| | Percent | Change ($cm^3$, STP) | Percent | Change ($cm^3$, STP) |
| $H_2$ | 0.10 | +0.3 | 0.14 | +0.5 |
| $H_2O$ | 0.94 | | 1.47 | |
| $N_2$ | 82.06 | | 82.64 | |
| $O_2$ | 12.71 | −36 | 11.76 | −40 |
| Ar | 1.01 | | 0.98 | |
| $CO_2$ | 3.18 | +12 | 3.01 | +11 |
| Hydrocarbons | <0.01 | | <0.01 | |

[a]Original gas volumes (STP) were 237 ml in the fuel autoclave and 163 ml in the diffusion system. The oxygen content of the gas in the latter system was not available for reaction while the fuel specimen was at a high temperature.

## RADIOCHEMICAL RESULTS

Radiochemical analyses were obtained for the two experiments. Eight fission products and uranium were determined throughout each experiment so that a complete fission product balance was obtained. The eight fission products were those usually determined in fission product release experiments. The pretransient irradiation for fission product buildup was planned to be 160 times as great as the irradiation received during the transient so that the experiment would simulate an accident with reactors containing aged fission products. However, the actual pretransient irradiation was only 16.5 times that of the transient. Since 30 days decay time occurred between the pretransient irradiation and the transient, much of the $^{131}I$, $^{140}Ba$, and other short-half-life isotopes decayed to low levels before the transient was performed. Consequently, the transient-formed fission products of mass numbers 131 and 140 were of relatively significant quantity. These isotopes interfered with the investigation of the release of $^{131}I$ and $^{140}Ba$, since nearly all the transient-formed fission products were born as short-half-life isotopes, which behaved differently in the experiment than the longer-half-life isotopes into which they later decayed.

The decay chains for fission products of interest were presented and discussed previously[1] for experiments 1 and 2. In all cases the short-half-life precursors have half-lives of the order of seconds and minutes, so that these experiments cannot be examined and analyzed before precursors have decayed into the isotopes of interest. In most cases the precursors behave differently, both physically and chemically, from the daughters. For example, the mass 131 yield from fissioning is mostly $^{131}Sn$, $^{131}Sb$, and $^{131}Te$, which decay progressively by beta emission with half-lives of the order of minutes into $^{131}I$.

When experiments 3 and 4 were analyzed, only 56% of the $^{131}I$ found was actually $^{131}I$ at the time of the transient. The remaining 44% was formed during the transient and was released and distributed as short-half-life precursors $^{131}Sn$, $^{131}Sb$, and $^{131}Te$. Therefore, the results of experiments 3 and 4 show the release of certain mixtures of fission products and their precursors. The percentage of each fission product and the percentage of its principal precursors are listed in a footnote of Table 1.10, but are not repeated for Tables 1.11 and 1.12. The effect of the precursors may be qualitatively inferred from the results of experiment 2, in which all the fission products were released as precursors, although

UNCLASSIFIED
ORNL DWG. 64-9812

**Table 1.10. Distribution of Fission Products and Fuel in Experiments 3 and 4 Including Transient-Formed Fission Products**

| Location of Material | Percentage in Each Location[a] | | | | | | | | |
|---|---|---|---|---|---|---|---|---|---|
| | $^{131}I$ | $^{129}Te$ | $^{137}Cs$ | $^{106}Ru$ | $^{89}Sr$ | $^{140}Ba$ | $^{95}Zr$ | $^{144}Ce$ | $UO_2$ |
| **Experiment 3** | | | | | | | | | |
| $UO_2$ fuel | 61 | 69 | 61 | 92 | 94 | 90 | 97 | 97 | 97 |
| Stainless steel cladding[b] | 12 | 12 | 0.61 | 0.033 | 0.52 | 0.48 | 0.50 | 0.53 | 0.36 |
| Alumina heater | 19 | 12 | 29 | 3.6 | 0.82 | 4.5 | 0.62 | 0.66 | 0.44 |
| Autoclave liner | 3.3 | 5.9 | 6.6 | 2.5 | 1.5 | 2.5 | 1.4 | 1.3 | 1.9 |
| Fuel autoclave walls | 3.6 | 0.82 | 1.4 | 1.4 | 0.98 | 1.3 | 0.95 | 0.89 | 0.86 |
| Aerosol-transport zone[c] | 0.59 | 0.086 | 0.86 | 0.0033[d] | 1.1 | 1.1 | 0.00099 | 0.0011 | 0.00066 |
| Filters[c] | 0.115[d] | 0.013 | 0.017 | 0.00092[d] | 0.11 | 0.074 | 0.00012 | 0.00004 | 0 |
| Gas-collection autoclave[c] | 0.16 | 0.0046 | 0.95 | 0.00024[d] | 1.3 | 0.054 | 0.00014 | 0.00009 | 0.00014 |
| **Experiment 4** | | | | | | | | | |
| $UO_2$ fuel | 66 | 73 | 68 | 98.8 | 95 | 91 | 99.3 | 99.3 | 99.3 |
| Stainless steel cladding[b] | 4.7 | 7.4 | 1.1 | 0.38 | 0.039 | 0.018 | 0.024 | 0.012 | 0.00011 |
| Alumina heater | 18 | 14 | 24 | 0.77 | 1.2 | 5.3 | 0.56 | 0.62 | 0.59 |
| Autoclave liner | 5.1 | 4.3 | 3.9 | 0.040 | 0.77 | 1.8 | 0.073 | 0.076 | 0.062 |
| Fuel autoclave walls | 4.4 | 0.52 | 0.94 | 0.0042 | 0.18 | 0.54 | 0.0084 | 0.010 | 0.0053 |
| Aerosol-transport zone[c] | 0.86 | 0.22 | 1.6 | 0.004[d] | 1.5 | 1.6 | 0.0018 | 0.0026 | 0.00078 |
| Filters[c] | 0.093 | 0.013[d] | 0.10 | 0.022 | 0.090 | 0.071 | 0.00024 | 0.00004 | 0.00001 |
| Gas-collection autoclave[c] | 0.052[d] | 0.00062[d] | 1.1 | 0.0018[d] | 1.5 | 0.012 | 0.00009 | 0.00002 | 0.00022 |

[a]The distribution of radiochemically analyzed fission products is shown. At the time of the transient each listed isotope was a mixture of the isotope and its chain precursors. Mass chain 131 was 56% I and 44% Sn, Sb, and Te. Mass chain 129 was 90% Te and 10% Sn and Sb. Mass 137 was 94% Cs and 6% I and Xe. Mass 106 was 94% Ru and 6% Mo and Tc. Mass 89 was 92% Sr and 8% Br and Kr. Mass 140 was 77% Ba and 23% Xe and Cs. Mass 95 was 94% Zr and 6% Rb and Sr. Mass 144 was 94% Ce and 6% Ba and La.

[b]$UO_2$ and its normally associated fission products which adhered to the stainless steel samples were removed by a surface leach of the stainless steel and included as part of the "$UO_2$ fuel" above. In both experiments this amounted to approximately 1.5% of the $UO_2$.

[c]Only approximately 60% of the transient-generated aerosol enters the aerosol-transport system. Only approximately 40% of the transient-generated aerosol enters the filter and gas-collection autoclave.

[d]Error ± 100%.

UNCLASSIFIED
ORNL DWG. 64-9813

**Table 1.11. Distribution of Material Released from Transient-Heated $UO_2$ in Experiment 3 Including Transient-Formed Fission Products**

| Release Zone | Percent of Total Inventory[a] | | | | | | | | |
|---|---|---|---|---|---|---|---|---|---|
| | $^{131}I$ | $^{129}Te$ | $^{137}Cs$ | $^{106}Ru$ | $^{89}Sr$ | $^{140}Ba$ | $^{95}Zr$ | $^{144}Ce$ | $UO_2$ |
| Total release from $UO_2$ fuel | 39 | 31 | 39 | 7.6 | 6.3 | 10 | 3.4 | 3.4 | 3.5 |
| Release from high-temperature zone[b] | 4.5 | 0.92 | 3.3 | 1.4 | 3.5 | 2.6 | 0.95 | 0.89 | 0.86 |
| Transported release[c] | 0.86 | 0.10 | 1.82 | 0.0044 | 2.5 | 1.3 | 0.0013 | 0.0013 | 0.00080 |

[a]The distribution of fission products as radiochemically analyzed is shown. At the time of the transient the amount of each fission product in precursor isotope form was: 44% of $^{131}I$, 10% of $^{129}Te$, 8% of $^{89}Sr$, 23% of $^{140}Ba$, and 6% of $^{137}Cs$, $^{106}Ru$, $^{95}Zr$, and $^{144}Ce$.

[b]The high-temperature zone includes the fuel, cladding, heater, and autoclave liner.

[c]Gas-transport zone, filters, and gas-collection autoclave.

UNCLASSIFIED
ORNL DWG. 64-9814

**Table 1.12. Distribution of Material Released from Transient-Heated $UO_2$ in Experiment 4 Including Transient-Formed Fission Products**

| Release Zone | Percent of Total Inventory[a] | | | | | | | | |
|---|---|---|---|---|---|---|---|---|---|
| | $^{131}I$ | $^{129}Te$ | $^{137}Cs$ | $^{106}Ru$ | $^{89}Sr$ | $^{140}Ba$ | $^{95}Zr$ | $^{144}Ce$ | $UO_2$ |
| Total release from $UO_2$ fuel | 34 | 27 | 32 | 1.2 | 5.3 | 9.3 | 0.67 | 0.72 | 0.66 |
| Release from high-temperature zone[b] | 5.4 | 0.76 | 3.8 | 0.033 | 3.2 | 2.2 | 0.011 | 0.013 | 0.0063 |
| Transported release[c] | 1.0 | 0.24 | 2.9 | 0.029 | 3.1 | 1.7 | 0.0021 | 0.0027 | 0.0010 |

[a]The distribution of fission products as radiochemically analyzed is shown. At the time of the transient the amount of each fission product in precursor isotope form was: 44% of $^{131}I$, 10% of $^{129}Te$, 8% of $^{89}Sr$, 23% of $^{140}Ba$, and 6% of $^{137}Cs$, $^{106}Ru$, $^{95}Zr$, and $^{144}Ce$.

[b]The high-temperature zone includes the fuel, cladding, heater, and autoclave liner.

[c]Gas-transport zone, filters, and gas-collection autoclave.

only 65% of the fuel melted in experiment 2 and the atmosphere was argon.

From radiochemical results, pretransient irradiation for fission product buildup was calculated to be $2.4 \times 10^{16}$ fissions in experiment 3 and $2.1 \times 10^{16}$ fissions in experiment 4. The transient irradiation amounted to $1.36 \times 10^{15}$ and $1.31 \times 10^{15}$ fissions for experiments 3 and 4, respectively, calculated from the reactor integrated power. Table 1.10 shows the detailed distribution of fission products, including both pretransient- and transient-produced fission products, in the two experiments.

The large piece of melted stainless steel cladding was analyzed in each experiment. Most of the fission products and uranium associated with the stainless steel sample were found in a nitric acid leach of the surface, indicating entrainment of $UO_2$. Most of the $^{131}I$ and $^{129}Te$ was found in the solution of the previously leached stainless

steel. The $^{129}Te$ was probably alloyed with the stainless steel, and the Sn and Sb precursors of $^{131}I$ also probably alloyed with the cladding.

Fission products found on the alumina heater were predominantly the volatile fission products I, Te, and Cs. Next in abundance was $^{140}Ba$, whose precursors are Xe and Cs, with the other fission products approximately equal to the percentage of $UO_2$. The autoclave liner and fuel autoclave walls of experiment 3 contained significantly more $UO_2$ and nonvolatile fission products than did experiment 4. Nothing was observed during disassembly of the assemblies that would account for this difference.

Tables 1.11 and 1.12 summarize data on the distribution of fission products in the two experiments. Release values are expressed as the percent of the total inventory of each fission product or fuel. Values are given for release from the $UO_2$ fuel, release from the high-temperature zone, and for "transported release," which is material carried out of the fuel autoclave through the aerosol sampling system by a low-velocity gas stream; it includes only gaseous material and small particles formed by the transient heating.

The high-temperature zone includes the fuel autoclave liner and all equipment within the liner such as the wires and insulators between the alumina heater and the fuel autoclave cap, the heater, stainless steel cladding, and the fuel. Except for the outside of the liner, the high-temperature zone represents surfaces which were above approximately 500°C. Release from the high-temperature zone includes transported release and material deposited on the fuel autoclave walls and cap. The relatively large quantity of uranium and nonvolatile fission products (Zr and Ce) found on the fuel autoclave walls of experiment 3 was probably introduced during disassembly of fuel autoclave components.

The values for total release from $UO_2$ fuel are subject to variation because of the difficulty of separating melted $UO_2$ from melted stainless steel and from the alumina heater. Therefore, no significance is attached to the difference between experiments 3 and 4 with respect to release of fuel and nonvolatile fission products within the fuel autoclave.

The transported release values found in experiment 4 are greater than those of experiment 3. The greater amount of steam formed in the fuel autoclave of experiment 4 might be expected to force a greater fraction of the fission-product-containing mixture from the fuel autoclave into the gas-transport zone than was transferred in experiment 3. This better flushing of the fuel autoclave in experiment 4 may have been responsible for the greater transported release values observed in this experiment.

The data from experiments 3 and 4 would be more useful for predicting fission product release from accidental power reactor excursions if the transient-generated fission products in experiments 3 and 4 could be distinguished from those formed during the preliminary irradiation. The distribution and amount of transient-generated fission products can be approximated by using the results of experiment 2, in which all of the fission products were formed during the transient. This use of the data from experiment 2 may result in corrections that are not absolutely correct because of minor differences between experiment 2 and experiments 3 and 4. The greatest difference is in the atmospheres employed, but data obtained by other experimenters suggest that there should be no large effect of atmosphere on the release of fission products from melted $UO_2$. By using the distribution of transient-generated fission products found in experiment 2, adjusted for differences in transient energy, the transient-formed fission products in experiments 3 and 4 can be calculated and subtracted from the fission products formed during the preliminary irradiation. Table 1.13 shows the results of applying this correction to the distribution of fission products; Table 1.14 presents a summary of the corrected distribution of released material.

These tables show a consistent pattern of release and distribution of fission products from transient-heated $UO_2$ fuel. The corrections resulted in negative values or numbers with no significance for some locations because of the normal variation found in radiochemical analysis and because of minor experimental differences mentioned previously. Generally good agreement between experiments 3 and 4 is evident, and the materials having comparable volatilities such as I-Te-Cs, Sr-Ba, and Zr-Ce-$UO_2$ show consistent behavior.

UNCLASSIFIED
ORNL DWG. 64-9815

Table 1.13. Distribution of Fission Products in Experiments 3 and 4 with Transient-Formed Precursors Removed[a]

| | $^{131}I$ | $^{129}Te$ | $^{137}Cs$ | $^{106}Ru$ | $^{89}Sr$ | $^{140}Ba$ | $^{95}Zr$ | $^{144}Ce$ | $UO_2$ |
|---|---|---|---|---|---|---|---|---|---|
| | | | | Experiment 3 | | | | | |
| $UO_2$ fuel | 55 | 68 | 62 | 92 | 98 | 97 | 96 | 97 | 97 |
| Stainless steel cladding[b] | 5.5 | 12 | 0.58 | 0.035 | 0.55 | 0.41 | 0.53 | 0.56 | 0.36 |
| Alumina heater | 26 | 13 | 30 | 3.7 | 0.26 | 0 | 0.61 | 0.21 | 0.44 |
| Autoclave liner | 5.5 | 6.5 | 6.6 | 2.7 | 1.2 | 1.9 | 1.4 | 1.4 | 1.9 |
| Fuel autoclave walls | 5.8 | 0.78 | 0.93 | 1.5 | 0 | c | 1.0 | 0.92 | 0.86 |
| Aerosol-transport zone | 0.87 | 0.090 | 0.07 | 0 | 0 | 0.65 | 0.0005 | 0.0003 | 0.00066 |
| Filters | 0.036 | 0.012 | c | 0.0005 | c | c | 0 | c | 0 |
| Gas-collection autoclave | 0.27 | 0.0028 | 0.15 | 0.0002 | 0 | 0.05 | 0.0001 | c | 0.00014 |
| | | | | Experiment 4 | | | | | |
| $UO_2$ fuel | 59 | 72 | 69 | 98.8 | 98.4 | 97 | 99.4 | 99.8 | 99.3 |
| Stainless steel cladding[b] | c | 6.6 | 1.1 | 0.40 | 0.023 | c | 0.019 | 0.0071 | 0.00011 |
| Alumina heater | 24 | 14 | 25 | 0.81 | 0.68 | 0.63 | 0.55 | 0.17 | 0.59 |
| Autoclave liner | 8.2 | 4.7 | 3.7 | 0.043 | 0.42 | 0.89 | 0.073 | 0.073 | 0.062 |
| Fuel autoclave walls | 6.8 | 0.45 | 0.40 | 0.0043 | c | c | 0.0013 | c | 0.0053 |
| Aerosol-transport zone | 1.3 | 0.24 | 0.89 | 0.0016 | 0.35 | 1.2 | 0.0014 | 0.0019 | 0.00078 |
| Filters | 0 | 0.011 | 0 | 0.023 | c | c | 0.00013 | c | 0.00001 |
| Gas-collection autoclave | 0.08 | c | 0.33 | 0.0018 | 0.21 | c | 0.00007 | c | 0.00022 |

[a]Transient-formed fission products were subtracted using the distribution found in Experiment 2 and the amounts given in footnote (a) of Table 1.10. No correction was applied to $UO_2$.

[b]A nitric acid leach of the stainless steel was included in the "$UO_2$ fuel."

[c]The method of correction resulted in a negative value.

Table 1.14. Distribution of Material Released from Transient-Heated $UO_2$ with Transient-Formed Precursors Removed

| Release Zone | $^{131}I$ | $^{129}Te$ | $^{137}Cs$ | $^{106}Ru$ | $^{89}Sr$ | $^{140}Ba$ | $^{95}Zr$ | $^{144}Ce$ | $UO_2$ |
|---|---|---|---|---|---|---|---|---|---|
| | | | | Experiment 3 | | | | | |
| Total release from $UO_2$ fuel | 45 | 32 | 38 | 8 | 2 | 3 | 4 | 3 | 3 |
| Release from high-temperature zone | 7.0 | 0.88 | 1.2 | 1.5 | 0 | 0.7 | 1.0 | 0.92 | 0.86 |
| Transported release | 1.2 | 0.10 | 0.22 | 0.0007 | 0 | 0.7 | 0.0006 | 0.0003 | 0.0008 |
| | | | | Experiment 4 | | | | | |
| Total release from $UO_2$ fuel | 41 | 28 | 31 | 1.2 | 1.6 | 3 | 0.6 | 0.2 | 0.7 |
| Release from high-temperature zone | 8.2 | 0.70 | 1.6 | 0.031 | 0.56 | 1.2 | 0.003 | 0.002 | 0.006 |
| Transported release | 1.4 | 0.25 | 1.2 | 0.026 | 0.56 | 1.2 | 0.002 | 0.002 | 0.001 |

## CONCLUSIONS

Experiments 3 and 4 gave data for the release of fission products and fuel from transient-heated trace-irradiated stainless-steel-clad $UO_2$ in air-steam atmospheres. The fuel autoclave of experiment 3 contained 3 vol % steam, and experiment 4 contained enough water to provide equal volumes of steam and air when fully vaporized, although only approximately one-fifth of the water was vaporized at the beginning of the transient. No significant differences between these two experiments in which 75% of the $UO_2$ melted were observed. No special effect of the oxidizing steam-air atmospheres was noticed when the results and the specimens in experiments 3 and 4 were compared with those in experiments 1 and 2 conducted with an argon atmosphere in the fuel autoclave. This may have been due to the fact that a large fraction of the oxygen in the fuel autoclaves was consumed during experiments 3 and 4.

Interpretation of the data from experiments 3 and 4 was complicated by the presence of a mixture of fission products formed during the transient and during the pretransient irradiation. Corrections were made by subtracting the transient-formed fission product release values on the basis of the results of experiment 2. The corrected results show the behavior of aged fission products released from fuel during a reactor transient.

In these experiments the transient release of aged fission products from $UO_2$ was less than the release of fission products formed during the transient because the recently born fission products were more volatile than their daughters. A comparison of the transient release of aged fission products with the release of aged fission products by slow melting (Section 3) shows that the pattern of release is similar and that the percent release is in all cases less for transient heating. Release values for the low-volatility fission products Sr, Ba, Zr, and Ce correspond to the release of uranium in both types of experiments. Large fractions of the volatile fission products are released from the fuel, but most of these materials remain in the high-temperature zone. In the transient release experiments approximately one-third of the volatile fission products I, Te, and Cs were released from the fuel, but only 1% was released from the fuel autoclave.

# 1.3 Behavior of Fission Products Released During In-Pile Destruction of Reactor Fuels

W. E. Browning, Jr.
C. E. Miller, Jr.
R. P. Shields
B. F. Roberts

In-pile experiments of the type previously reported[6] are being continued to study the characteristics and behavior of fission products released during simulated reactor accidents. In these experiments fission products are released by melting miniature stainless-steel-clad $UO_2$ fuel elements in the ORR. Three additional experiments have been conducted and analyzed. Studies have been made of the effects of atmosphere and of sustained overheating below the melting point of $UO_2$ on the behavior of released fission products.

Previous experiments on the effects of gas velocity have shown that release of fission products from the fuel itself does not appear to be affected by flow rate over the linear velocity range 60 to 350 fpm. Release of fission products from the high-temperature zone, however, was affected by flow rate. The sweep gas in those experiments was helium. Two of the experiments described in detail in the following sections were performed to determine the effects of an oxidizing atmosphere with the expectation that changes in chemical form of fission products due to reaction with the atmosphere could affect the behavior of the released fission products and the release from the high-temperature zone.

The third experiment described in detail in the following sections was performed to study the effects of sustained overheating of the fuel below its melting point. This type of experiment simulates an accident where fuel cladding is melted but the fuel itself does not melt. Variations in release of fission products from the fuel as a function of temperature are expected. The behavior of the released fission products and their release from the high-temperature zone should be influenced more by atmosphere and other conditions outside of the fuel.

In all these experiments physical examination of the fuel residues and of other parts of the high-temperature zone yields valuable information. Inherent variation of fission power in a specific position of the reactor lattice over a period of many cycles causes a considerable spread in the maximum temperatures in the various experiments. Thus, in order to study the effects of a specific variable, those effects due to temperature variation must be recognized. Analysis of the physical appearance makes it possible to group experiments having similar temperature histories, and further interpretation of data can be made within these groups. Useful information can be obtained about the state of the atmosphere during meltdown and its effects on the materials. In addition, the physical conditions of fuel, cladding, and other visible materials can shed light on the behavior of the corresponding materials under the same conditions in reactor accidents. This information will assist in the construction of concepts of the sequence of events in the core during an accidental meltdown. Some features of the fuel region of the experimental assemblies which physically change with specific changes in conditions have been found to do so in reproducible ways. These features are appearance of fuel residue, position of stainless steel "dew line," form of cladding residue, size and color of "filter cake," and extent of cracking of parts. In the detailed sections to follow, some physical features of the experiment are described which have proved to be good indications of temperature history, of atmosphere conditions, and of the behavior of core materials under accident conditions.

## EFFECTS OF ATMOSPHERE ON BEHAVIOR OF RELEASED FISSION PRODUCTS

Experiments 12 and 13 were performed to study the effects of atmosphere on the release and behavior of fission products. Atmospheres of moist helium in the 12th experiment and moist air in the 13th experiment were used. The dew point was 23°C in each case. The fuel specimens were preirradiated for 48 hr to accumulate fission products,

[6] W. E. Browning, Jr., *et al.*, *Nucl. Safety Program Semiann. Progr. Rept. Dec. 31, 1963*, ORNL-3547, pp. 42–59.

and they were held near the melting temperature for 5 min.

### Moist Helium

Visual examination of the fuel specimen from experiment 12 showed that the fuel did not melt. However, it reached a slightly higher temperature than the fuel in experiment 7, which was run in dry helium. The stainless steel cladding from experiment 12 apparently was at least partially oxidized in the moist helium. These conclusions were reached by making the following comparisons between 12 and 7. Portions of the fuel cylinders from experiments 12 and 7 (Fig. 1.17) show that the cavity in the experiment 12 fuel is larger than that in the experiment 7 fuel, indicating a higher temperature in experiment 12. Portions of the fuel remaining in the $ThO_2$ holders are shown for comparison in Fig. 1.18 for experiments 12 and 7. A large amount of stainless steel cladding can be seen in the experiment 7 holder; only a few droplets can be seen in the experiment 12 holder. This also would indicate that the temperature was higher in experiment 12. Other evidence indicates that the cladding in experiment 12 perhaps reacted with the moisture in the helium. In an experiment such as 7, where the stainless steel is heated to high temperature, droplets of steel are found on most of the pieces of the high-temperature zone. In experiment 12 very little stainless steel could be found. Figure 1.19 shows for comparison the $ThO_2$ exit ports of the melting chamber from experiments 12 and 7. Shiny stainless steel droplets can be seen in the experiment 7 port, while none can be seen in the experiment 12 opened port.

Comparison of the radiochemical results of experiment 12 with those of experiment 7 shown in Table 1.15 shows that the presence of moisture in the atmosphere had no appreciable effect on the release of fission products from the fuel itself. The slight increase in release of nonvolatile fission products was probably due to the slightly higher temperature of the fuel in experiment 12. The release of iodine and tellurium from the high-temperature zone (Table 1.16) was increased when moisture was present in the atmosphere. The release of ruthenium decreased. The release of nonvolatile fission products did not change.

### Moist Air

Visual examination of experiment 13 in the hot cell showed that the fuel melted completely and that the stainless steel had been oxidized. As evidenced by the similarity in appearance of fuel residue, the fuel reached a temperature comparable

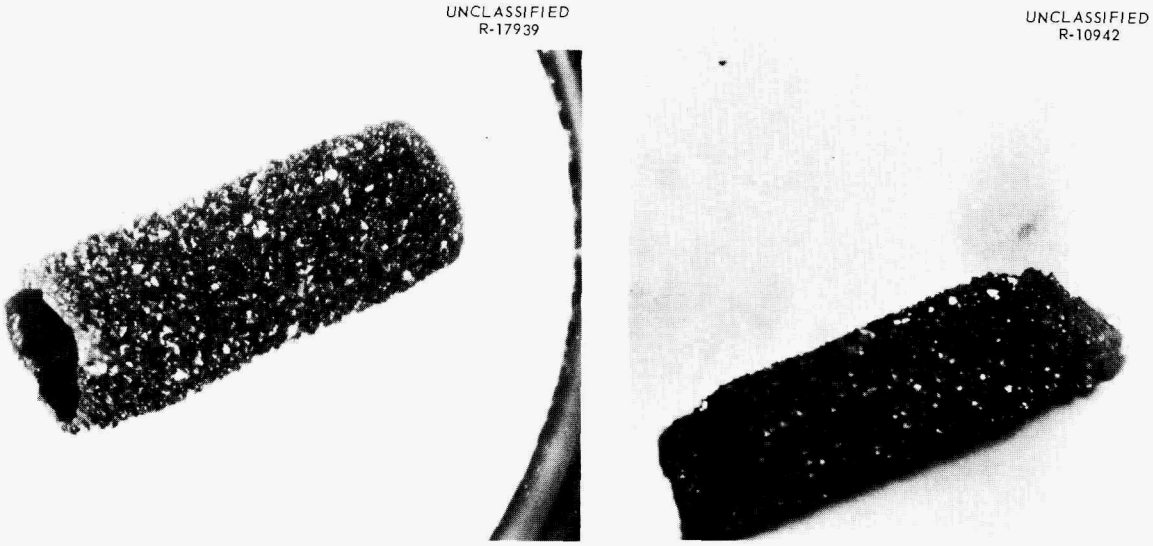


Fig. 1.17. Portions of $UO_2$ Fuel Cylinders from Experiments 12 (Left) and 7 (Right) for Comparison of Temperatures.

Fig. 1.18. $UO_2$ Fuel Remaining in Holders from Experiments 12 (Left) and 7 (Right) for Comparison of Temperatures.

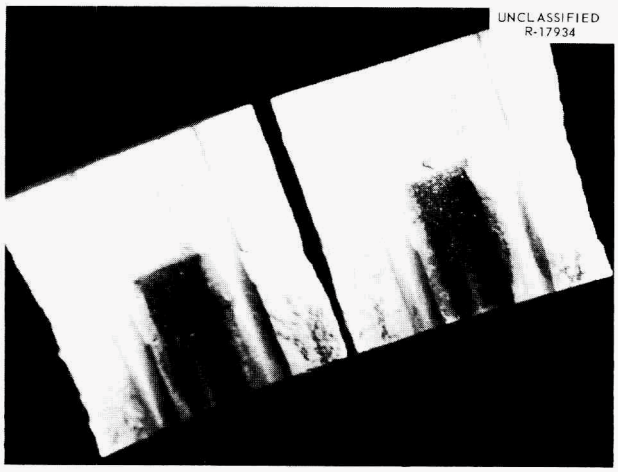


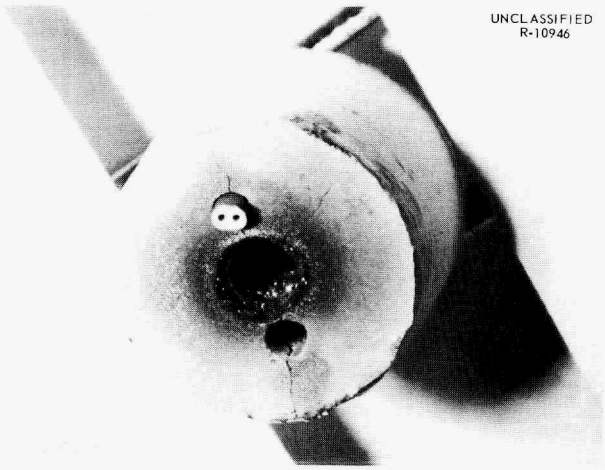


Fig. 1.19. Melting Chamber Exit Ports, Indicating Oxidation of Stainless Steel Cladding in Moist Helium Atmosphere in Experiment 12 (Left) Compared to Dry Helium in Experiment 7 (Right).

Table 1.15. Material Released from the Fuel in $UO_2$ Melting Experiments

| Experiment No. | Percent of $UO_2$ Melted | Atmosphere | Flow Rate (fpm) | Material Released (%) | | | | | | |
|---|---|---|---|---|---|---|---|---|---|---|
| | | | | $^{131}I$ | $^{132}Te$ | $^{137}Cs$ | $^{106}Ru$ | $^{89}Sr$-$^{140}Ba$ | $^{95}Zr$-$^{144}Ce$ | $UO_2$ |
| 7 | 0–20 | He | 60 | 96 | | 96 | 11 | 9.6 | 1.7 | 0.72 |
| 6, 8 | 80–90 | He | 60 | 99.0 | 96.5 | 99.0 | 58 | 55 | 52 | 42 |
| 4, 5, 9 | 100 | He | 60 | 99.6 | 99.2 | 98 | 88 | 71 | 57 | 49 |
| 10 | 97 | He | 125 | 97 | 96 | 96 | | 70 | 58 | 56 |
| 11 | 70–80 | He | 350 | 98 | 99.4 | 96 | 48 | 22 | 10 | 5.1 |
| 12 | 0–20 | $H_2O$-He | 60 | 94 | 88 | 92 | 24.4 | 14 | 3.7 | 1.8 |
| 13 | 100 | $H_2O$-air | 25 | 97 | 96 | 96 | 44 | 32 | 32 | 33 |
| 14 | 100 | $H_2O$-air, 100 min | 60 | 66 (Sn-Sb) | 63 (Sn-Sb) | 73 (Xe) | 64 | 45 (Kr-Xe) | 21 (Y-Ce) | 20 |

Table 1.16. Material Released from High-Temperature Zone of the Furnace in $UO_2$ Melting Experiments

| Experiment No. | Percent of $UO_2$ Melted | Atmosphere | Flow Rate (fpm) | Material Released (%) | | | | | | |
|---|---|---|---|---|---|---|---|---|---|---|
| | | | | $^{131}I$ | $^{132}Te$ | $^{137}Cs$ | $^{106}Ru$ | $^{89}Sr$-$^{140}Ba$ | $^{95}Zr$-$^{144}Ce$ | $UO_2$ |
| 7 | 0–20 | He | 60 | 50 | 12 | 74 | 2.0 | 0.72 | 0.19 | 0.015 |
| 6, 8 | 80–90 | He | 60 | 94 | 67 | 85 | 1.4 | 0.90 | 0.11 | 0.16 |
| 4, 5, 9 | 100 | He | 60 | 86 | 85 | 70 | 5.0 | 1.5 | 0.25 | 0.11 |
| 10 | 97 | He | 125 | 89 | 72 | 81 | | 2.4 | 1.9 | 0.29 |
| 11 | 70–80 | He | 350 | 89 | 80 | 88 | 0.15 | 5.4 | 0.88 | 1.6 |
| 12 | 0–20 | $H_2O$-He | 60 | 86 | 63 | 71 | 0.21 | 0.79 | 0.24 | 0.18 |
| 13 | 100 | $H_2O$-air | 50 | 95 | 95 | 92 | 22 | 1.4 | 0.75 | 1.1 |
| 14 | 100 | $H_2O$-air, 100 min | 60 | 49 (Sn-Sb) | 42 (Sn-Sb) | 49 (Xe) | 45 | 2.1 (Kr-Ze) | 3.8 (Y-Ce) | 5.0 |

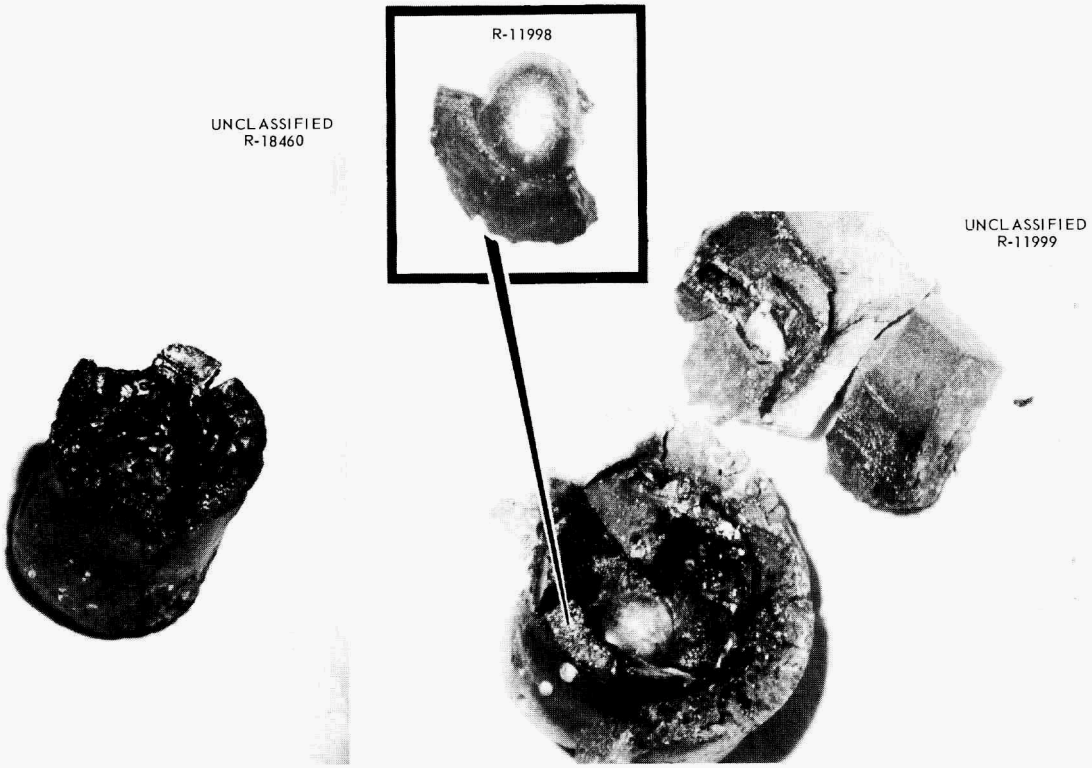


Fig. 1.20. $UO_2$ Fuel Residues After In-Pile Melting in Moist Air of Experiment 13 (Left) and in Helium, Experiment 9 (Right).

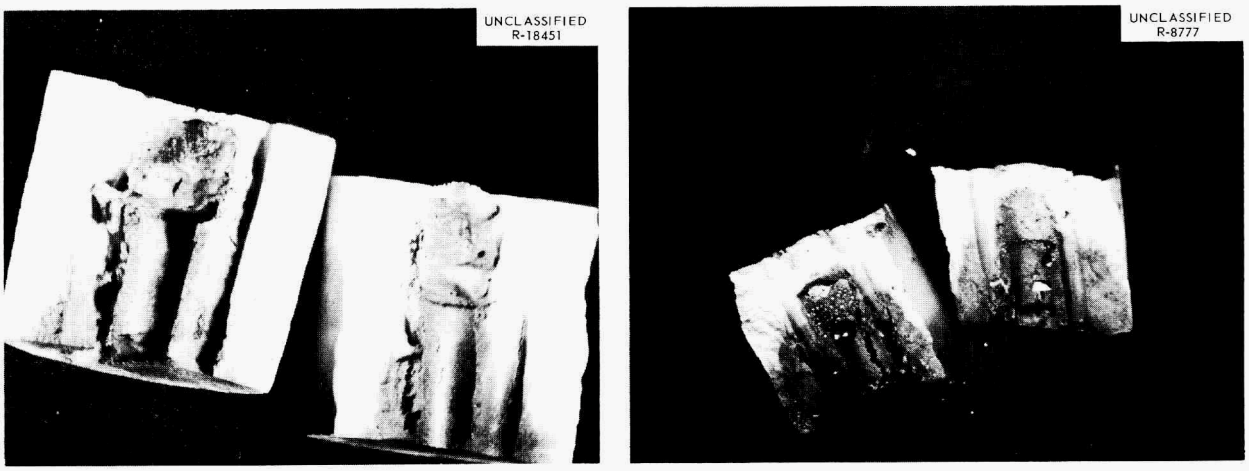


Fig. 1.21. Melting Chamber Exit Ports, Indicating Oxidation of Stainless Steel Cladding in Moist Air in Experiment 13 (Left) Compared to Helium in Experiment 4 (Right).

to that of experiments 4, 5, and 9, all of which were run in dry helium. Figure 1.20 shows the $ThO_2$ holders and fuel remains for experiments 13 and 9. A shiny drop of stainless steel which had apparently refluxed can be seen in the experiment 9 holder. No droplets of steel were found in experiment 13. Figure 1.21 shows the comparison of the $ThO_2$ exit ports from the melting chamber in experiments 13 and 4. Again, the absence of metallic droplets indicates that the stainless steel has been oxidized.

Comparison of the radiochemical results of experiment 13 with those of experiments 4, 5, and 9 shows that the air atmosphere had no effect on the fraction of strontium, barium, zirconium, and cerium remaining in the fuel itself. There was also no change in the release of volatile fission products from the fuel. The amount of $UO_2$ transported from the fuel zone was reduced (Table 1.15). The release of iodine, tellurium, and cesium from the high-temperature zone was increased in moist air. The distribution of iodine in experiment 13 indicated that it was in the elemental form, having been oxidized by the air atmosphere, and was able to penetrate the filters but was retained by the charcoal. This is discussed further in a later section. Ruthenium was released to a greater extent. There was no change in the release of strontium, barium, zirconium, and cerium.

## EFFECTS OF SUSTAINED OVERHEATING IN MOIST AIR

Experiment 14 was performed to study the effect of long irradiation at high temperature on the behavior and release of fission products. The fuel in this experiment was not preirradiated but was held at a temperature above the melting point of the stainless steel cladding but below the melting point of $UO_2$ for 105 min. The sweep gas was moist air having a dew point of 23°C. Visual examination showed that the fuel appeared to have melted, contrary to all indications that the fuel temperature was below the melting point of $UO_2$. Figure 1.22 shows the appearance of a part of the fuel and holder in the $ThO_2$ cylindrical side wall of the melting chamber. This figure may be compared with Fig. 1.20, which shows the fuel residues and holders from experiments 13 and 9. The fuel was completely destroyed in each case. No stainless steel droplets were found in the experiment 14 melting chamber. A comparison of the temperatures of the fuel may be made by comparing the appearance of the melting chamber exit ports from experiment 12 (Fig. 1.19, left), experiment 13 (Fig. 1.21, left), and experiment 14, shown in Fig. 1.23. The temperature of the fuel in experiment 12, which was run in moist helium, was well below the melting point of $UO_2$, while the temperature of the fuel in experiment 13, which was run in moist air, was above the melting point of $UO_2$. On comparing the exit ports and considering the longer period of heating, it appears that the temperature of the fuel in experiment 14 was less than that in experiment 12. Thermocouples which survived in experiment 14 also indicated that the temperature was less than that in experiment 12.

The apparent melting of the fuel in moist air at a temperature well below the melting point of $UO_2$ in experiment 14 is of potential significance in predicting the movement of fuel in reactor accidents. A possible explanation can be developed by considering the liquidus curves for mixtures of $UO_2$ and oxides of the metal components of stainless steel. These curves are not available directly from the literature, but their general nature may be inferred by reference to available data for mixtures with $ZrO_2$, which is similar to $UO_2$ in many respects. Figure 1.24 illustrates this similarity for $Al_2O_3$ for which data are available[7] on both the $UO_2$ and the $ZrO_2$ systems. Aluminum oxide is also similar to $Fe_2O_3$, which is of principal interest here. Figure 1.25 shows the liquidus curves for mixtures of $ZrO_2$ with the oxides of iron, chromium, and nickel, the constituents of stainless steel.[8] Also shown in Fig. 1.25 is a single point which has been reported for the system $UO_2$-$Fe_2O_3$ (ref. 9). Of these oxides, $Fe_2O_3$ has the most pronounced effect; as little as 25 mole % could depress the melting point to 2000°C. The fuel residue shown in Fig. 1.22 may consist of a relatively low-melting flux of $UO_2$-$Fe_2O_3$ with the undissolved excess of $UO_2$ dispersed as fine grains. This material would be expected to have a

[7] E. M. Levin, H. F. McMurdie, and F. P. Hall, *Phase Diagrams for Ceramicists*, part I (1956), Figs. 121 and 149, American Ceramic Society, Columbus, Ohio, 1956.

[8] E. M. Levin *et al.*, *ibid.*, part I (1956), Figs. 148 and 149, and part II (1959), Fig. 1035.

[9] S. G. Tresvyatskii and V. I. Kushakovskii, *At. Energ.* **8**, 56–8 (1960).

UNCLASSIFIED
R-19115

Fig. 1.22. Residue of Stainless-Steel-Clad $UO_2$ Fuel Element Overheated in Experiment 14 for 105 min in Moist Air Below the Melting Point of $UO_2$, Indicating Reaction with Oxidized Cladding.

slushy consistency and may not flow rapidly from the overheated part of a reactor core, but at the same time it could release fission products readily.

The results of radiochemical analyses of experiment 14 are given in Tables 1.15 and 1.16. These results should not be compared directly with those of other experiments since there were no aged fission products present in the experiment 14 fuel. The results depend upon the precursor form of the fission product rather than the analyzed form. By comparing the results of experiment 14 with those of experiment 13, selected because of similar atmospheres and similar extent of fuel destruction, the effects of precursors may be seen. The release of iodine and tellurium from the fuel itself was reduced (Table 1.15). These elements have nonvolatile precursors (tin and antimony). The release of cesium, strontium, and barium occurred as volatile precursors (xenon and krypton). Other fission products, such as zirconium and cerium, and the transported fuel were released to the small degree expected for a maximum fuel temperature

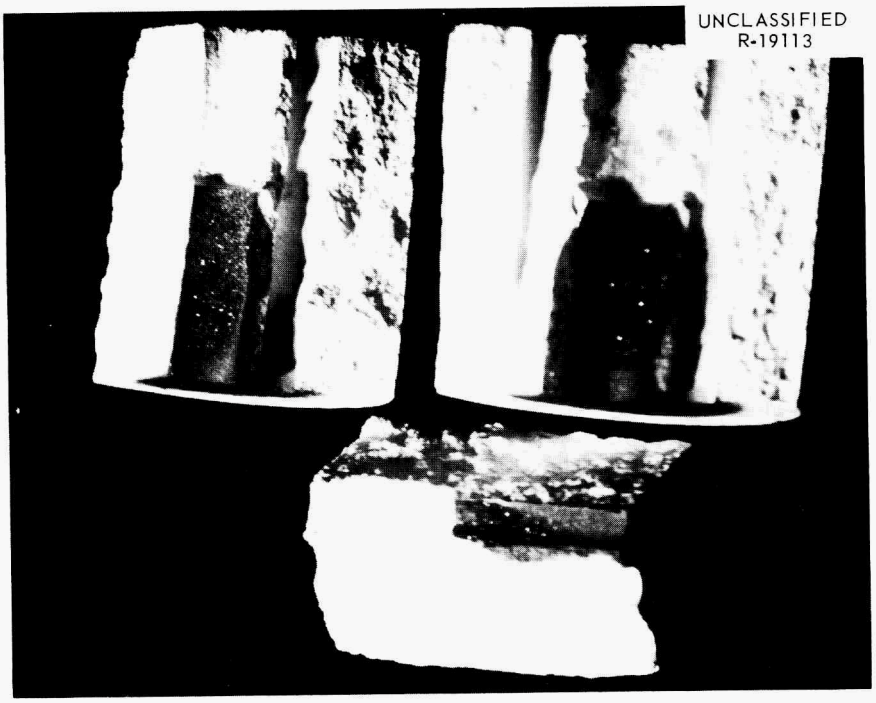


Fig. 1.23. Melting Chamber Exit Port from Experiment 14, Stainless-Steel-Clad $UO_2$ Overheated in Moist Air for 105 min.

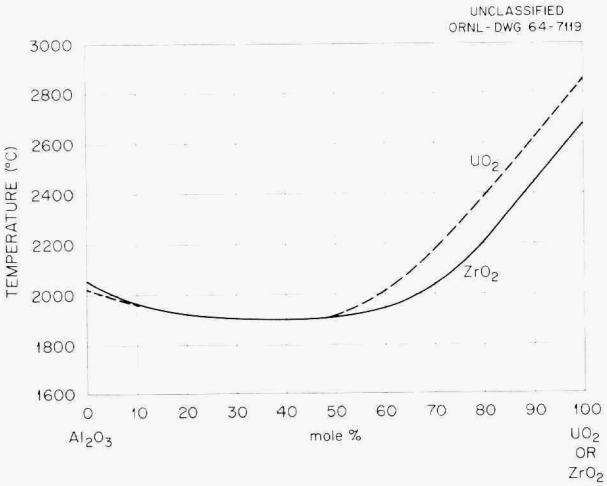


Fig. 1.24. Comparison of Liquidus Curves of the Systems $Al_2O_3$-$UO_2$ and $Al_2O_3$-$ZrO_2$ to Justify the Use of $ZrO_2$ as a Stand-In for $UO_2$ in Phase Diagrams.

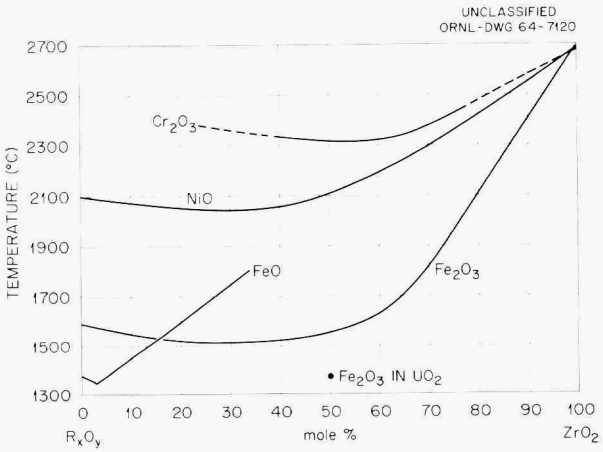


Fig. 1.25. Depression of Melting Point of $ZrO_2$, a Stand-In for $UO_2$, by Oxides of Stainless Steel.

less than that of experiment 12, but for a longer duration. The release of fission products from the high-temperature zone (Table 1.16) again indicates the effects of precursors and the long time period. The iodine and tellurium release was lower than in other experiments, again because the precursor elements actually released were nonvolatile. The strontium and barium release was higher, and large fractions of these elements were found in the filter section. The high release of zirconium, cerium, and $UO_2$ fuel is believed to be due to the long time period of sweeping.

Samples of the gas penetrating the filters and adsorbers in this experiment were analyzed by gamma spectrometry, and the results are discussed separately in a subsequent section.

## EQUIPMENT FOR IN-PILE MELTING OF STAINLESS-STEEL-CLAD $UO_2$ IN A HIGH-CONCENTRATION STEAM ATMOSPHERE

Most present-day nuclear power reactors use pressurized water as a coolant, and during a reactor accident, at least initially, the fuel would be exposed to an atmosphere of steam. In previous experiments miniature $UO_2$ fuel elements have been melted in-pile in helium, air, moist helium, and moist air atmospheres to investigate the behavior of released fission products. In the series of experiments now being started, the fuel will be melted in the presence of steam to simulate conditions in a water-cooled reactor during an accident. The use of a steam atmosphere has necessitated considerable modification of the present equipment to provide controlled steam injection, to prevent premature condensation, and finally to condense the steam.

The problem of supplying the steam at a controlled rate was solved by designing an injector which will supply water at 0.28 $cm^3$/min. This, when evaporated and added to the 50 $cm^3$/min of air, produces a 90% steam–10% air mixture flowing at the rate of 400 $cm^3$/min, which is normally used in the in-pile meltdown experiments. The water injector, Fig. 1.26, consists of a 1-in.-ID cylinder with highly polished inside walls and a piston with an O-ring seal. The piston is driven by a screw that is turned by a gear. The unit is mounted vertically so that any air in the system

UNCLASSIFIED
PHOTO 66647

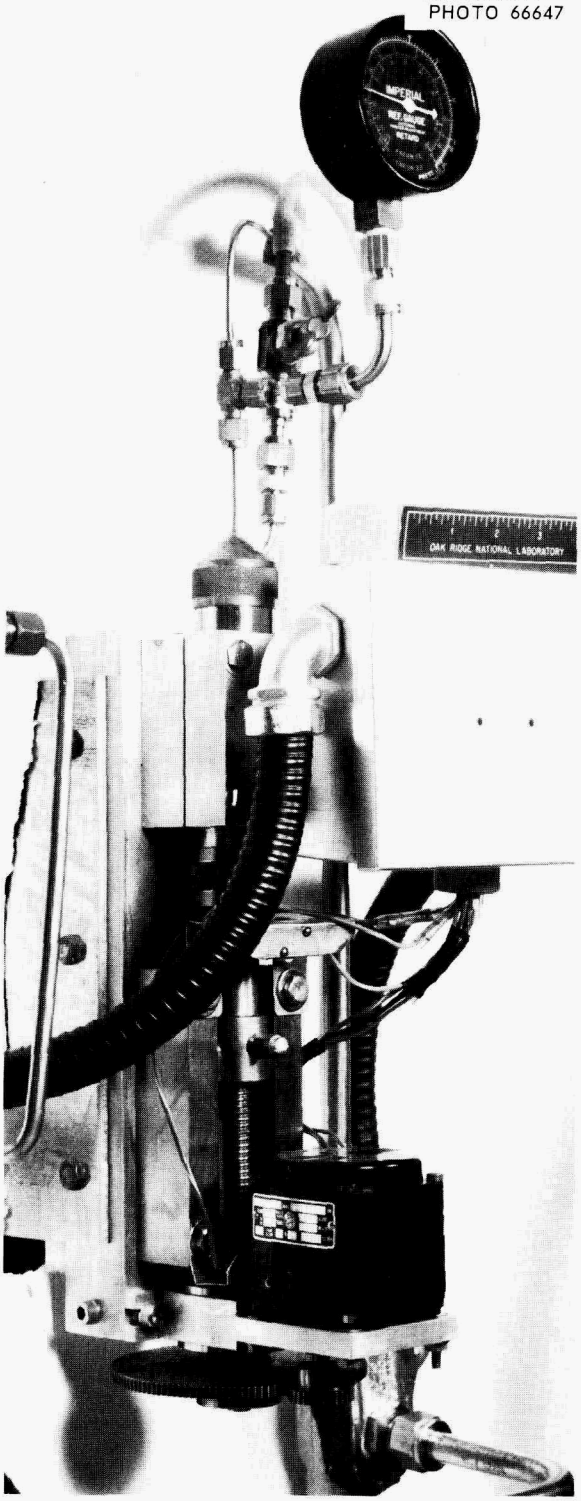


Fig. 1.26. Water Injector for Generating Steam at a Controlled Rate During In-Pile Melting of $UO_2$.

collects in the cone-shaped upper end of the cylinder, where it can be discharged through a $\frac{1}{8}$-in. tube and valve. It is necessary to remove air from the entire injection system so that it cannot compress during a temporary blockage and then cause delivery of water at too high a rate. The delivery tube for the water is a $\frac{1}{16}$-in. stainless steel tube to within 5 ft of the furnace. Here it is changed to a 0.035-in. capillary, which penetrates the $\frac{1}{8}$-in. gas inlet line and continues concentrically with the gas line to a point inside the furnace. A small tube is used so that steam formation above the outlet cannot suddenly cause the delivery of a large pulse of water. Water is not admitted until the furnace is above 100°C so that the water will evaporate as fast as it enters to cause a constant vapor flow through the furnace and out the gas exit tube.

In all the in-pile experiments the gas exit tube has served the dual functions of a delivery tube which transports released fission products to the filters and of a diffusion tube which provides analytical information relative to particle size and to the activities associated with the particles. In the experiments using a steam atmosphere, it is mandatory that the temperature over the full 40-in. length of this tube remain above 100°C to prevent the condensation of water in the tube. Premature condensation could have two adverse effects: (1) allow the return of water into the furnace with a consequent pulsation of sweep and possible damage to the containment and (2) disturb the particle deposits in the diffusion tube. The necessary temperature is maintained by surrounding the exit tube with a steam jacket in the form of a flexible metal hose. Figure 1.27 shows the assembly which was developed. Steam for the jacket is provided by heating water in the lower part of the jacket with a platinum-wound heater. The air is eliminated from the jacket by heating the water to the boiling point; this causes the air to be driven into the top of the jacket, where it can be released. When all air is removed, three thermocouples monitoring the top, middle, and bottom of the exit tube read the same at all power levels. The possibility of cold spots where condensate could form is thus eliminated. The isothermal condition gives added dividends when analyzing the diffusion tube data because it eliminates the possibility of temperature effects along the tube.

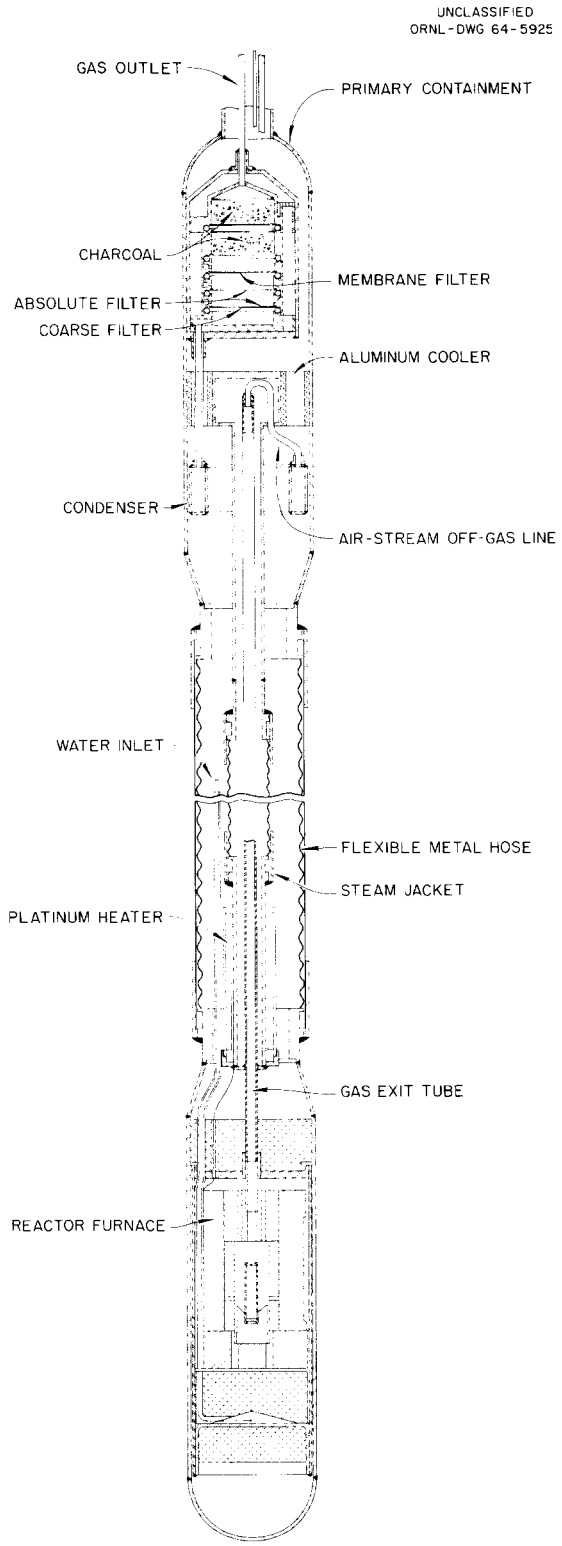


**Fig. 1.27. Experimental Assembly for Controlling Condensation During In-Pile Melting of $UO_2$.**

Heat balance for the steam jacket system is a compromise between keeping the heater power required in the retracted position low and providing sufficient heat dissipation to keep the jacket pressure at a safe level during full insertion into the reactor core. The platinum-wound heater at the base of the steam jacket maintains the temperature while the experiment is retracted. With the experiment inserted, approximately 300 w of gamma heat is generated. To dissipate heat, an aluminum block is mounted on the top of the steam jacket, and, when its temperature increases, it fits tightly against the wall of the secondary container which is maintained at reactor water temperature. A recording potentiometer responding to a thermocouple inside the steam jacket turns off the heater power when the temperature reaches 120°C. If the temperature reaches 225°C (300 psia in the steam jacket), the experimental assembly is retracted automatically as a safety measure. This steam jacket, supplying its own steam produced by the heater and dissipating gamma heat automatically, provides an efficient and safe way to maintain the exit tube at a predetermined isothermal temperature.

The water vapor in the sweep gas, leaving the steam jacket region, must be condensed and separated from the air. The condenser is an annular can 2.5 in. OD and $1\frac{3}{4}$ in. ID designed to make good contact with the water-cooled secondary wall. Stainless steel inlet and outlet tubes $\frac{1}{8}$ in. in diameter penetrate the top at a 45° angle and continue halfway around the inside circumference, to prevent direct drainage of the condensate when the experiment is laid in a horizontal position in the hot cells. These tubes are silver soldered to the inside wall to provide the heat dissipation necessary to condense the vapor. The condenser must be located below the top of the steam jacket as shown in Fig. 1.27 to avoid return of condensate at the furnace. Uncondensed gas passes from the condenser to the filter package. Measurement of the fission products retained in the condenser will give valuable information which will help in understanding the behavior of fission products during steam condensation under reactor accident conditions.

The operation of the experiment revised for steam atmosphere is only slightly different from the usual operating procedure. Irradiation of the fuel prior to melting is done using helium as the sweep gas to protect cladding and other parts from corrosion. Before inserting to melt the $UO_2$, the sweep is changed to air, and, after the temperatures are constant and above 100°C everywhere in the primary container of the furnace and in the exit tube, the air flow is reduced to 50 $cm^3$/min and the water injector is started. A flow of water vapor is indicated by a thermocouple on the condenser inlet line. Without water vapor flow the temperature is 50 to 60°C, and as soon as condensate starts through the tube, it increases to 100°C. With this sweep flow at 400 $cm^3$/min (350 $H_2O$–50 air) the experiment is inserted all the way into the lattice to melt the $UO_2$. As the experiment is being retracted, the water injector is shut off and the air flow is replaced by helium; after 10 min of helium sweep the heater power to the steam jacket is turned off.

Simultaneously with the modifications just described, the design of the filter unit was also changed to include several improvements: (1) to provide means of testing each filter in place, (2) to make changes for easier handling in the hot cell, and (3) to increase filter area. Special ports, which are accessible after mounting of the filters and which can be sealed after testing, are provided before and after each filter. Testing the filters consists in drawing air with a known particle content in through one port, through the filter, and out the port above the filter. A condensation nucleus particle detector is used for determination of particle concentrations. The percentage of particles stopped is a measure of filter efficiency. The filter parts and the assembled unit are shown in Fig. 1.28. The capability for in-place testing of the filters makes it possible to detect and eliminate leaks which might otherwise diminish filter efficiencies indicated for released fission products.

One in-pile experiment has been conducted in which a miniature stainless-steel-clad $UO_2$ fuel element was melted in a high-concentration steam atmosphere with a small amount of air. The experimental assembly has been disassembled and examined in the hot cells. The $UO_2$ was fully melted, and no metallic stainless steel was found. Radioassay of the samples from this experiment is in progress, and the results are expected to help to predict the behavior of fission products in an accidental meltdown in a water-cooled reactor.

Fig. 1.28. In-Pile Filter Package, Modified to Permit In-Place Testing.

## RETENTION OF RELEASED FISSION PRODUCTS PRODUCED BY COMPONENTS OF THE OFF-GAS SYSTEM

The amounts of released fission products and uranium collected by the relatively cold wall surrounding the furnace, the diffusion tube, the filters, the charcoal adsorber, and other parts of the off-gas system are determined by radiochemical analysis for each in-pile fuel destruction experiment. These parts simulate various components which would be encountered by released fission products as they would be carried from the melted fuel to the containment vessel and into a filter-adsorber system in an actual reactor accident. From these radioassay data an estimate of the effectiveness of the components of the gas-cleaning system can be obtained. The amounts of material found downstream from the fuel and from the high-temperature zone, expressed as percent of the total inventory of that material, are the release data which have been presented previously for experiments where $UO_2$ was melted[6] and where uranium carbide–graphite fuel was burned.[10] The present discussion concerns material found downstream of selected components of the off-gas system. Table 1.17 shows the amount of each material downstream of the diffusion tube also expressed as percent of the total inventory of that material. The difference between a value in this table and the corresponding value in tables of material released from the high-temperature zone of the furnace gives the fraction of the inventory deposited on the cool metal surfaces of the furnace chamber and the diffusion tube. These components simulate the reactor vessel and pipes leading to the containment vessel of an actual reactor. A comparison of these data so calculated with the data on the release from the high-temperature zone of the furnace generally shows similar values for the nonvolatile ruthenium, strontium, barium, zirconium, cerium, and uranium. On the other

[10] W. E. Browning, Jr., *et al.*, *Nucl. Safety Semiann. Progr. Rept. June 30, 1963*, ORNL-3483, pp. 22–26.

**Table 1.17. Material Found Downstream of the Diffusion Tube**

Expressed as percent of the total inventory of material

| Experiment[a] | Conditions[b] | $^{131}I$ | $^{132}Te$ | $^{137}Cs$ | $^{106}Ru$ | $^{89}Sr$ | $^{140}Ba$ | $^{95}Zr$ | $^{144}Ce$ | U |
|---|---|---|---|---|---|---|---|---|---|---|
| G-1 | Burned in air | 9 | 13 | 24 | 35 | 1.0 | 0.39 | 0.59 | 5.2 | 0.30 |
| G-3 | Burned in air | 7 | 5.2 | 15 | 2.1 | 0.8 | 0.44 | 0.23 | 0.8 | 0.048 |
| 2 | He atm | | | 6 | 0.1 | 7.1[c] | 7–11[c] | 0.026 | 0.16 | 1.4 |
| 3 | He atm | 4.4 | | 14 | 0.5 | 0.37 | 0.26 | 0.09 | 0.032 | 0.0023 |
| 4 | He atm | 26 | 28 | 22 | 3 | 1.3 | 0.46 | 0.01 | 0.1 | 0.029 |
| 5 | He atm | 47 | 51 | 41 | 2.6 | 1.1 | 1.3 | 0.014 | 0.18 | 0.10 |
| 6 | He atm | 55 | 32 | 32 | 0.7–1.3 | 0.39 | 0.30 | 0.09 | 0.034 | 0.021 |
| 7 | He atm | 0.7 | 4.4 | 3.5 | 0.9 | 0.50 | 0.35 | 0.012 | 0.17 | 0.0051 |
| 8 | He atm | 11 | 23 | 14 | 1.2 | 0.57 | 0.071 | 0.018 | 0.17 | |
| 9 | He atm | 43 | 14 | 32 | 3.6 | 0.50 | 0.29 | 0.047 | 0.12 | 0.0050 |
| 10 | High flow He | 53 | 29 | 33 | 0.005–0.009 | 0.9 | 1.0 | 2.1 | 0.23 | 0.10 |
| 11 | Very high flow He | 39 | 30–50 | 26 | 0.03–0.07 | 0.8 | 1.7 | 0.011 | 0.26 | 0.15 |
| 12 | Moist He | 42 | 33 | 32 | 0.13 | 0.38 | 0.15 | 0.0035 | 0.029 | 0.007 |
| 13 | Moist air | 70 | 36 | 35 | 6.1 | 0.56 | 0.34 | 0.22 | 1.0 | 0.20 |
| 14 | Not preirradiated; moist air, 105 min | 32[c] | 17[c] | 35[c] | 3.7 | 14[c] | 9[c] | 0.034[c] | 1.3 | 1.4 |

[a]"G" prefix indicates experiments with uranium carbide–graphite fuel. Others were with $UO_2$.

[b]Duration was 5 min except where noted otherwise.

[c]Reflects behavior of precursors.

**Table 1.18. Material Found Downstream of the Diffusion Tube**

Expressed as percent of that released from the high-temperature zone of the furnace

| Experiment[a] | Conditions[b] | $^{131}I$ | $^{132}Te$ | $^{137}Cs$ | $^{106}Ru$ | $^{89}Sr$ | $^{140}Ba$ | $^{95}Zr$ | $^{144}Ce$ | U |
|---|---|---|---|---|---|---|---|---|---|---|
| G-1 | Burned in air | 33 | 38 | 65 | 87 | 84 | 78 | 85 | 82 | 80 |
| G-3 | Burned in air | 49 | 37 | 35 | 40–60 | 61 | 65 | 18 | 28 | 28 |
| 2 | He atm | | | 29 | 3 | 34[c] | 39[c] | 22 | 27 | 36 |
| 3 | He atm | 9 | | 30 | 84 | 30 | 35 | 70–90 | 1.8 | 4.5 |
| 4 | He atm | 28 | 61 | 51 | 50–70 | 56 | 49 | 20–40 | 20–40 | 38 |
| 5 | He atm | 54 | 63 | 50 | 51 | 76 | 58 | 73 | 55 | 44 |
| 6 | He atm | 58 | 61 | 39 | 96 | 42 | 55 | 97.0 | 50 | 7 |
| 7 | He atm | 1.4 | 38 | 4.7 | 30–50 | 58 | 60 | 33 | 52 | 34 |
| 8 | He atm | 12 | 29 | 16 | 71 | 45 | 9 | 35 | 69 | |
| 9 | He atm | 53 | 16 | 55 | 94 | 52 | 26 | 38 | 41 | 39 |
| 10 | High flow He | 60 | 40 | 41 | 4–8 | 43 | 35 | 74 | 22 | 35 |
| 11 | Very high flow He | 44 | 50 | 30 | 20–40 | 28 | 21 | 1.9 | 21 | 9 |
| 12 | Moist He | 48 | 53 | 45 | 63 | 37 | 27 | 1.6 | 12 | 3.6 |
| 13 | Moist air | 73 | 38 | 38 | 28 | 47 | 22 | 62 | 91 | 19 |
| 14 | Moist air, 105 min; not preirradiated | 65[c] | 41[c] | 72[c] | 8 | 57[c] | 56[c] | 1.2[c] | 27 | 28 |

[a] "G" prefix indicates experiments with uranium carbide–graphite fuel. Others were with $UO_2$.

[b] Duration was 5 min except where noted otherwise.

[c] Reflects behavior of precursors.

Table 1.19. Material Found Downstream of First Intact High-Efficiency Filter

Expressed as percent of the total inventory of material

| Experiment[a] | Conditions[b] | $^{131}I$ | $^{132}Te$ | $^{137}Cs$ | $^{106}Ru$ | $^{89}Sr$ | $^{140}Ba$ | $^{95}Zr$ | $^{144}Ce$ | U |
|---|---|---|---|---|---|---|---|---|---|---|
| G-1 | Burned in air, 15 min | 5.4 | 0.067 | 21 | 25 | 0.43 | 0.26 | 0.31 | 4.9 | 0.17 |
| G-3 | Burned in air, 15 min | 1.5 | 0.07 | 14 | 1.1 | 0.47 | 0.38 | 0.18 | 0.7 | |
| 2 | He atm, 10 min | | | 0.13 | 0–0.10 | 0.008[c] | 4[c] | 0.005 | 0.024 | |
| 3 | He atm | 0.8 | | 10 | 0.002–0.010 | 0.19 | 0.019 | 0.0037 | 0.011 | 0.003 |
| 5 | He atm | 3.5 | 0.4 | 19 | 2.3 | 0.63 | 0.22 | 0.008 | 0.13 | 0.008 |
| 6 | He atm | 15 | 22 | 12 | 0.66 | 0.20 | 0.18 | 0.08 | 0.027 | 0.012 |
| 7 | He atm | 0.16 | 0.06 | 2.9 | 0.7 | 0.48 | 0.32 | 0.012 | 0.16 | 0.0051 |
| 9 | He atm | 2.8 | 12 | 4.2 | 1.3 | 0.25 | 0.13 | 0.013 | 0.035 | 0.0033 |
| 10 | High flow He | 1.3 | 0.022 | 2.5 | 0.0011 | 0.23 | 0.23 | 1.2 | 0.13 | 0.008 |
| 11 | Very high flow He | 2.9 | 0.19 | 2.7 | 0.022 | 0.023 | 0.17 | 0.0011 | 0.017 | 0.0006 |
| 12 | Moist He | 0.81 | 0.111 | 1.1 | 0.06 | 0.15 | 0.053 | 0.0030 | 0.022 | 0.005 |
| 13 | Moist air | 45 | 0.61 | 1.0 | 0.02–0.06 | 0.071 | 0.11 | 0.0012 | 0.019 | 0.002 |
| 14 | Not preirradiated; moist air, 105 min | 1.5[c] | 2.7[c] | 26[c] | 0.32 | 5.9[c] | 7[c] | 0.0063[c] | 0.16 | 0.12 |

[a] "G" prefix indicates experiments with uranium carbide–graphite fuel. Others were with $UO_2$.

[b] Duration was 5 min except where noted otherwise.

[c] Reflects behavior of precursors.

Table 1.20. Material Found Downstream of First Intact High-Efficiency Filter

Expressed as percent of that released from the high-temperature zone of the furnace

| Experiment[a] | Conditions[b] | $^{131}I$ | $^{132}Te$ | $^{137}Cs$ | $^{106}Ru$ | $^{89}Sr$ | $^{140}Ba$ | $^{95}Zr$ | $^{144}Ce$ | U |
|---|---|---|---|---|---|---|---|---|---|---|
| G-1 | Burned in air, 15 min | 20 | 0.19 | 58 | 61 | 35 | 51 | 67 | 79 | 47 |
| G-3 | Burned in air, 15 min | 10.6 | 0.5 | 33 | 20–40 | 35 | 56 | 14 | 24 | |
| 2 | He atm, 10 min | | | 0.60 | 1 | 0.036[c] | 18[c] | 0.4 | 4.0 | |
| 3 | He atm | 1.5 | | 20 | 0.3–1.5 | 15 | 2.6 | 3.5 | 0.6 | 0.0 |
| 5 | He atm | 3.9 | 0.5 | 24 | 45 | 44 | 10 | 41 | 41 | 3.4 |
| 6 | He atm | 15 | 42 | 14 | 50–90 | 22 | 33 | 94.8 | 40 | 40 |
| 7 | He atm | 0.32 | 0.6 | 3.9 | 20–40 | 56 | 55 | 33 | 49 | 34 |
| 9 | He atm | 3.5 | 13 | 7.2 | 33 | 26 | 11 | 10 | 12 | 26 |
| 10 | High flow He | 1.4 | 0.031 | 3.1 | 0.9 | 11 | 8 | 42 | 13 | 2.7 |
| 11 | Very high flow He | 3.3 | 0.24 | 3.1 | 14 | 0.77 | 2.1 | 0.20 | 1.4 | 0.037 |
| 12 | Moist He | 0.9 | 0.18 | 1.6 | 29 | 15 | 9 | 1.4 | 9 | 3.0 |
| 13 | Moist air | 47 | 0.64 | 1.1 | 0.2 | 6.0 | 7.0 | 0.33 | 1.7 | 0.2 |
| 14 | Not preirradiated; moist air, 105 min | 3.0[c] | 6.3[c] | 53[c] | 0.72 | 23[c] | 39[c] | 0.23[c] | 3.4 | 2.3 |

[a]"G" prefix indicates experiments with uranium carbide–graphite fuel. Others were with $UO_2$

[b]Duration was 5 min except where noted otherwise.

[c]Reflects behavior of precursors.

hand, these data for tellurium and cesium are usually considerably smaller and are much smaller for iodine than are the corresponding data on release from the high-temperature zone. These results reflect the fact that much iodine deposits on the cool metal surface of the reactor furnace and considerable iodine, tellurium, and cesium deposit in the diffusion tube. In experiment 13, iodine was probably oxidized by the air to elemental vapor and thus was not deposited on the metal surfaces as in previous experiments. In experiment 14 the fuel was not preirradiated to build up fission products, and mass numbers 89 and 140 were released as volatile precursors while mass 131 was retained because its precursor is nonvolatile.

In Table 1.18, the material downstream of the diffusion tube is expressed as a percentage of the amount of that material released from the high-temperature zone of the furnace. The data are displayed in this form in order to show explicitly the effectiveness of the components of the off-gas system between the high-temperature zone of the furnace and the far end of the diffusion tube for the retention of released fission products. The isotopes which show greatest release from the high-temperature zone also are the ones which are retained to the greatest extent on the cold wall of the furnace and in the diffusion tube. Although there is wide variation, generally less than half of the material released from the high-temperature zone of the furnace is found downstream of the diffusion tube.

Table 1.19 shows the amounts of material found downstream of a "high-efficiency" filter expressed as percent of total inventory of that material, and Table 1.20 shows the same quantities expressed as percent of that material released from the high-temperature zone of the furnace. Only data for filters which remained intact during the entire experimental run are presented. Where an experimental assembly contained more than one such filter, data for the initial one are shown. The "high-efficiency" filter material is either Gelman type E glass, HV-70, or Flanders F-700. The difference between values in one of these tables and those in the corresponding tables of materials downstream of the diffusion tube gives the fraction of material deposited on the "high-efficiency" filter and, in many experiments, also on a roughing filter. From Table 1.19, it is seen that only very small fraction of the total inventory of nonvolatile elements (ruthenium, strontium, barium, zirconium, and uranium) and slightly larger amounts of volatile elements, (iodine, tellurium, and cesium) are found downstream of a "high-efficiency" filter. The data presented in Table 1.20 generally indicate that for the volatile isotopes smaller fractions of the material released into off-gas systems escape capture by the "high-efficiency" filter than is the case for the nonvolatile ones. This probably reflects the fact that greater amounts of these materials are released into the off-gas system. Calculated efficiencies of the "high-efficiency" filters for the various fission products follow the same pattern. The large amounts of iodine shown for experiment 13 are probably due to its oxidation to the elemental form by the moist air atmosphere. In this form the iodine was deposited to a lesser extent prior to the charcoal, and only 0.7% penetrated the first 2 in. of charcoal.

The data in Tables 1.19 and 1.20 are of interest in assessing the performance of filters in removing fission products released in reactor accidents. Because the amounts of fission products which escape the high-temperature zone are so small, the data are susceptible to interference by contamination (e.g., in the hot cells). Although great care is exercised to prevent such contamination, its occurrence cannot be ruled out entirely. At the present time, however, the data in Tables 1.19 and 1.20 generally must be considered as upper limits, and judgment must be withheld about the implied low filter efficiencies. The data in Table 1.19 represent upper limits for the fractions of the fission-product inventories which would be found beyond an absolute filter in a reactor accident.

## ANALYSIS OF OFF-GAS FROM IN-PILE FUEL MELTING EXPERIMENTS

The off-gas which has passed from the in-pile meltdown experiments through the filters and the charcoal trap is processed in a permanent part of the ORR facility to determine the extent to which the various fission products can penetrate these components. This unit has been revised recently and now performs the following functions: (1) monitoring of the radioactivity of the gas during operation, (2) collection of rare gases in a refrigerated charcoal trap, (3) transfer of the collected gases into an evacuated 21-liter tank by heating

the charcoal trap, and (4) collection of gaseous aliquots in 7-$cm^3$ biological serum bottles. Collection of gas samples is accomplished by piercing the rubber tops of the serum bottles in the manifold system with hypodermic needles. The bottles can then be evacuated, with a vacuum pump installed in the system, and filled either directly from the gas stream before the refrigerated charcoal trap or from the 21-liter tank which contains the gases removed from the charcoal. Removing samples from the line before the trap permits the detection of nuclides which would otherwise remain fixed on the trap. The revised unit was used for experiment 14, and the results have been partially interpreted.

Construction of experiment 14 was identical to that of previous experiments. The stainless-steel-clad $UO_2$ fuel specimen was surrounded by thoria insulation through which sweep gas passed to carry released fission products through filters, a charcoal trap, and on to the part of the facility described above. The analysis discussed in this section deals only with samples removed from the gas stream in this part of the facility. Operation of experiment 14 differs from previous experiments in that the fuel was not preirradiated but was inserted immediately into the lattice of the reactor to a point where the temperature of the $UO_2$ was $\sim 2000°C$. It was irradiated for 105 min with moist air sweeping over the fuel at 400 $cm^3$/min. Seven-cubic-centimeter samples of the gas were taken at 10-min intervals beginning 10 min after insertion. After the experiment the contents of the charcoal trap were discharged into an evacuated tank, and this gas also was analyzed. The gas samples were found to contain small amounts of the 131, 132, 133, and 135 chains. Preliminary analysis of the mass 132 data indicates that some antimony or tellurium penetrated the gas-cleaning system during the initial 20 min of operation but not later. On the other hand, the mass 133 data indicate that not more than 0.36% of the antimony was released, 0.0034% of the tellurium, a vanishingly small fraction of the iodine, or 50% of the xenon formed 10 min after the start.

It can be concluded from this analysis that either antimony or tellurium is released in a detectable, but very small, amount from $UO_2$ fuel heated to $\sim 2000°C$ and that the released material passes through a roughing filter, a charcoal trap at 40°C, and about 30 ft of $\frac{1}{8}$-in. tubing. This method of analysis has proved to be highly sensitive and is being developed further with the expectation of setting limits on the amounts of various fission-product elements which penetrate a gas-cleaning system.

# 1.4 Characterization and Control of Accident-Released Fission Products

## IODINE DISTRIBUTION AMONG CHEMICAL FORMS AND PARTICLE SIZES IN AGED AEROSOLS

G. W. Parker G. E. Creek W. J. Martin

### Aerosol from 7000 Mwd/ton Burnup $UO_2$

An experiment (run C) was described in Sect. 1.1 of this report in which highly irradiated $UO_2$ (7000 Mwd/ton burnup) was melted in air and the resulting aerosol was transferred to the confinement tank of the CMF. Diffusion tube data obtained from sample streams withdrawn at three points in the filter pack while 3-hr-aged aerosol passed through the pack are given in Figs. 1.29, 1.30, and 1.31. Figure 1.29 presents data on the unfiltered mixed aerosol entering the analyzer; Fig. 1.30 gives data on the aerosol after filtration by "absolute" (CWS) filter paper; and Fig. 1.31 gives data on the iodine remaining after adsorption of the elemental iodine on eight activated copper screens. The diffusion tube plots were used to calculate the iodine distribution data displayed in

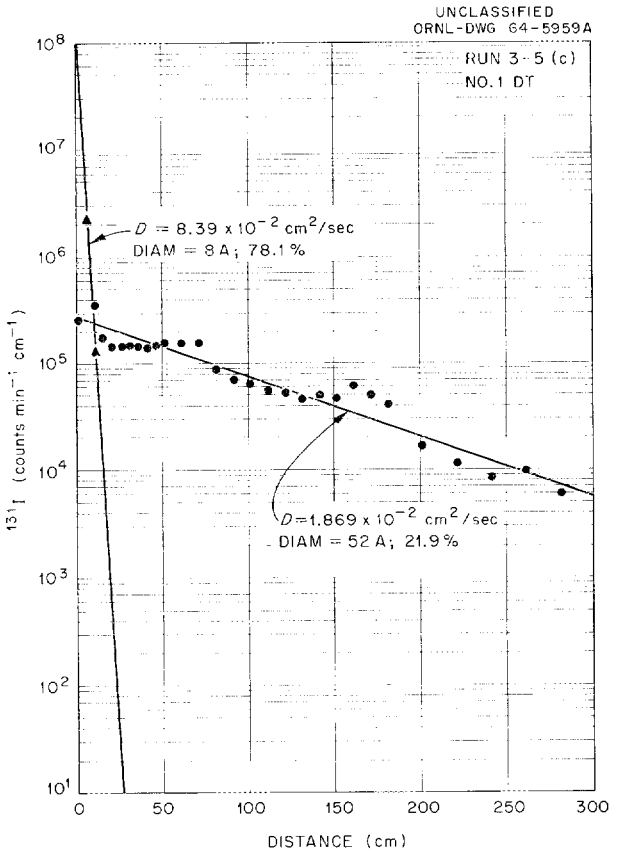


Fig. 1.29. Diffusion Tube Data for Unfiltered Aged Aerosol from 7000-Mwd/ton $UO_2$.

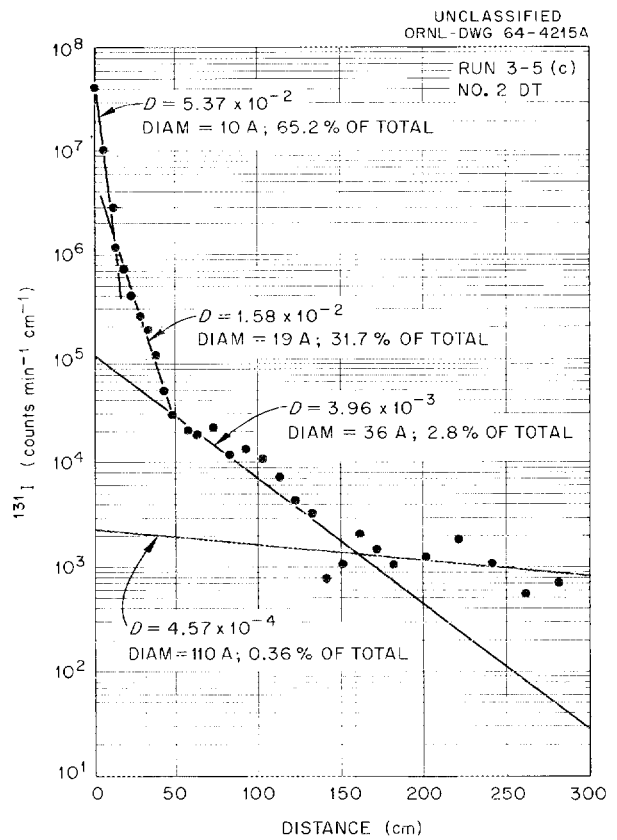


Fig. 1.30. Diffusion Tube Data for Filtered Aged Aerosol from 7000-Mwd/ton $UO_2$.

Table 1.21. Some additional data on larger size particles were obtained by use of the Andersen sampler; however, the amount of iodine (0.2%) associated with particles collected by the sampler can be neglected.

It is especially interesting that a frequently observed particle size (20 to 30 A) is the only one seen in Fig. 1.31 after the sample had passed through the copper screens.

Additional data which support the existence of this particulate form of iodine are given in the plot (Fig. 1.32) of the relative amount of iodine on individual copper screens. The occurrence of an additional form of iodine is indicated by the plot of the charcoal cartridge data, Fig. 1.33. The slope of the data obtained with the last three cartridges is attributed to a "penetrating organic form."

Table 1.21. Distribution of Iodine States and Particles from 7000-Mwd/ton $UO_2$ Melted in Air[a]

| Form | Method | Percent of Airborne Iodine | |
|---|---|---|---|
| | | Before Filtration | After Filtration |
| $I_2$ | Diffusion tube | 70 | 65 |
| 20–30 A | Diffusion tube | 25 | 32 |
| 30–50 A | Diffusion tube | | 2.0 |
| 100–240 A | Diffusion tube | 2 | 0.4 |
| 240 A–0.7 $\mu$ | Abs filter | 2 | 0 |
| 0.7–3 $\mu$ | Impactor | 0.2 | |
| Organic + desorbed $I_2$ | Charcoal | 0.8 | 1.5 |

[a]Airborne after 3 hr in containment.

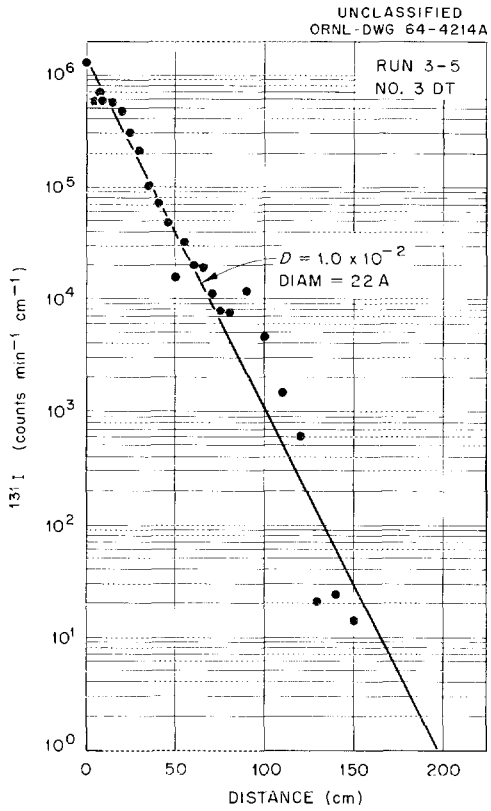


Fig. 1.31. Diffusion Tube Data for Aged Aerosol from 7000-Mwd/ton $UO_2$ After Passing Through a Filter and Copper Screens.

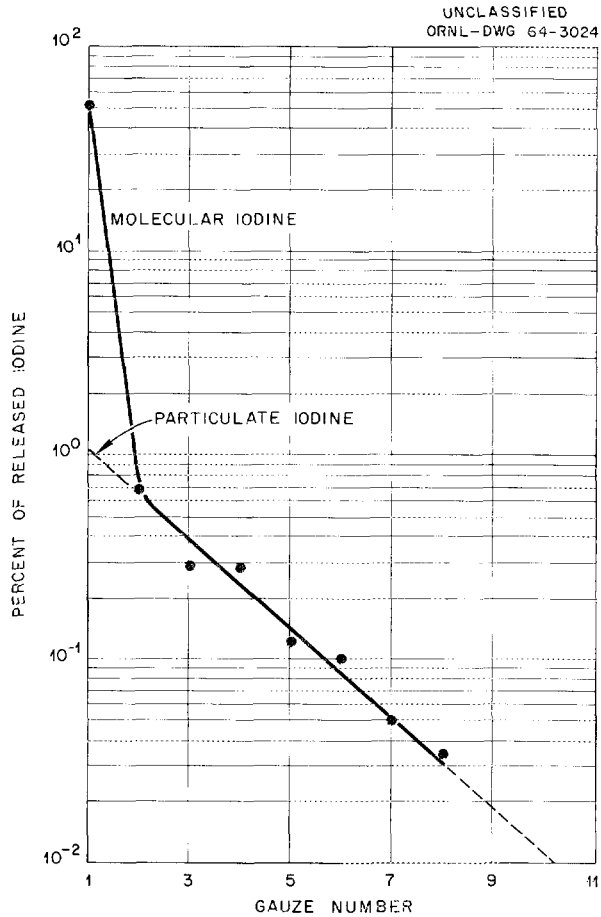


Fig. 1.32. Distribution of Iodine on Copper Screens.

### Aerosol from Molten $UO_2$–Iodine Tracer (Run D)

Diffusion tube data obtained with aged aerosol, unfiltered and filtered, are shown in Figs. 1.34 and 1.35 respectively. It is clear from these data that passage through an absolute filter had little effect on the distribution of iodine among molecular iodine and small particles deposited in the diffusion tubes.

Distribution data obtained in various experiments involving release of iodine in the presence of vaporized $UO_2$ are compared in Table 1.22.

The largest variation noted is in the iodine associated with particles in the 50- to 100-A size range. The difference between the results obtained in runs A and B can probably be attributed to the presence of unfiltered air in run B. It seems significant that when a realistic concentration of iodine (2 mg/m$^3$) is present initially in the confinement tank the fraction of iodine attached to particles in the 50- to 100-A size range is quite small. It is not clear whether the variation in the fraction of iodine attached to the small particles (18 to 22 A) has any significance. As was mentioned previously in this report, the molecular $^{127}I$ with tracer $^{131}I$ employed in run D was transferred to the confinement tank before the unirradiated $UO_2$ specimen or its stainless steel cladding melted, and this may have given less opportunity for the iodine to adsorb on or react with these small particles.

### Aerosol from Iodine Tracer Experiment

Several tests were compared to obtain the ratio of various forms of iodine produced in the experiment (run E) described in Sect. 1.1 of this report, in which molecular $^{127}I$ with tracer $^{131}I$ was introduced into the containment tank (of the CMF)

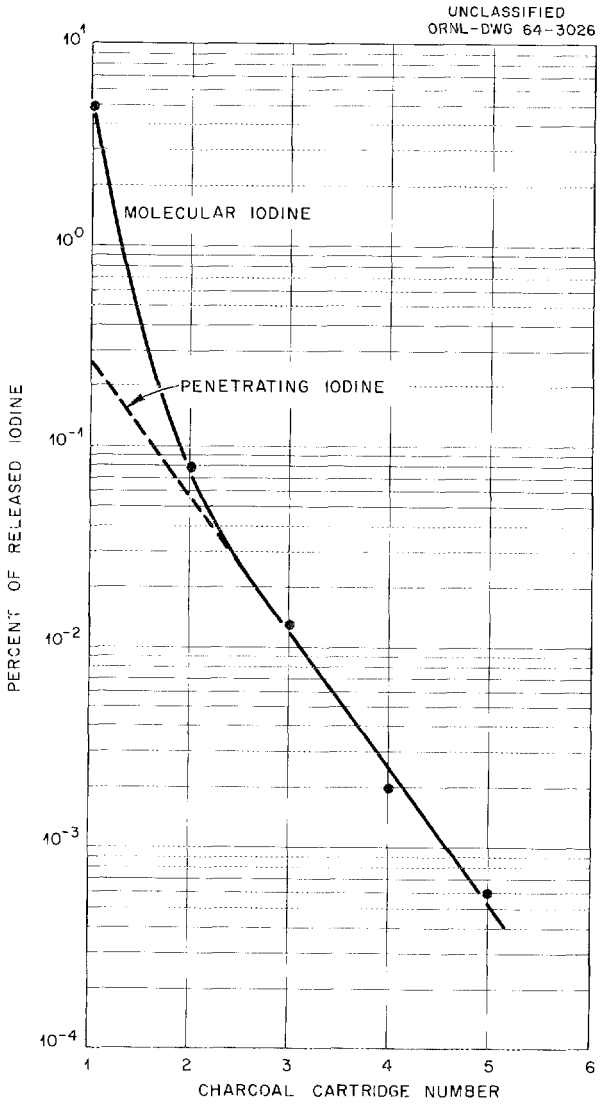


Fig. 1.33. Distribution of Iodine in the Charcoal Adsorber Pack.

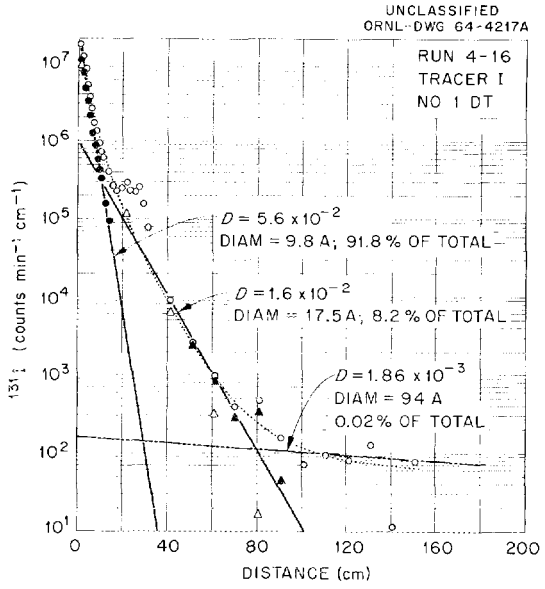


Fig. 1.34. Diffusion Tube Data for Unfiltered Aged Aerosol from $UO_2$-$^{131}I$ Simulation Experiment.

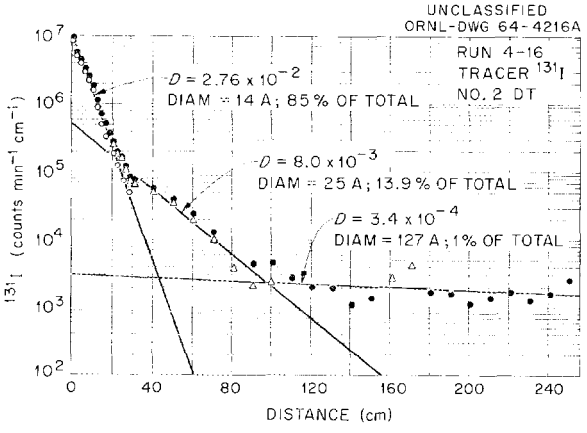


Fig. 1.35. Diffusion Tube Data for Filtered Aged Aerosol from $UO_2$-$^{131}I$ Simulation Experiment.

Table 1.22. Comparison of Distribution of Iodine Among Different Particle Sizes

| Size Range (A) | Percent of Airborne Iodine | | | |
|---|---|---|---|---|
| | Run A | Run B | Run C | Run D |
| 8–14 ($I_2$) | 80 | 68 | 78 | 92 |
| 18–22 | 14 | 12 | 22 | 8 |
| 50–100 | ~5 | 20 | | 0.02 |
| >100 | 0.4 | | 0.4 | |

filled with air at 15 psig. Since some unfiltered air was present in the containment tank, it was expected that some particulate iodine and some organo-iodine compounds would be found. The first means of differentiation were the filter pack and the diffusion tubes. Separate filter packs and diffusion tubes were used at three stages in the experiment. Absolute filters preceding the diffusion tubes removed only part of the very small (near molecular size) particles. The silver-copper screen combination (three silver-plated screens followed by five copper screens) was probably

Table 1.23. Particle Size of Airborne and Desorbed Iodine in Iodine-Tracer Experiment (Run E)

| Fraction Analyzed | Iodine Collected on Filters | | Iodine Passing Through Filters | | |
|---|---|---|---|---|---|
| | Particles of Undetermined Size: Held by Absolute Filter[a] | Particles >60 A: Held by Filter After Diffusion Tube | Molecular or Ionic Iodine Held on Silver-Copper Screen | Reactive Small Particles Held on Charcoal Paper | Penetrating Forms Held on Charcoal Beds |
| | Percent of Total Iodine Removed in Each Fraction | | | | |
| Air pressure release (2.8% of total) | 1 | 0.6 | 64 (37 + 27)[b] | 32 | 2.9 |
| Argon sweep (7.0% of total) | 1 | 1.7 | 71 (45 + 26)[b] | 23 | 2.8 |
| Air sweep (2.9% of total) | 10 | 1.5 | 72 (39 + 33)[b] | 16 | 1.4 |

[a]Absolute filter is composed of 2-in. disk of CWS-6 or AEC-type "high-efficiency" air filter and one membrane-type filter.

[b]Total amount is determined by adding the iodine held on a "polypore" filter paper after penetration of the normal CWS paper.

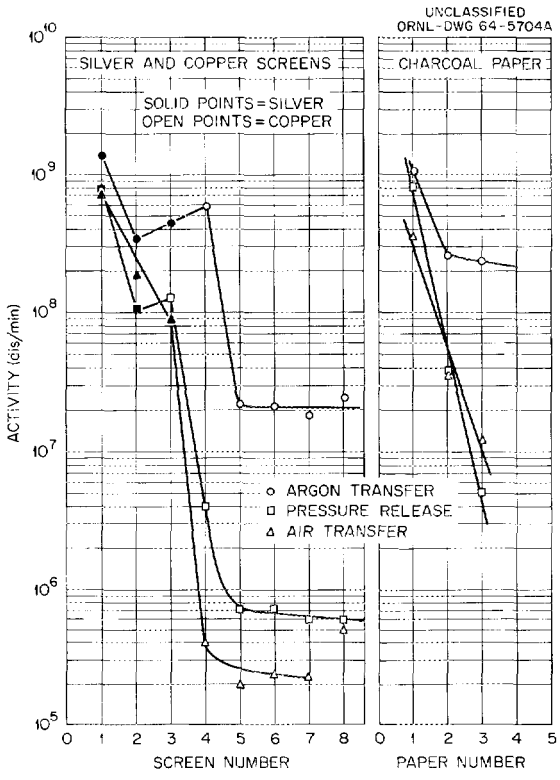


Fig. 1.36. Iodine Collected on Silver-Copper Screens and on Charcoal-Loaded Filter Paper During Iodine Tracer Experiment (Run E).

effective in removing HI and molecular or atomic iodine. Data plotted in Fig. 1.36 show that the copper was more effective than silver. The remainder of the small particulate fraction was presumably collected in the charcoal filter paper, and the organic or penetrating fraction was retained in the charcoal cartridges. The distribution given in Table 1.23 is based on this method of fractionation. The size of the particles at each stage was determined from the diffusion tube plot.

## IDENTIFICATION OF CHEMICAL FORMS OF IODINE BY A LIQUID CONTACTOR METHOD

G. W. Parker G. E. Creek J. G. Wilhelm

One method used to determine the chemical state of radioiodine is that which makes use of equilibration of tracer iodine between two solvents such as water and carbon tetrachloride ($CCl_4$). The accepted value for the distribution of elemental iodine is approximately 80 parts in $CCl_4$ to 1 in water, while $I^-$, $IO_3^-$, and $IO_4^-$ concentrate in water on equilibration. It appears, therefore, that the distribution of iodine between solvents should afford a method for determining whether iodine is present as $I_2$ or in another valence state.

However, this method, as it is currently used, gives results of questionable value in fission product release experiments because: (1) organoiodine compounds may extract into $CCl_4$, for example, and become identified as $I_2$; (2) submicron particles carrying iodine may possibly distribute between solvents without reference to the state of oxidation of the radioiodine; (3) a rapid change in oxidation state may occur due to reaction with impurities in the solvents, especially at very low concentrations of iodine; and (4) rapid isotopic exchange of radioiodine in one state with that in another previously added as a carrier to the solvent systems is possible. Information derived without due regard for these various possibilities is likely to be in error.

Studies conducted to date have not quantitatively defined any of the above-mentioned effects, but preliminary tests of the liquid-contactor method were performed in an effort to supplement data obtained by use of the modified May pack and diffusion tubes.

An experiment was performed in which ambient air carrying a mixture of $^{131}I$ and $^{127}I$ was introduced into a stainless steel tank. This experiment (run D) is described in more detail in Sect. 1.1 of this report. After the aerosol had aged for 5 hr and the pressure in the tank had been reduced from 15 to 2.5 lb, a gas stream from the aerosol tank was removed and split into two parts. One stream was directed to the $CCl_4$ system, and the other to the $CH_3I$ system, as shown in the block diagram, Fig. 1.37, which also gives the observed distribution data.

In the $CH_3I$ system, the gas stream passed through eight silver screens to remove $I_2$ and any HI that might be present. The screens removed about 81% of the airborne iodine. The distribution of iodine among the eight screens suggests that part of the deposited iodine was attached to small particles. There seems to be little doubt that interpretation of distribution data would be simplified by use of filters having a high efficiency for removal of small particles. The gas was then bubbled through $CH_3I$ (maintained at approximately 6°C) which extracted most of the iodine not removed by the screens. This solvent should remove organic iodine compounds, such as $CH_3I$, but, as mentioned above, part of the 18.8% of iodine found in this scrubber may have been due to particles. After passing through the $CH_3I$, the gas flowed through a water scrubber and a charcoal trap.

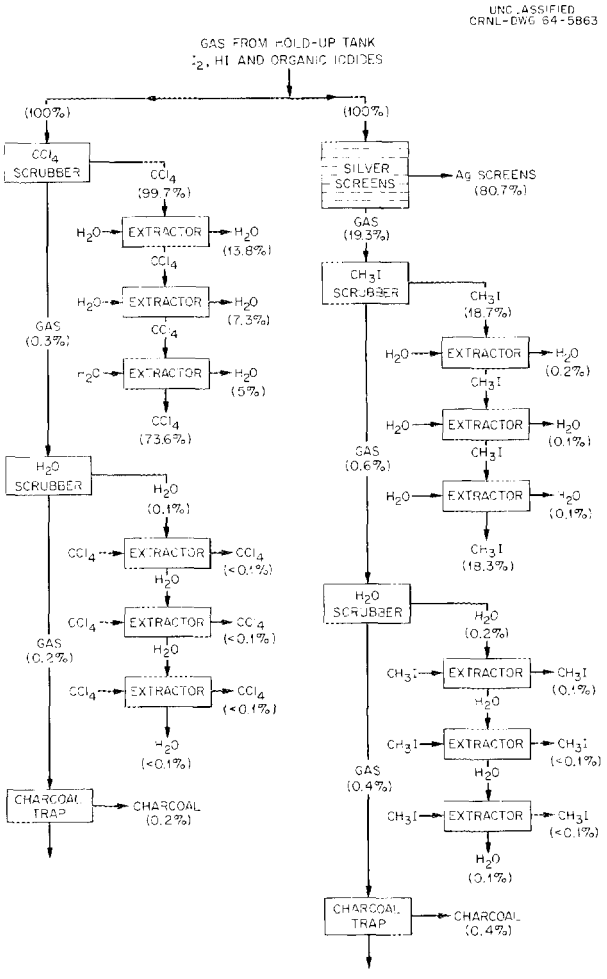


**Fig. 1.37. Distribution of Iodine in Water and Organic Solvents.**

In the $CCl_4$ system, the gas was first scrubbed with $CCl_4$, which was cooled to approximately 6°C. This treatment removed $I_2$ and, presumably, organic iodine compounds as well. Nearly all (99.8%) of the airborne iodine was removed by this scrubber. The $CCl_4$-scrubbed gas was bubbled through water to remove HI and any other water-soluble iodine compounds present and then passed through a charcoal trap.

A significant amount (~26%) of the total activity in $CCl_4$ was extracted by three water washes. This indicated the presence of nonelemental iodine, which could be due to a change in state of some of the original elemental iodine in solution or to water-soluble iodine compounds, such as might be carried by particles trapped in the $CCl_4$. The distribution of iodine activity between the three

successive backwashes and the $CCl_4$ indicated however that little, if any, of the iodine in the $CCl_4$ was present as HI. Very little water-soluble iodine was found in the $CH_3I$ scrubber.

It appears that part of the radioiodine that remained airborne for more than 5 hr and was extracted from air by $CCl_4$ was later in a form which was water-extractable. This fraction was not found in the $CH_3I$ and, therefore, must have been retained on silver screens. More data will be required to determine the effect of iodine concentration on the fraction of iodine in $CCl_4$ converted to the extractable form and, in general, the value of distribution data for characterizing the chemical form of gas-borne radioiodine.

## INVESTIGATION OF IODINE BEHAVIOR IN MAY PACKS BY MEANS OF COMPOSITE DIFFUSION TUBES

W. E. Browning, Jr. R. D. Ackley

Iodine samplers referred to as May packs have been extensively employed by British workers in studying the nature and behavior of radioiodine in gas streams.[11,12] The May pack, named after F. G. May, consists of components intended to distinguish between elemental iodine, iodine on particulates, and two classes of volatile iodine compounds – one class being those readily adsorbed on charcoal and the other those adsorbed less readily. More recently, American workers have also instituted the use of iodine samplers of this type.[13] They are being used in the Nuclear Safety Pilot Plant (NSPP) and have been considered for use in the Containment Systems Experiment (CSE) and the Loss of Flow Test (LOFT). In view of the widespread application of these samplers, it is desirable that their capability for discriminating between the various forms of iodine which are encountered be investigated. The use of composite diffusion tubes for the characterization of molecular forms of iodine has been previously described,[14,15] and application of this technique appeared to provide a suitable means for investigating iodine behavior in May packs. Accordingly, an experimental program based on the foregoing considerations was initiated.

One experiment has been completed and is reported herein. It involved the use of iodine which, as volatilized, was 99.7% elemental and 0.3% iodine compounds, carried by a stream of relatively dry, filtered air. A second experiment, similar except for the use of air at a relative humidity of approximately 60%, has been performed, and radioactivity determinations and data treatment are under way; results will be reported later.

### Experimental

The May pack, as recently described,[12] consisted of a brass holder $2\frac{1}{2}$ in. long by 2 in. in diameter, containing the following: (1) two or more copper mesh disks to remove elemental iodine vapor, (2) a membrane filter to remove particulate matter, (3) two or more charcoal-loaded filter papers to remove readily adsorbed iodine compounds, and (4) a plug of granular charcoal to remove less readily adsorbed iodine compounds.

The top right portion of Fig. 1.38 shows the selection of components for duplicating the above apparatus. The copper gauze, mounted in a stainless steel holder, was cut from wire cloth; was degreased with acetone, and was then pretreated with 4 *N* HCl solution. The membrane filter was Millipore, MF type PH. The carbon-loaded paper was Alex Pirie 2/21-100GSM. The granular activated carbon was Pittsburgh PCB, which was retained in a 6-in. section of glass pipe. The overall May pack assembly was made with appropriately machined Teflon parts using Teflon O-rings where necessary, all held together under slight compression by a metal rod framework with end pieces. Teflon was selected because of its low absorption capacity for iodine and its compounds. Five of the Teflon parts were drilled radially for insertion of diffusion tubes, each of

[11] W. J. Megaw and F. G. May, *J. Nucl. Energy: Pt. A & B* 16, 427–36 (1962).

[12] A. C. Chamberlain *et al.*, *J. Nucl. Energy: Pt. A & B* 17, 519–50 (1963).

[13] G. W. Parker *et al.*, *Nucl. Safety Program Semiann. Progr. Rept. Dec. 31, 1963*, ORNL-3547, pp. 3–25.

[14] W. E. Browning, Jr., and R. D. Ackley, *Nucl. Safety Program Semiann. Progr. Rept. June 30, 1963*, ORNL-3483, pp. 26–28.

[15] W. E. Browning, Jr., R. D. Ackley, and R. E. Adams, *Nucl. Safety Program Semiann. Progr. Rept. Dec. 31, 1963*, ORNL-3547, pp. 60–64.

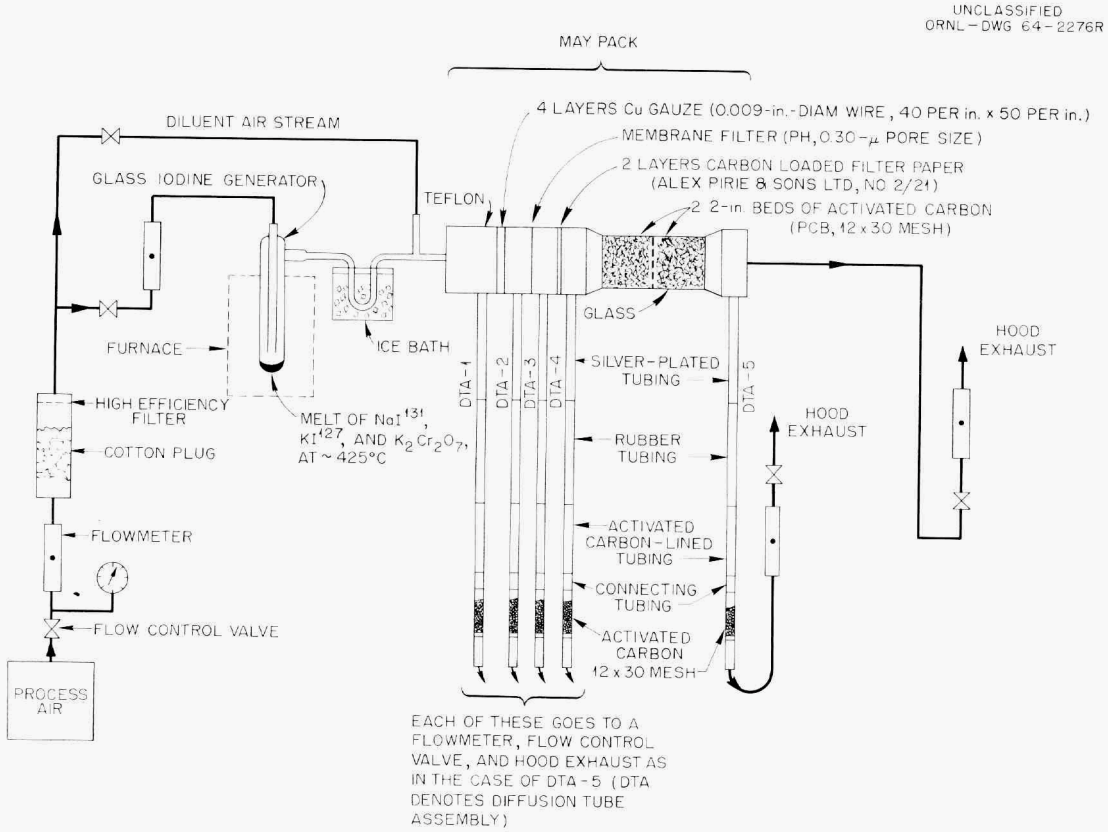


Fig. 1.38. Experimental Setup for Investigation of Iodine Behavior in a May Pack by Means of Diffusion Tubes.

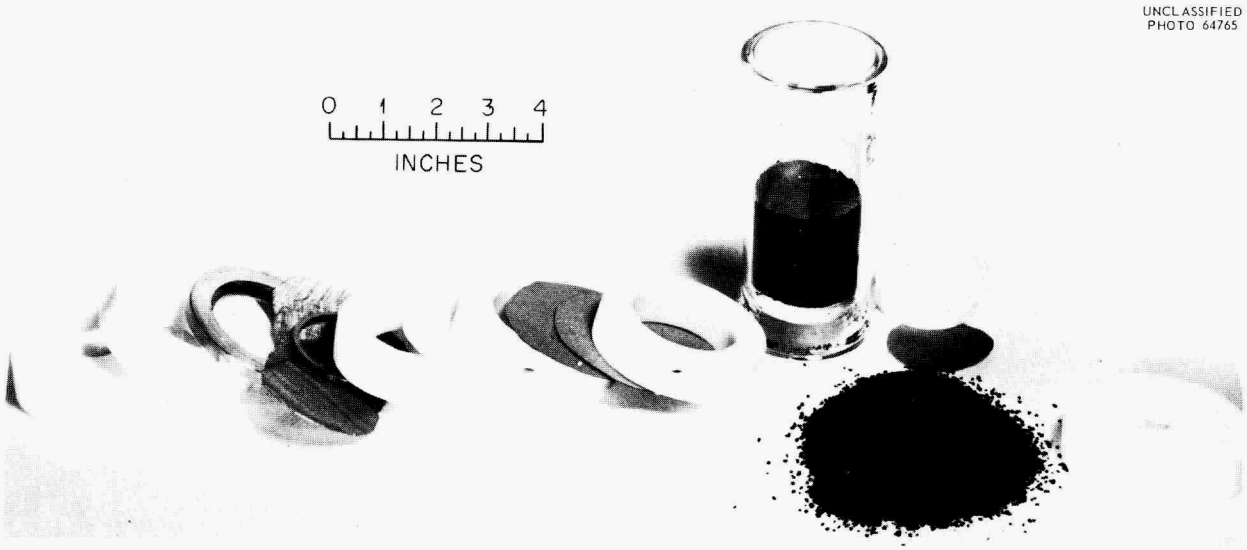


Fig. 1.39. May Pack Components.

which was held in place by friction. The disassembled May pack is shown in Fig. 1.39; Fig. 1.40 shows it after assembly with diffusion tubes inserted. The inside diameter of most of the May pack was 2 in.

Each of the diffusion tubes presented to the flowing gas successive inner surfaces of silver, rubber, and activated carbon, which are intended to distinguish between various chemical species. The tubing lengths corresponding to these three surfaces were 30, 30 (exclusive of overlap), and 20 cm, respectively, and the inside diameters were each about 0.8 cm. The silver surface was obtained by plating; the rubber surface was obtained simply by using translucent amber latex rubber tubing; and the activated carbon surface

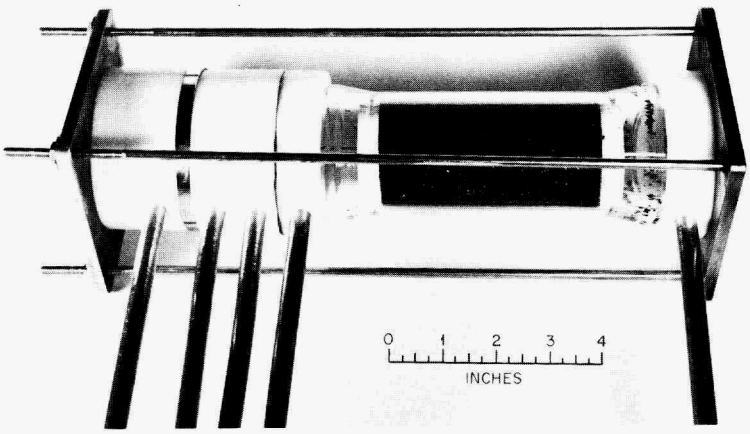


Fig. 1.40. May Pack Assembly with Diffusion Tubes.

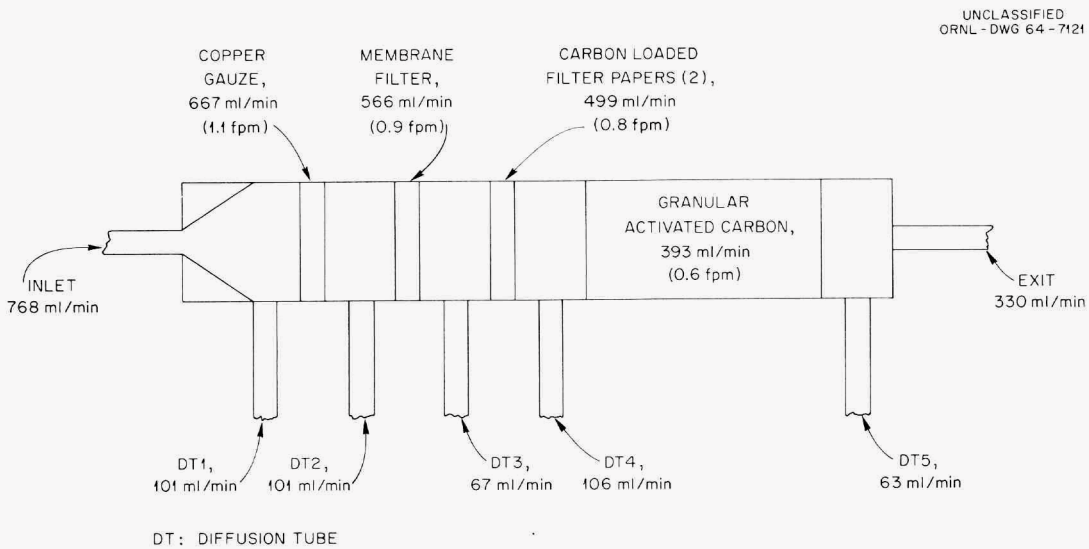


Fig. 1.41. Air Flow Rates and Velocities in May Pack Experiment.

was obtained by coating the inside of an adhesive-lined copper tube with dust obtained by grinding Pittsburgh PCB activated carbon to pass a No. 80 sieve. The traps at the exit of the diffusion tubes each contained a 2-in.-long, $^3/_8$-in.-diam column of Pittsburgh PCB 12 × 30 activated carbon.

Figure 1.38 shows the essentials of the entire experimental setup. As indicated, $I_2$ was generated and evolved by melting a 0.5-in.-deep layer of potassium dichromate covering a dried residue from a solution of $Na^{131}I$ (0.25 mc) plus $K^{127}I$ (1 mg). During the actual transfer of $I_2$, which required roughly 1 hr, the air entering the May pack contained about 15 mg of $I_2$ per $m^3$ of air. The more pertinent air flow rates and velocities which were involved are illustrated in Fig. 1.41. These flow conditions were maintained for 2 hr after the $I_2$ transfer was essentially complete. Subsequently, the setup was disassembled, the necessary samples were prepared, and the amounts of $^{131}I$ radioactivity were determined.

## Results

The data obtained with the five diffusion tubes are shown in Fig. 1.42, except that points corresponding to less than $10^2$ dis $min^{-1}$ $cm^{-1}$ (before applying the graphing factor used in the figure) have been omitted. Deposition profiles in this figure have not been normalized for the varying diffusion tube flow rates, as has been done for some of the results to be given. The diffusion coefficients were calculated, where straight lines are shown, from the equation

$$D = 0.2004Q(\Delta \log_{10} y)/\Delta Z \ , \qquad (1)$$

where

$D$ = the diffusion coefficient, $cm^2$/sec,
$Q$ = the volumetric flow rate in the diffusion tube, $cm^3$/sec,
$y$ = deposited radioactivity per unit length, dis $min^{-1}$ $cm^{-1}$,
$Z$ = distance from diffusion tube entrance, cm.

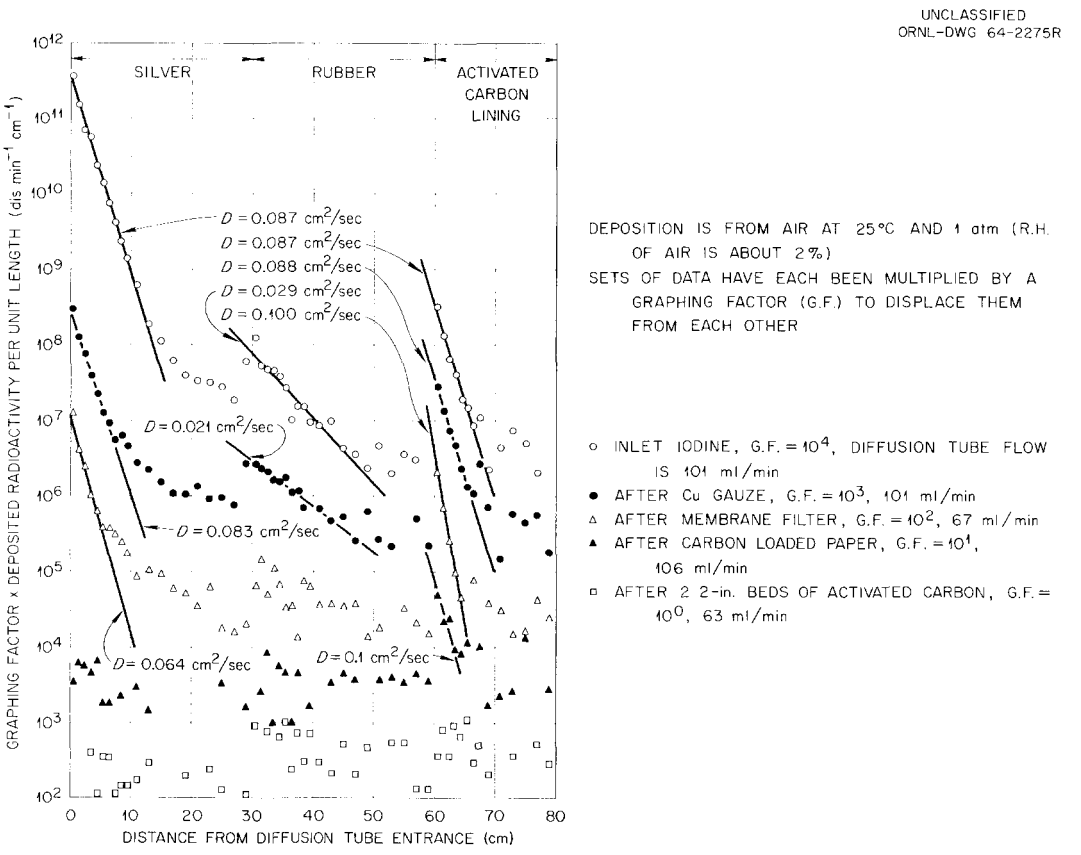


**Fig. 1.42. Penetration of May Pack Components by Airborne Iodine as Indicated by Diffusion Tubes.**

The basis for Eq. (1) is the Gormley and Kennedy equation for diffusion to the wall of a cylinder through which laminar flow is occurring.[16] For present purposes, its minor exponentials were dropped, and it was then differentiated. Considering the deposits on the silver sections, which are intended for the deposition of elemental iodine, data points at some distance from the entrance and above the straight lines shown reflect the presence of nonelemental iodine. This material, which is measured by the vertical distance above the straight lines, will be referred to as non-$I_2$. Somewhat similarly, the deposits on rubber will be referred to as "rubber, $D \doteq 0.025$ cm$^2$/sec" and "rubber, residual"; and the deposits on activated carbon will be referred to as "activated carbon, $D = 0.1$ cm$^2$/sec" and "activated carbon, residual." The value $D \doteq 0.025$ cm$^2$/sec is representative of part of the data on rubber herein, and the value $D = 0.1$ cm$^2$/sec is approximately representative of the data on activated carbon and, also, of other data obtained previously.[15] Where the data points for the three diffusion tube surfaces were at too low a level of radioactivity and were too scattered for determining straight lines, upper limits for materials corresponding to $I_2$ on silver, $D \doteq 0.025$ cm$^2$/sec on rubber, and $D = 0.1$ cm$^2$/sec on activated carbon were evaluated. This was done in each case by first selecting, at the beginning of a section having a particular surface, a maximum value for the intercept for material possibly present and having the diffusion coefficient 0.085 cm$^2$/sec, 0.025 cm$^2$/sec, or 0.1 cm$^2$/sec respectively. For example, considering the deposit on silver represented by solid triangles in Fig. 1.42, the intercept selected was $1 \times 10^4$ after multiplying by the graphing factor. Using the intercept so obtained, the appropriate value of $D$, and the theoretical relationship for the decrease in deposition with distance, the upper limit for the amount of each iodine species which could have been present was determined by integration.

The amounts of radioactivity observed on the May pack components and on the diffusion tube surfaces in terms of various iodine species are given in Table 1.24; also included are the results of the above described calculations of upper limits of species. The data were normalized, for purposes of comparison, to the flow rate through the copper gauze (667 ml/min) by multiplying them

[16]P. G. Gormley and M. Kennedy, *Proc. Roy. Irish Acad., Sect. A* **52**, 163–69 (1949).

**Table 1.24. Distribution of Radioiodine Species Among May Pack Components and Diffusion Tubes**

| Component or Diffusion Tube | Radioactivity Relative to Inlet Gas (%) | | | |
|---|---|---|---|---|
| | Total | $I_2$ | On Rubber, $D \doteq 0.025$ cm$^2$/sec | On Activated Carbon $D = 0.1$ cm$^2$/sec |
| Diffusion tube No. 1 | 100.000[a] | 99.724 | 0.068 | 0.095 |
| Copper gauze (4 layers) | 106[b] | | | |
| Diffusion tube No. 2 | 1.048 | 0.854 | 0.035 | 0.096 |
| Membrane filter (PH) | 0.127 | | | |
| Diffusion tube No. 3 | 0.641 | 0.483 | $\leq 0.013$ | 0.080 |
| Carbon-loaded filter papers (2) (Pirie, No. 2/21) | 0.594 | | | |
| Diffusion tube No. 4 | 0.045 | $\leq 0.002$ | $\leq 0.009$ | $\leq 0.016$ |
| Activated carbon bed (4 in. of PCB, 12/30 mesh) | 0.011 | | | |
| Diffusion tube No. 5 | 0.056 | $\sim 10^{-5}$ | $\leq 0.009$ | $\leq 0.004$ |

[a]Totals include contributions of less important species not listed.

[b]This number exceeds 100% due to experimental variation.

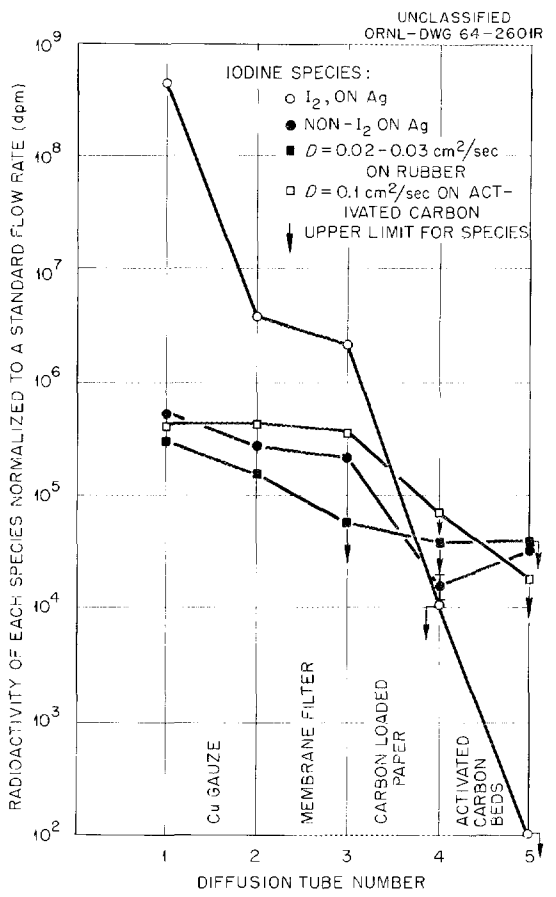


Fig. 1.43. Penetration of May Pack Components by Various Iodine Species.

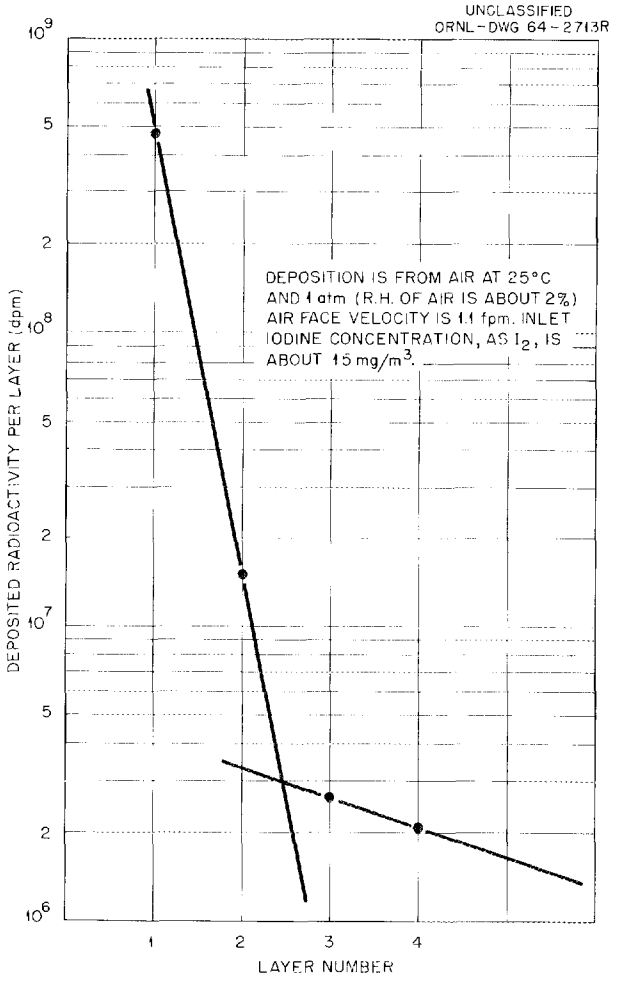


Fig. 1.44. Deposition of Airborne Iodine on Successive Layers of Copper Gauze.

by $667/F$, where $F$ (ml/min) is the flow rate through the part for which the data were being normalized. This treatment is based on the premise that the amount of radioactivity entering the May pack was given by the normalized total found in the first diffusion tube assembly, that is, the numbers are on the basis that $4.60 \times 10^8$ dis/min is equivalent to 100%. Figure 1.43 illustrates the behavior of certain of the iodine species in the May pack. The iodine deposition on the different layers of copper gauze is shown in Fig. 1.44.

## Discussion

The diffusion tube plots, Fig. 1.42, are similar to those observed previously for volatile iodine produced by the dichromate method when carrier iodine and fairly dry air were employed.[15] Some points of difference are that the diffusion coefficients corresponding to deposition on rubber are somewhat lower, and on activated-carbon-lined tubes they are lower in two instances. The diffusion coefficients, given as 0.064 cm²/sec and 0.1 cm²/sec in the figure, are based on data which cover such a narrow ordinate range that these values are of dubious accuracy. The degree of attenuation of the various iodine species is given by this figure, but a more direct quantitative evaluation is provided by considering the summations of the groups of data points in Table 1.24.

From a perusal of Table 1.24, it appears that the only pronounced discrepancy occurs in the amount of radioactivity found on the membrane

filter. This amount is low by a factor of 3 as compared to the difference between the amounts found in diffusion tubes 2 and 3. No satisfactory explanation appears to be available; however, this does not appear to be a matter for great concern since, in general, the data are internally consistent.

Figure 1.43 provides a summary of the behavior of the various iodine species in the May pack as indicated by diffusion tubes. The concentration of elemental iodine was diminished by a factor of about 100 by the copper gauze; that remaining was diminished by a factor of about 2 by the membrane filter and then by a factor of >100 by the carbon-loaded filter paper. The "non-$I_2$ on Ag" fraction did not appear to be appreciably retained except by the carbon-loaded paper. Radioactivity levels downstream of the carbon-loaded paper, including the diffusion tube surfaces, were in most instances close enough to background that the associated results cannot be regarded as having more than a tenuous significance. The species "$D$ = 0.02–0.03 $cm^2$/sec on rubber" appeared to be retained by the membrane filter, but the reason for this is not obvious since the membrane filter is composed of cellulose esters, a material dissimilar to rubber. This species is apparently not particulate in nature as evidenced by the increase in deposition on going from silver to rubber. The species characterized by $D$ = 0.1 $cm^2$/sec on activated-carbon-lined tubing penetrated the copper gauze and the membrane filter but was at least 80% removed by the carbon-loaded paper; the remainder was essentially completely removed by granular activated carbon. Generally, the rubber and activated carbon residuals were present at such low levels that discussing them in much detail is not warranted.

Various mechanisms have been studied briefly in an effort to explain the observed deposition on the layers of copper gauze, but the results were inconclusive. It does appear, however, that elemental iodine is incompletely removed by four layers of copper gauze under the experimental conditions employed.

In summary, the behavior of volatile iodine in the May pack, as indicated by diffusion tubes, was observed, in this one test with fairly dry air, to be generally consistent with the designed function of the May pack components. On the other hand, about 1% of the elemental iodine apparently was not retained by the copper gauze; if this is a usual occurrence, then May pack measurements could incorrectly label part of the elemental iodine as nonelemental. This extent of mislabeling could be of considerable significance in connection with the design of iodine-removal systems of high efficiency.

## INVESTIGATION OF IODINE BEHAVIOR IN COMPOSITE DIFFUSION TUBES BY VARYING THEIR INTERNAL ARRANGEMENT OR THEIR TEMPERATURE

W. E. Browning R. D. Ackley

Composite diffusion tubes developed to distinguish and measure various airborne forms of iodine have been described previously.[14,15] An experiment has been performed to investigate certain anomalies which have been observed in the use of these devices and to prepare for an investigation of the possibility of reducing interference by moisture by heating the diffusion tubes; the results are reported in this section.

The diffusion tubes, which are simply consecutive segments of tubing of various materials, distinguish between the various vapor species according to their tendencies to react with or sorb on the different surfaces and measure the rates of deposition for each species under laminar-flow conditions. Where gas-phase diffusion is the rate-limiting step in deposition, interpretation of the distribution of iodine in the diffusion tube is fairly straightforward. The data fall on an approximately straight line in a semilog plot of radioactivity vs position in the tube, and the diffusion coefficient may be obtained from the slope of the line. A deposit resulting from aerosol particles can be recognized by its slope, which is smaller than that of most molecular species, and by its continuity through a boundary between different wall materials. The forces of adherence of a small particle to a surface would exceed the forces tending to dislodge it by so large a margin that there should be no variation in the amount deposited on various materials under laminar-flow, diffusion-controlled conditions, whereas the deposit from a volatile molecular vapor should exhibit a discontinuity at the boundary between materials having different affinities for the vapor. Composite diffusion tubes have in general yielded the expected distribution patterns, and they have

been quite useful in distinguishing and measuring the various forms of radioiodine in gases.

Similar deposition distributions can result from rate-limiting processes other than diffusion, and there is reason to suspect that such may be the case under certain conditions. In some instances, apparent diffusion coefficients of approximately 0.025 $cm^2/sec$ have been obtained for deposition of volatile iodine on a rubber surface, following removal of the elemental iodine by a silver surface. This diffusion coefficient would correspond to a molecular weight of the order of 1000; the presence of such iodine compounds seems rather unlikely. Furthermore, particles are contraindicated because of the discontinuity in the amount deposited at the boundary between the silver and the rubber surface. Certain rearrangements in the order of wall materials in diffusion tubes were made in the present experiment to provide information on this problem.

The deposit of radioiodine on an activated-carbon-lined tube could be explained in terms of elemental iodine vapor formed by slow dissociation of an iodine compound. A silver-lined tube was provided, preceding the carbon-lined tube, to test this possibility.

Air carrying elemental iodine and iodine compounds, which are to be characterized by diffusion tubes, may have been mixed with steam and contain considerable amounts of moisture. At a temperature of 25°C, for example, the moisture would adsorb or condense on diffusion tube surfaces and probably interfere with proper deposition of the volatile iodine. At higher temperatures, the relative humidity and extent of adsorption of moisture would be reduced, thereby reducing the interference. Accordingly, the experiment was designed to determine whether the deposition behavior of iodine in dry air was seriously altered by heating one of the diffusion tubes.

## Experimental

Six diffusion tubes having various arrangements of wall material were supplied with air, bearing iodine, through a Teflon header. One of the tubes was heated to 100°C throughout its length by a heating jacket. Iodine was generated by the dichromate method and introduced into the air stream as in the experiment described in the preceding section, except that the flow rate of the air entering the header was approximately 600 ml/min. This resulted in an iodine concentration of about 20 mg per $m^3$ of air. The amount of $^{131}I$ at the time of radioactivity determinations was about 1 mc. The Teflon header and diffusion tube arrangements that were employed are shown in Fig. 1.45, which also gives the various flow rates. Composite diffusion tube sections, except for variations in order and overall lengths, were the same as in the recent experiments. The diffusion tube exit traps, however, were redesigned so as to contain more activated carbon.

## Results

Deposition data for the six diffusion tubes are shown in Figs. 1.46–1.50. The data for tubes 1 and 6 (DT1 and DT6) are both given in Fig. 1.46 since they were essentially duplicates.

To aid in interpretation of the data, the apparent amount of activity associated with each deposition pattern extrapolated to infinity was calculated by evaluating the integral of the radioactivity for the indicated species, even in instances where it was not too well defined, over two sets of limits, from the beginning of the diffusion tube segment to infinity and from the end of the segment to infinity. This was done analytically, except for the activated-carbon segment of DT5, making use of the fact that the depositions are of the form $y = ae^{-bx}$ and using the slopes and appropriate intercepts of the straight lines representative of the various iodine species. The straight lines in the figures are labeled with the corresponding calculated diffusion coefficients. To simplify the calculations, the lines were fitted generally in regions where the data points for one species were negligibly influenced by the contribution to them due to a different species. For the activated-carbon part of DT5, simple summation was employed for the first 10 cm, and the remainder was evaluated analytically; the two results were then added together to give the integral. The results of these evaluations are given in Table 1.25, together with the percentages of the radioactivity due to $I_2$ as indicated by the individual diffusion tubes. These percentages were evaluated in a slightly different manner, as a result of a different treatment of non-$I_2$ activity on silver, than was used in the previous section since here the integral

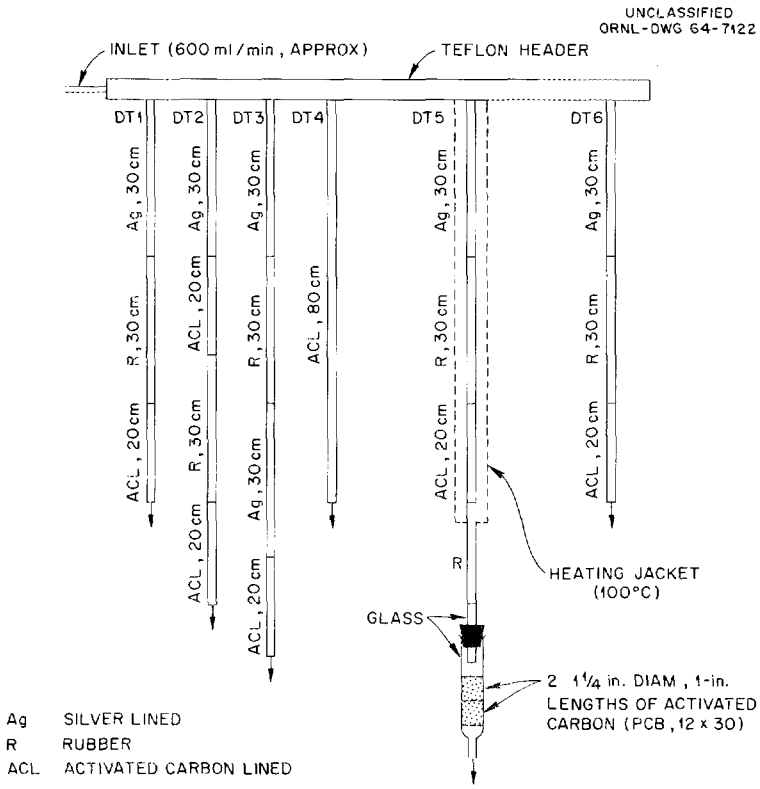


**Fig. 1.45. Wall Material Sequences for Investigating Iodine Behavior in Composite Diffusion Tubes.** Each diffusion tube (DT) was connected to a trap (as shown for DT5), then to a flowmeter, a flow control valve, and a hood exhaust. DT flow rates were 100, 102, 100, 103, 125 (at 100°C), and 100 ml/min respectively.

over the section was employed to obtain the amount of this substance.

The pieces of rubber tubing connecting the diffusion tubes to the charcoal traps, the rubber stoppers from the latter, and the two 1-in. lengths of charcoal in the traps were separately radioassayed for $^{131}I$. Each of the 24 samples gave $\leq$100 dis/min, a negligible fraction of the radioiodine.

### Discussion

Diffusion tubes (DT's) 1 and 6 of this experiment would be expected to yield results similar to those observed for the upstream diffusion tube, preceding the copper gauze, of the previous experiment. However, relative to the other surfaces, the deposition on rubber in DT1 and DT6 was higher by a factor of roughly 10 than was previously observed for this particular diffusion tube, after allowance was made for the higher level of radioactivity involved in the present study. It is thus suggested that some minor variation in experimental technique produces a large variation in the proportion of the iodine species which deposits in a characteristic fashion on a rubber surface. Other than this feature, comparable data from the two experiments are notably similar. Observations and conclusions which may be obtained from Figs. 1.46–1.50 with the aid of data in Table 1.23 will be discussed in the paragraphs that follow.

Figure 1.46 shows that the depositions on rubber in DT1 and DT6 differ in magnitude by a factor of about 2 whereas those on silver, as well as those on activated carbon, agree excellently. No

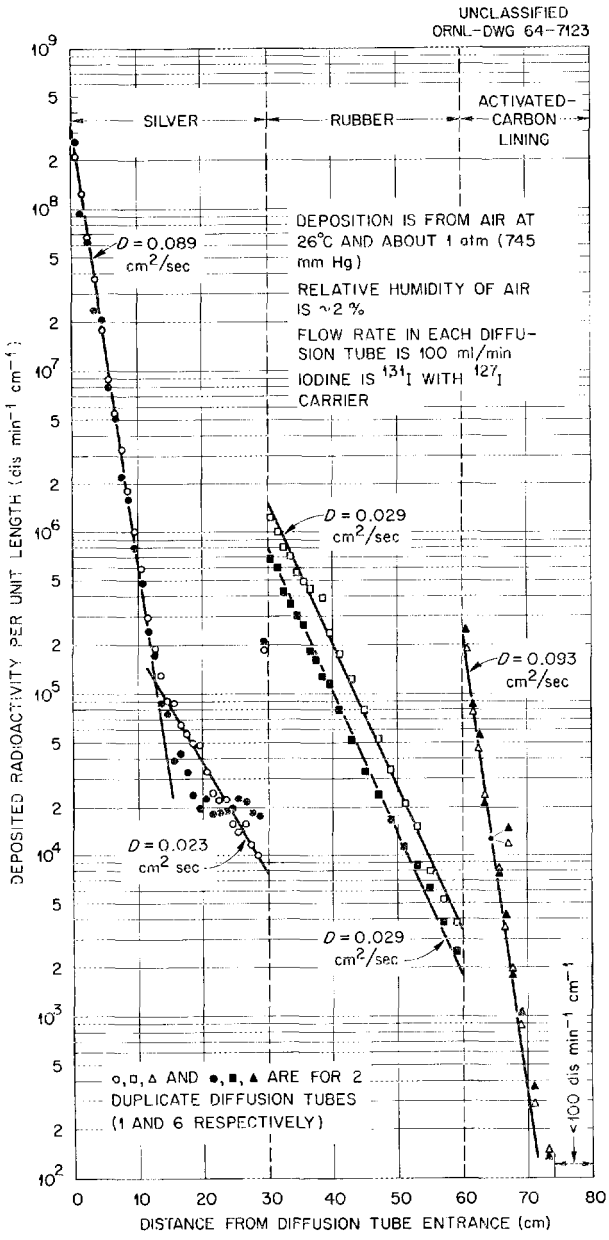


**Fig. 1.46. Deposition of Volatile Radioiodine Species in Composite Diffusion Tubes of the Usual Sequence.**

explanation for the difference appears to be available although it may be due to a loss or change of one species on passing through the header either at room temperature or while passing through the warm region of the header in the vicinity of the heated diffusion tube. The deposit on rubber appears too large to be an extension of that observed on the part of the silver surface where $I_2$ deposition is low. This would suggest that the latter deposit represents a species distinct from that which produces the deposit on rubber. However, the potential magnitude of the deposit on silver may be grossly understated by the extrapolation employed for its estimation in which event it may be reflecting one or more of the compounds deposited more efficiently downstream. Also, it appears that the deposit on activated carbon is too large to be an extension of that on silver or rubber. This suggests that the deposit on carbon is a species distinct at least in part from that which deposits on rubber. Thus, at least two vapor forms of iodine, in addition to elemental iodine, are indicated.

In Fig. 1.47 we see that the deposition on the first segment of activated carbon surface is at a high level and initially has a steep slope. As shown in Table 1.23, the integral of the steeply sloped portion exceeds the integral of the deposit on carbon in Fig. 1.46 by a factor of more than 10. This indicates that the compound(s) depositing on the rubber of Fig. 1.46 is partially being deposited on the carbon of Fig. 1.47 at a more rapid rate than in Fig. 1.46. However, not all is rapidly deposited as is evidenced by the indicated diffusion coefficient of 0.044 $cm^2$/sec. The average of the totals of the deposited radioactivity downstream of silver in Fig. 1.46 is compatible with that total of Fig. 1.47. The deposit on rubber in Fig. 1.47 still behaves as in Fig. 1.46, but its extent has been reduced by a factor of ~1000 by traversing the activated-carbon-lined segment. The fact that there is a very slight but noticeable deposit on the second activated-carbon-lined segment, even though the deposit on rubber dwindled to negligible amounts, is consistent with the behavior of these iodine compounds as observed at higher concentrations. These observations imply that the deposit on rubber in Fig. 1.46 may be reflecting the presence of at least two compounds, one of which can be induced to deposit more rapidly on carbon.

Figure 1.48 shows that the deposition on silver, first section, and on rubber are in good agreement with the analogous depositions of Fig. 1.46. The deposition on the second section of silver indicates the generation during passage through the rubber tubing of a small amount of some substance which rapidly reacts with silver such as $I_2$ or HI. The amount of this substance, characterized by $D$ = 0.134 $cm^2$/sec, is roughly 50% of the value

Table 1.25. Radioactivity Integrals for Volatile Iodine Species Deposited on Diffusion Tube Surfaces[a]

| Diffusion Tube | Surface | Calculated Diffusion Coefficient ($cm^2/sec$) | $\int_0^\infty y\,dx$ | $\int_{end}^\infty y\,dx$ (ref. b) | Calculated $I_2$ Purity (%) |
|---|---|---|---|---|---|
| 1 | Silver | 0.089 | $9.0 \times 10^{-1}$ | $<4 \times 10^{-7}$ | 97.0 |
| 1 | Silver | 0.023 | $1.1 \times 10^{-2}$ | $9.6 \times 10^{-5}$ | |
| 1 | Rubber | 0.029 | $1.5 \times 10^{-2}$ | $3.7 \times 10^{-5}$ | |
| 1 | Activated carbon | 0.093 | $7.6 \times 10^{-4}$ | $<4 \times 10^{-7}$ | |
| 6 | Silver[c] | 0.089 | $9.0 \times 10^{-1}$ | $<4 \times 10^{-7}$ | 97.8 |
| 6 | Silver[c] | 0.023 | $1.1 \times 10^{-2}$ | $9.6 \times 10^{-5}$ | |
| 6 | Rubber | 0.029 | $8.2 \times 10^{-3}$ | $1.9 \times 10^{-5}$ | |
| 6 | Activated carbon[c] | 0.093 | $7.6 \times 10^{-4}$ | $<4 \times 10^{-7}$ | |
| 2 | Silver | 0.097 | 1.0 | $<4 \times 10^{-7}$ | 97.7 |
| 2 | Silver | 0.016 | $8.4 \times 10^{-3}$ | $3.3 \times 10^{-4}$ | |
| 2 | Activated carbon | 0.081 | $1.1 \times 10^{-2}$ | $<4 \times 10^{-7}$ | |
| 2 | Activated carbon | 0.044 | $4.9 \times 10^{-3}$ | $1.2 \times 10^{-5}$ | |
| 2 | Rubber | 0.029 | $1.2 \times 10^{-5}$ | $<1 \times 10^{-6}$ | |
| 2 | Activated carbon | ~0.05 | $1.3 \times 10^{-6}$ | $<6 \times 10^{-7}$ | |
| 3 | Silver | 0.085 | $8.1 \times 10^{-1}$ | $<4 \times 10^{-7}$ | 97.2 |
| 3 | Silver | 0.016 | $5.5 \times 10^{-3}$ | $2.2 \times 10^{-4}$ | |
| 3 | Rubber | 0.027 | $1.7 \times 10^{-2}$ | $6.5 \times 10^{-5}$ | |
| 3 | Silver | 0.134 | $3.9 \times 10^{-5}$ | $<4 \times 10^{-7}$ | |
| 3 | Silver | 0.004 | $4.9 \times 10^{-5}$ | $2.2 \times 10^{-5}$ | |
| 3 | Activated carbon | 0.085 | $4.9 \times 10^{-4}$ | $<4 \times 10^{-7}$ | |
| 4 | Activated carbon | 0.090 } d | $8.8 \times 10^{-1}$ | $<4 \times 10^{-7}$ | e |
| 4 | Activated carbon | 0.078 } d | | | |
| 5 | Silver | 0.129 | $9.0 \times 10^{-1}$ | $<4 \times 10^{-7}$ | 99.3 |
| 5 | Silver | 0.017 | $3.9 \times 10^{-3}$ | $2.5 \times 10^{-4}$ | |
| 5 | Rubber | 0.057 | $1.3 \times 10^{-3}$ | $<8 \times 10^{-7}$ | |
| 5 | Rubber | 0.018 | $3.9 \times 10^{-4}$ | $2.2 \times 10^{-5}$ | |
| 5 | Activated carbon | 0.128 | $7.8 \times 10^{-4}$ | $<4 \times 10^{-7}$ | |

[a]Data expressed as a fraction of $4.9 \times 10^8$ dis/min, the activity of the largest integral.

[b]In general, where a "less than" sign (<) is employed, the magnitude of the integral is much less than indicated by the number given.

[c]Diffusion coefficient and integrals taken to be the same as for diffusion tube No. 1.

[d]Radioactivities corresponding to the two diffusion coefficients not evaluated separately.

[e]Not evaluated since separating $I_2$ deposition from that of other species is not feasible for this particular diffusion tube.

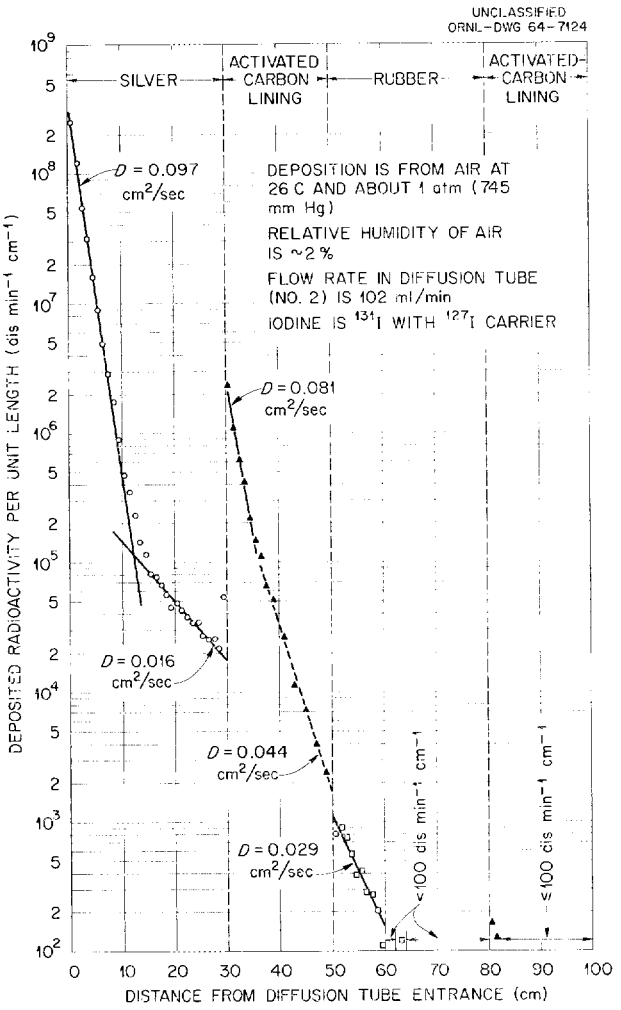


**Fig. 1.47. Deposition of Volatile Radioiodine Species in a Composite Diffusion Tube Designed to Investigate the Low Diffusion Coefficient Observed with a Rubber Surface.**

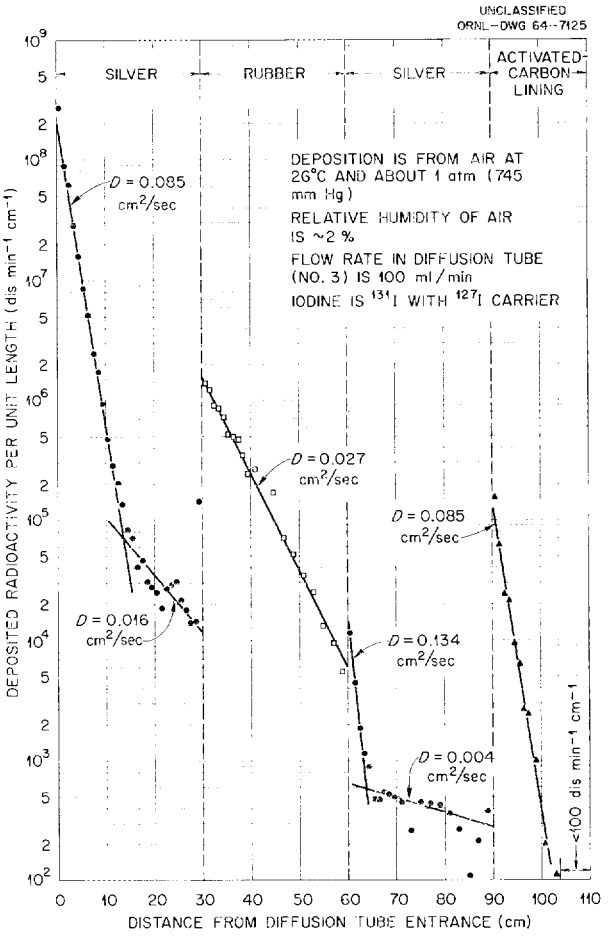


**Fig. 1.48. Deposition of Volatile Radioiodine Species in a Composite Diffusion Tube Designed to Detect Compound Decomposition.**

obtained by extrapolation of the deposit on rubber to infinity (i.e., from the end of the rubber section to infinity). The diffusion coefficient of 0.134 $cm^2/sec$ is based on too few data to make a distinction between $I_2$ and HI, but it is suggested that the deposit is due to the latter since the accepted value for $I_2$ under these conditions is 0.085 $cm^2/sec$ and the estimated value for HI is 0.117 $cm^2/sec$. If the poorly defined deposits on the separated silver sections represent the same substance and if their extent of deposition varies as concentration to the first power as a linear projection would imply, this substance would appear to be different from the deposit on rubber since the ratio of the latter deposit to that of the adjacent deposit on silver changes by a factor of 10 (from $10^2$ to $10^1$) from the entrance of the rubber section to its exit. Or similarly, it may be reasoned that if the poorly defined deposit on the first silver section and the deposit on rubber are the same substance, then the poorly defined deposit on the second silver section is a different substance. On the other hand, the depositions under consideration, on rubber and silver, may be manifestations of the same material if the extent of the deposition on silver varies as concentration to an appropriate power or powers less than 1. The slope of the poorly defined deposit on the

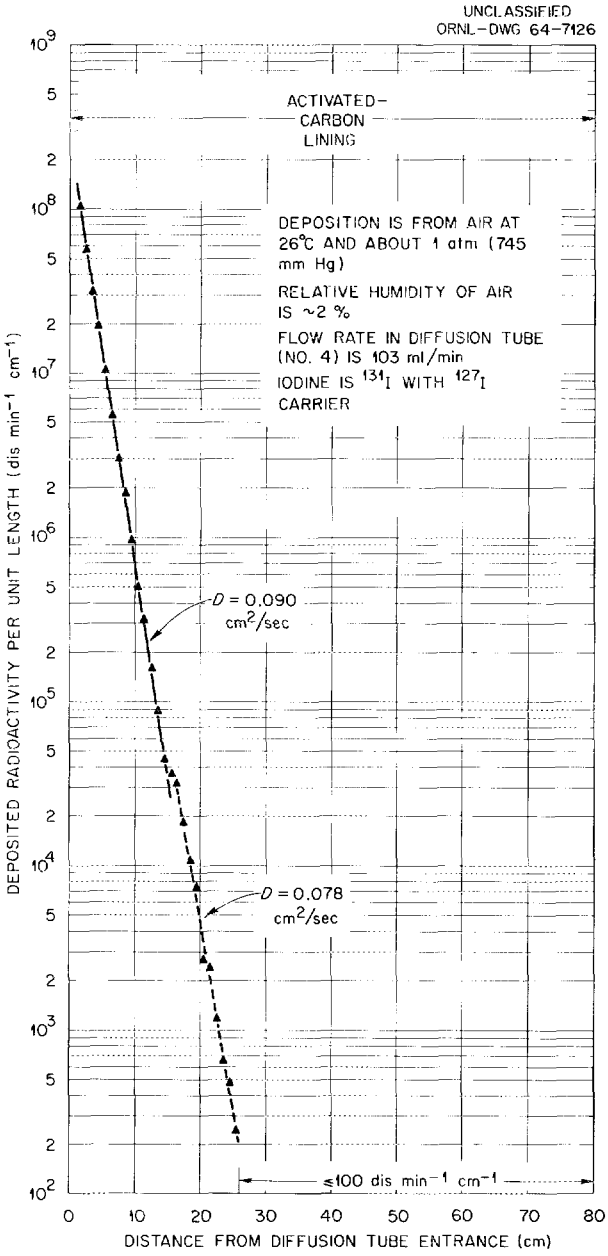


**Fig. 1.49. Deposition of Volatile Radioiodine Species in an Activated-Carbon-Lined Diffusion Tube.**

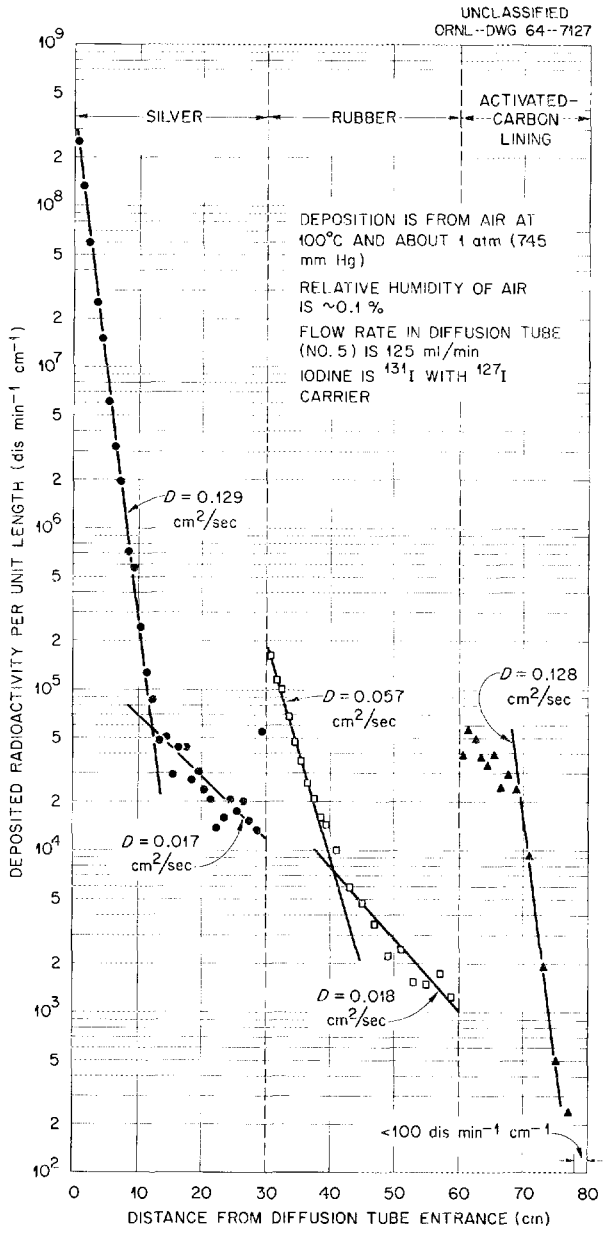


**Fig. 1.50. Deposition of Volatile Radioiodine Species in a Heated Composite Diffusion Tube.**

second silver section is so low and indefinite that it is conceivable, but does not appear probable, as shown in Table 1.23, that its extrapolation to infinity could be equivalent to the subsequent deposit on the activated-carbon surface. The latter deposit, which occurs immediately downstream of 25 cm of silver-lined tubing with a sparse deposition of radioactivity, is evidently neither $I_2$ nor HI since $I_2$ reacts quantitatively with silver, as seen in these and other experiments, and Perkins has reported that HI readily reacts with silver.[17] These observations indicate that a small amount of HI or $I_2$ is generated during

[17] R. W. Perkins, *Health Phys.* 9, 1113–22 (1963).

passage through rubber tubing but that the subsequent deposit on charcoal is distinct from HI or $I_2$.

In Fig. 1.49 we see that all of the various iodine species are apparently deposited at a rate corresponding to a relatively high diffusion coefficient. The value 0.090 $cm^2/sec$ corresponds, within the limits of experimental error, to that for $I_2$, and the deposit masks the deposits of other species. The region where the dashed line appears is probably showing evidence of the same sort of behavior exhibited in the lower portion of the first activated-carbon section of Fig. 1.47. The fact that iodine carried by particles was not a factor in this experiment is conclusively shown since their diffusion coefficients are relatively low and, if their concentration were appreciable, they would have produced a measurable deposit beyond 26 cm in this diffusion tube. The apparent diffusion coefficients of 0.027–0.029 $cm^2/sec$ observed with rubber are evidently an artifact; otherwise the corresponding species would have manifested itself at the diffusion tube distance of 30 cm to the extent of about $5 \times 10^3$ dis $min^{-1}$ $cm^{-1}$ as judged by the nature of the deposition on rubber in Figs. 1.46 and 1.48. That is, the data in Fig. 1.49 indicate that iodine compounds with molecular weights grossly in excess of that for $I_2$ are not present in appreciable quantities. Thus, a more complex mechanism is required to explain the depositions on rubber.

Figure 1.50 shows that at 100°C the $I_2$ deposition on silver is quite similar to that already observed after making allowance for the increase in diffusion coefficient with an increase in temperature. The increase observed is in good accord with theory. The same statement regarding diffusion coefficients is true for deposition on activated carbon in the region where the activated carbon appeared to behave as a perfect sink. The apparent diffusion coefficient, 0.057 $cm^2/sec$, observed on rubber, increased considerably more with increased temperature than theory predicts, again indicating that the process is more complex than the normal diffusion to a perfect sink of a high-molecular-weight iodine compound. The fact that the lower part of the plot of $^{131}I$ deposition on rubber suggests a lower diffusion coefficient is probably a superficiality. The extent of deposition on rubber in the heated diffusion tube is lower by a rather large factor than those in the similarly arranged unheated tubes. A more or less obvious interpretation is that the higher temperature has resulted in extensive decomposition of the corresponding substance or substances to $I_2$ or HI. The bulk of the postulated decomposition may have occurred in the first part of the silver section where $I_2$ initially present would have effectively masked its presence. The capacity of the activated carbon is severaly limited by the increase in temperature. While a lowering of capacity is of course to be anticipated, the effect is rather pronounced considering the low range of concentrations involved. However, the total amount deposited on activated carbon was essentially unaffected by the increase in temperature. This fact supports the previously noted indication that the substance depositing on activated carbon is distinct from that depositing on rubber. These observations indicate that heating a diffusion tube alters the deposition distribution of radioiodine compounds, but meaningful results are still obtained.

## Conclusions

The foregoing observations point to the presence of at least two distinct iodine species other than $I_2$, and one of the species is indicated to be relatively unstable. The results conceivably could be interpreted in terms of just one iodine compound, in addition to the $I_2$, but a rather complex mechanism seems to be required. The deposition rate on rubber tubes is primarily not diffusion limited but probably involves dissociation of an iodine compound to yield HI or $I_2$. Iodine carried by particulates is not a factor with the dichromate method. The deposit on charcoal following a rubber tube is associated with a species distinct from HI and $I_2$. A heated composite diffusion tube yields an altered but interpretable distribution and may be useful with moist atmospheres. While considerable additional information about the behavior of iodine substances in diffusion tubes was provided by this experiment, the interpretation of many aspects is still unclear, and additional work is planned to further elucidate the chemistry of volatile radioiodine.

## INVESTIGATION OF OCCURRENCE AND BEHAVIOR OF VOLATILE COMPOUNDS OF IODINE

W. E. Browning, Jr. R. E. Adams
Juergen Wilhelm[18]

Efforts are being directed toward the determination of the origin, identity, and behavior of the volatile compounds of iodine since the behavior of these compounds can greatly affect the fate of iodine in reactor accidents and the operating efficiency of iodine-removal systems. It has been reported previously[19] that iodine sources produced by either the palladium iodide or the dichromate method contain small amounts of at least two volatile compounds of iodine, in addition to elemental iodine.

[18]Karlsruhe Center for Nuclear Research and Development, Karlsruhe, West Germany.

[19]W. E. Browning, Jr., R. D. Ackley, and R. E. Adams, *Nucl. Safety Program Semiann. Progr. Rept. Dec. 31, 1963*, ORNL-3547, pp. 60–64.

When gas is passed over an iodine source held at a temperature of −70°C, there is a rapid initial transport of $^{131}I$ activity from the source followed by a slower, reasonably constant rate of transport. The initial, rapid release of $^{131}I$ activity indicates the presence of an iodine compound(s) more volatile than elemental iodine, and the gradual release of $^{131}I$ activity following the initial release is characteristic of either elemental iodine or a compound of similar volatility. These fractions have been arbitrarily labeled *A* and *B* respectively.

To aid in the study of the behavior of these iodine compounds under various conditions, the system illustrated in Fig. 1.51 is being utilized. Provisions were made to divide the main gas stream and to introduce one half upstream and the other half downstream of the first diffusion tube. A second diffusion tube was included farther downstream. This arrangement allows the first diffusion tube to characterize the iodine source

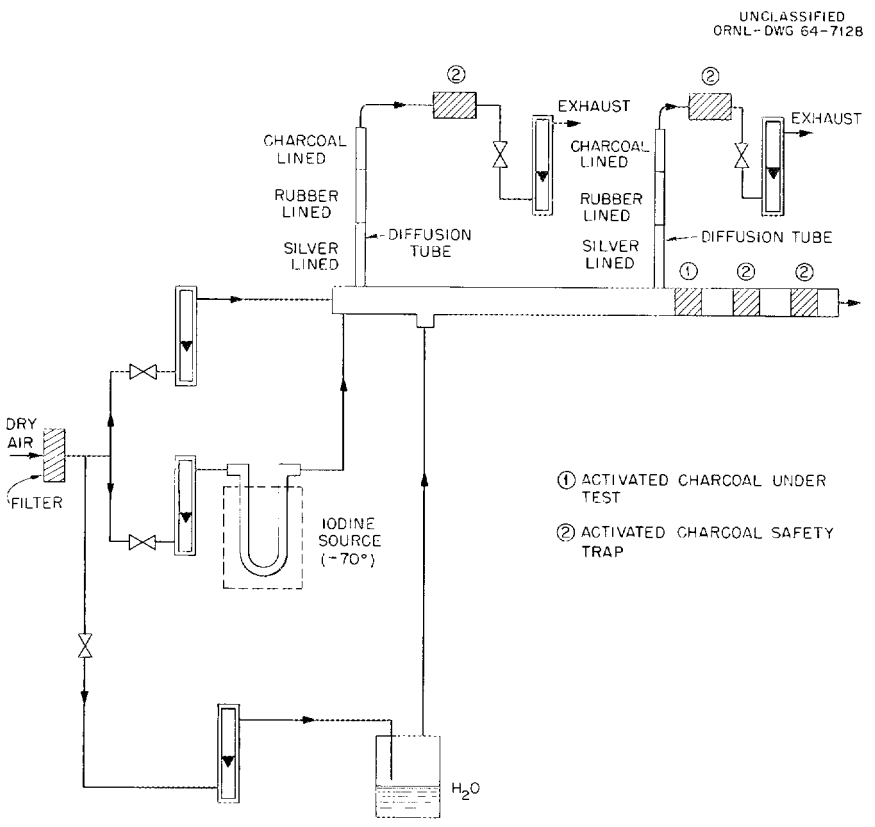


Fig. 1.51. Schematic of Laboratory Apparatus to Study Behavior of Iodine and Iodine Compounds by Diffusion Tube Analysis.

before any conditions are changed in the experiment. This is necessary due to slight variations in the iodine sources. The distribution of $^{131}I$ in the second diffusion tube indicates the extent of influence of any interfering gas or material introduced in the second half of the air sweep. Initial studies have included an assessment of the influences of moisture and of source temperature on the distribution pattern of iodine and iodine compounds in the diffusion tube. The experimental techniques devised for this study will be applied to observations of the influence of other added impurities, such as organic vapors and oil vapor, in the air stream.

The charcoal-lined portion of a diffusion tube assembly may be regarded as a macroscopic representation of the microscopic behavior of iodine compounds in a channel between granules in a charcoal adsorber. One would expect, on this basis, the response of the *A* fraction of an iodine source to moisture in a charcoal adsorber to be the same as it was in the diffusion tube. This similarity of response has been observed, and the results of experiments of this type are presented elsewhere in this section.

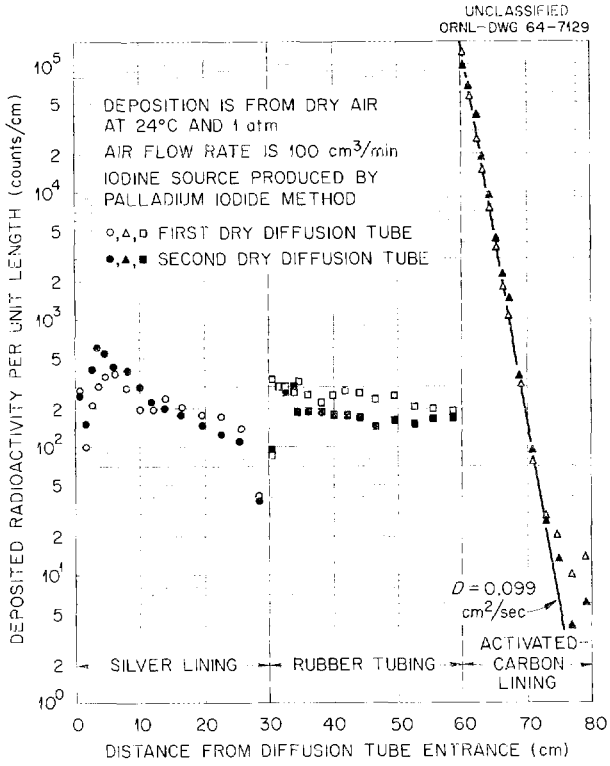


**Fig. 1.52. Diffusional Deposition of a Volatile Iodine Compound Under Dry Conditions.**

### In Dry Air

Experiments with dry air sweep (relative humidity <3%) at room temperature (22 to 24°C) carrying the *A* fraction separated from radioiodine produced by the palladium iodide method have yielded deposition profiles in the upstream and downstream diffusion tubes which are typified by the data in Fig. 1.52. These deposition patterns indicate that most of the radioiodine was in a form which deposited on activated carbon with a diffusion coefficient of 0.099 $cm^2/sec$ and that the composition did not change appreciably between the two points sampled. These and other similar results indicate that (1) there was no reaction or decomposition of the iodine compounds (fraction *A*) upon leaving a source at temperatures of −70, 0, or 22°C, (2) there was no reaction or decomposition (aging) of the iodine compounds during a system transit time ranging from 4 to 16 sec, (3) there was no selective loss of any of the iodine compounds to the walls of the system, and (4) there was a good reproducibility of measurements.

### In Moist Air

The addition of moisture to the second half of the air sweep, which entered downstream of the first diffusion tube, produced a very noticeable effect on the deposition profile of the *A* fraction in the charcoal-lined tube of the second diffusion tube assembly. The upstream diffusion tube indicated a normal behavior under dry conditions while the downstream diffusion tube exhibited a different behavior. The magnitude of this influence varied, depending upon whether or not all of the charcoal surface of the tube was saturated with the moisture in the system. Figure 1.53 illustrates the deposition profile obtained from an experiment when all of the diffusion tube was saturated with an air stream of approximately 30% relative humidity. Under partial saturation conditions a straight-line relationship was not obtained; a chromatographic type of wave pattern was produced. From the information obtained, it

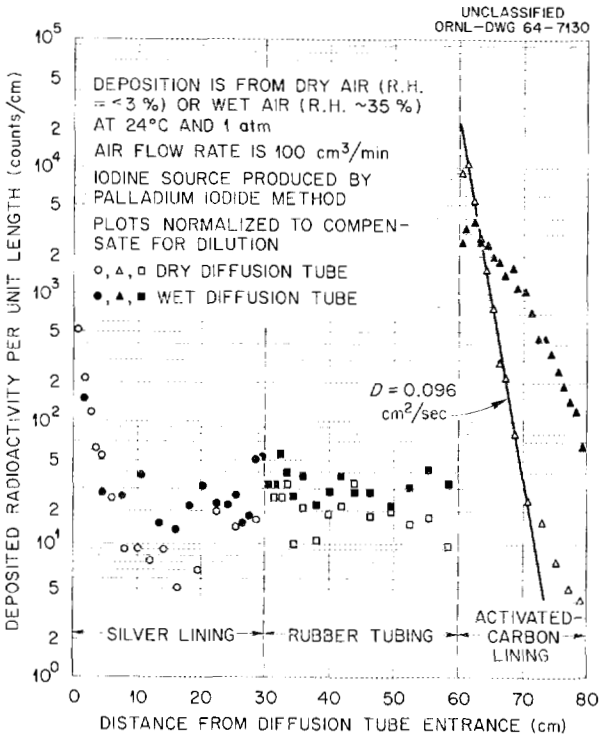


**Fig. 1.53. Comparison of Diffusional Deposition of a Volatile Iodine Compound Under Both Wet and Dry Conditions.**

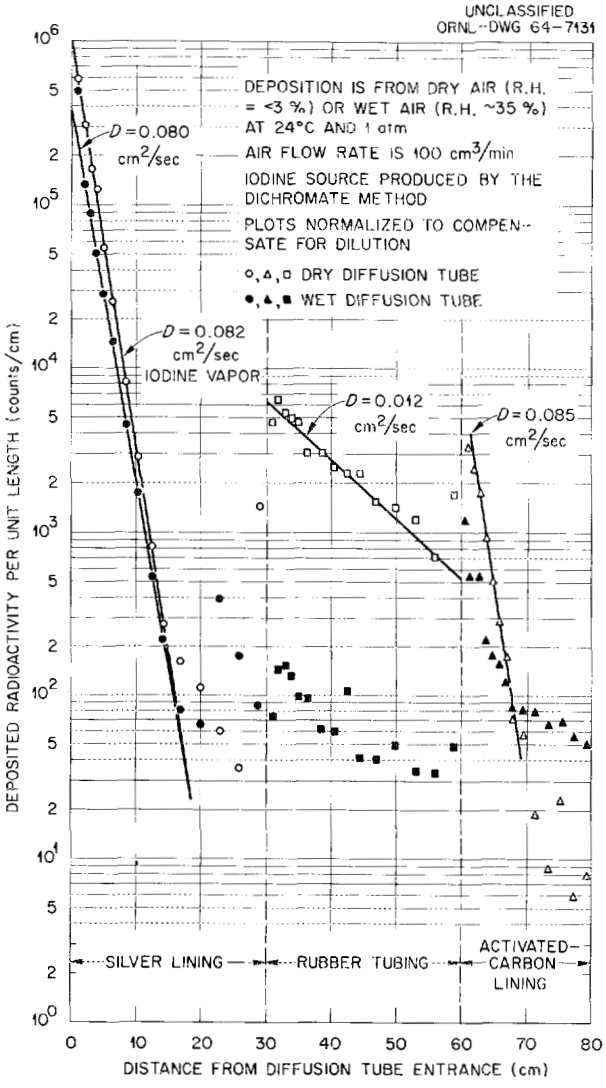


**Fig. 1.54. Comparison of Diffusional Deposition of Iodine Vapor and a Volatile Iodine Compound Under Both Wet and Dry Conditions.**

appears that moisture interferes with the adsorption of the iodine compounds at the charcoal surface rather than being instrumental in forming a new, less reactive compound of iodine. Moisture does not strongly affect the behavior of elemental iodine vapor, the principal constituent of the *B* fraction of an iodine source. The effect of moisture on the diffusion tube pattern of elemental iodine is illustrated in Fig. 1.54 where the elemental iodine resided on the silver portion of the diffusion tube; no influence due to moisture was noted. The data in Fig. 1.54 were obtained using iodine prepared by the dichromate method, and the deposition on rubber was similar to that described elsewhere in this report in the section entitled "Development of Methods for Measuring Forms of Gas-Borne Radioiodine." The introduction of moisture reduced this deposit fifty-fold, possibly as a result of interference by moisture adsorbed on the rubber surface.

## Solubility Behavior of Volatile Iodine Compounds

It has been demonstrated by diffusion tube analysis that iodine sources nominally in the elemental form can have a small fraction of the iodine existing in compound forms which are rather difficult to remove from air under certain conditions. At least three vapor species have been distinguished, and workers in England[20] have

[20] A. C. Chamberlain *et al.*, *J. Nucl. Energy: Pt. A & B* 17, 519–50 (1963).

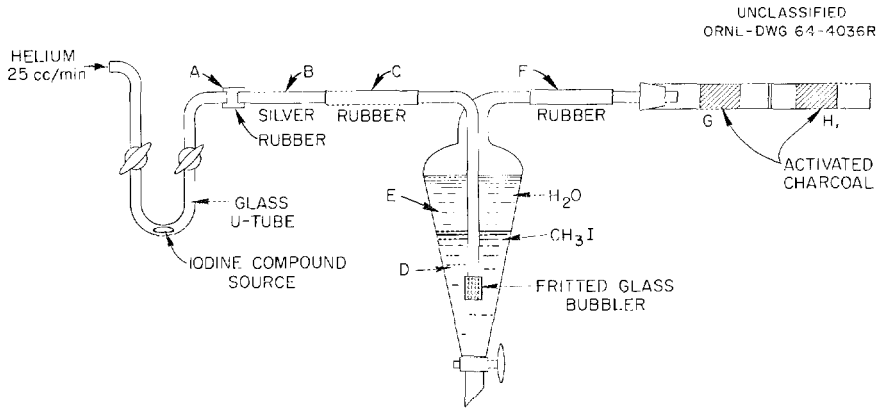


**Fig. 1.55. Apparatus for Investigating Solubility of Selected Iodine Vapor Species.**

identified one of the forms of gas-borne radioiodine as methyl iodide. Figure 1.55 illustrates the apparatus used to perform an experiment to determine whether methyl iodide is contained in the *A* fraction of iodine sources prepared by the palladium iodide method and also to investigate the applicability of differential solubility as a tool to characterize the volatile iodine compounds. Three experiments were performed. In the first two experiments the *A* fractions were separated from iodine sources by use of different techniques, were placed in independent containers, and were introduced into the experiments. In the third, pure methyl iodide vapor, tagged with radioactive methyl iodide (tagged methyl iodide obtained from Volk Radiochemical Co., Skokie, Ill.; produced by the exchange of $CH_3Br$ and $Na^{131}I$ in acetone), was introduced into the experiment. A gas sweep, containing the volatile iodine compound, was passed through a silver-lined tube and a rubber tube prior to entering the separatory funnel containing nonradioactive methyl iodide and water. In the first two experiments, the distribution coefficient between the two phases was about 55 in favor of methyl iodide. This corresponds approximately to the expected distribution considering the solubility of methyl iodide in water. The distribution coefficient in the third experiment using tagged methyl iodide was comparable. The results presented in Table 1.26 indicate that the mixture of iodine vapor species emanating from the iodine vapor source includes methyl iodide or an iodine compound of similar solubility.

**Table 1.26. Sorption and Solubility Behavior of Volatile Iodine Compounds**

| Sample Identity (see Fig. 1.55) | Relative Amount of Activity[a] | | |
|---|---|---|---|
| | Exp. 1[b] | Exp. 2[b] | Exp. 3[c] |
| A – rubber tube | 0.39 | 0.019 | 0.008 |
| B – silver tube | 0.92 | 0.023 | 0.001 |
| C – rubber tube | 0.69 | 0.32 | 0.92 |
| D – methyl iodide | 1.00 | 1.00 | 1.00 |
| E – water | 0.02 | 0.015 | 0.017 |
| F – rubber tube | 0.001 | 0.014 | 0.011 |
| G – charcoal | 0.008 | 0.053 | 0.073 |
| H – charcoal | 0.007 | 0.003 | 0.000 |
| Distribution coefficient ($CH_3I/H_2O$) | 49.6 | 61.9 | 46.2 |

[a]Data in each column normalized to methyl iodide sample = 1.00.

[b]Experiments using *A* fraction consisting of iodine compounds volatilized at −70°C.

[c]Experiment using $^{131}I$-labeled $CH_3I$.

## INNOCUOUS SIMULATION OF AEROSOLS PRODUCED BY REACTOR ACCIDENTS

W. E. Browning, Jr. R. E. Adams

A study is under way to develop ways of simulating the radioactive materials which would be released during a reactor accident, making use of

test materials which are less hazardous. Such innocuous "simulants" will be of value for investigating the behavior of released fission products in the various stages of reactor containment and in gas-cleaning systems. Information obtained in this program and in related iodine programs has been applied in developing an iodine-efficiency test procedure for full-scale operating charcoal adsorber systems. Either natural iodine in the elemental form or natural iodine tagged with $^{131}I$ has been applied previously in testing the 1500-cfm off-gas system of the Nuclear Ship "Savannah." More recently the applicability of these testing techniques has been explored by applying them to the 9000-cfm building ventilation system of the ORR. This system contains both particulate filters and activated-charcoal units for the decontamination of off-gases containing accident-released fission products.

Radioactive iodine vapor (100 mg of $^{127}I$ containing 15 mc of $^{131}I$) was introduced into the ventilation duct in the basement of the ORR, and a continuous sample of the off-gas was processed through small activated charcoal samplers. These samples were taken upstream and downstream of the filter pits which are approximately 100 ft from the point of iodine vapor injection. Four tests were run, and efficiencies of 99.93, 99.83, 99.86, and 99.78% were observed.

Consideration is now being given to possible assistance in the initiation of routine in-place tests of iodine adsorbers on the off-gas systems of several reactors under construction in the ORNL area.

## REMOVAL OF IODINE AND VOLATILE IODINE COMPOUNDS FROM AIR SYSTEMS BY ACTIVATED CHARCOAL

W. E. Browning, Jr. R. E. Adams

The effectiveness of activated charcoal adsorbers for the various forms of iodine must be known in order that the reliability of such engineered safeguards can be evaluated for containment of reactor accidents.

In experiments described earlier in this report, it was noted that when the iodine vapor source was divided into two fractions, the first (*A*) being that part which is vaporized in less than 10 min at −70°C and the second (*B*) being that which is vaporized after 10 min, the behavior of the *A* fraction in a charcoal adsorber was affected by moisture to a much larger extent than the *B* fraction was. This observation prompted the initiation of a more systematic study. The behavior of the *A* and *B* fractions of an iodine source (prepared by the palladium iodide method) toward three types of activated charcoal under varying degrees of temperature and humidity is being investigated by use of the test apparatus illustrated schematically in Fig. 4.4 of the previous report of this series.[19] The conditions of the tests were as follows: bed depth, 1.5 in.; gas velocity, 25 fpm; duration, 5 hr. The concentration of the *A* fraction evaluated over the 10-min injection period was 0.05 mg/m$^3$, while that of the *B* fraction over its 5-hr injection period was 0.01 mg/m$^3$. The three activated charcoals used in this study were selected mainly because of their availability in this laboratory and to typify three types of charcoals: bituminous coke (Pittsburgh BPL), coconut shells (Pittsburgh PCB), and a charcoal containing metallic impregnants (Whetlerite, BPL charcoal impregnated with silver, copper, and chromium). Equivalent activated charcoals produced by other manufacturers will probably produce comparable results.

Results obtained in this continuing study are presented in Table 1.27. The volatile fraction (*A*) is the one most difficult to remove from gases under humid conditions as is evidenced by experiments 1, 2, 4, and 6. Of the three charcoals, PCB (coconut) is the most effective for removing this fraction. Under dry conditions, approximately 3% relative humidity, all three charcoals are effective as shown by experiments 3, 5, and 7. The less volatile fraction (*B*), which is primarily elemental iodine but may contain other iodine forms, is removed efficiently by all three charcoals, but the coconut-base charcoal (PCB) appears to be somewhat more effective than the other two. In similar experiments (Nos. 8–14) at 100°C, both iodine source fractions were removed effectively by all three charcoals under varying conditions of humidity. Coconut charcoal, which was the best adsorber under the worst conditions (high humidity at room temperature), gave a minimum efficiency of 97% for the volatile fraction. This efficiency may be adequate since experience indicates that the nonelemental forms comprise only a small fraction of the iodine inventory.

Table 1.27. Removal of Iodine and Its Volatile Compounds from Air by Activated Charcoal[a]

| Experiment | Charcoal Type | Charcoal Temp (°C) | Iodine Fraction[b] | Relative Humidity (%)[c] | Efficiency (%) |
|---|---|---|---|---|---|
| 1 | Bituminous coke | 23 | *A* | 65 | 50.25 |
| | | | *B* | 77 | 97.87 |
| 2 | Bituminous coke | 20 | *A* | 77 | 73.42 |
| | | | *B* | 77 | 99.03 |
| 4 | Coconut | 20 | *A* | 77 | 97.34 |
| | | | *B* | 77 | 99.65 |
| 6 | Whetlerite[d] | 20 | *A* | 77 | 61.87 |
| | | | *B* | 77 | 96.11 |
| 3 | Bituminous coke | 24 | *A* | <3 | 99.97 |
| | | | *B* | <3 | 98.49 |
| 5 | Coconut | 23 | *A* | 4 | 99.89 |
| | | | *B* | <3 | 99.31 |
| 7 | Whetlerite | 23 | *A* | <3 | 99.91 |
| | | | *B* | (Not run) | |
| 8 | Bituminous coke | 100 | *A* | <3 | 99.89 |
| | | | *B* | (Not run) | |
| 9 | Bituminous coke | 100 | *A* | <3 | 99.87 |
| | | | *B* | <3 | 99.96 |
| 11 | Coconut | 100 | *A* | <3 | 99.99+ |
| | | | *B* | <3 | 99.66 |
| 13 | Whetlerite | 100 | *A* | <3 | 99.98 |
| | | | *B* | <3 | 99.89 |
| 10 | Bituminous coke | 100 | *A* | ~100 | 99.94 |
| | | | *B* | ~100 | 99.87 |
| 12 | Coconut | 100 | *A* | ~100 | 99.91 |
| | | | *B* | ~100 | 99.76 |
| 14 | Whetlerite | 100 | *A* | ~100 | 99.94 |
| | | | *B* | ~100 | 99.98 |

[a]Bed depth, 1.5 in.; gas velocity, 25 fpm; duration of tests, 5 hr.

[b]*A* is the volatile fraction (low-molecular-weight iodine compounds), and *B* is the less volatile fraction (primarily elemental iodine), when the iodine source is at −70°C. *A* is injected during initial 10 min of test at 0.05 mg/m$^3$, *B* over 5-hr test duration at 0.01 mg/m$^3$.

[c]Humidity of entering air evaluated at room temperature.

[d]Bituminous coke charcoal impregnated with salts of silver, copper, and chromium.

This series of experiments has demonstrated, under the conditions tested, that the anomalous behavior of iodine vapor in activated charcoal adsorbers under certain conditions can be explained by the occurrence of nonelemental forms of iodine and that selection of the proper charcoal type makes it possible to trap the more difficult-to-remove iodine fraction from air with a suitable efficiency.

## CHARACTERIZATION OF RADIOACTIVE AEROSOLS BY USE OF FIBROUS FILTERS

W. E. Browning, Jr. M. D. Silverman
L. F. Franzen[21]

Predicting the effectiveness with which fission products released in a reactor accident may be removed from gas streams requires a knowledge of the amounts associated with the different sizes of particles released. A method for characterizing radioactive aerosols has been developed which interprets the distribution of radioactive particles in a series of uniform fiber filters in terms of the three main mechanisms of filtration – diffusion, interception, and inertial impaction – and has been reported previously.[22] The data for this analysis are obtained by passing the radioactive aerosol through a series of uniform Dacron filters; the particle distribution vs depth in the filter bed, composed of discrete layers of fibers, is determined by radioassay. This method yields information about the behavior of aerosol particles within the fibrous bed in more minute detail than do other methods. It is thus possible to distinguish groups of particles according to size and in addition to devise new, more critical tests of filtration theory. Data from the initial series of experiments, which used a radioactive test aerosol containing $^{65}Zn$ particles in the diameter range 20 to 300 A and were conducted at linear velocities from 0.4 to 88 fpm, were analyzed in terms of the three mechanisms of filtration; analysis of the data in the diffusion region has been reported.[23,24]

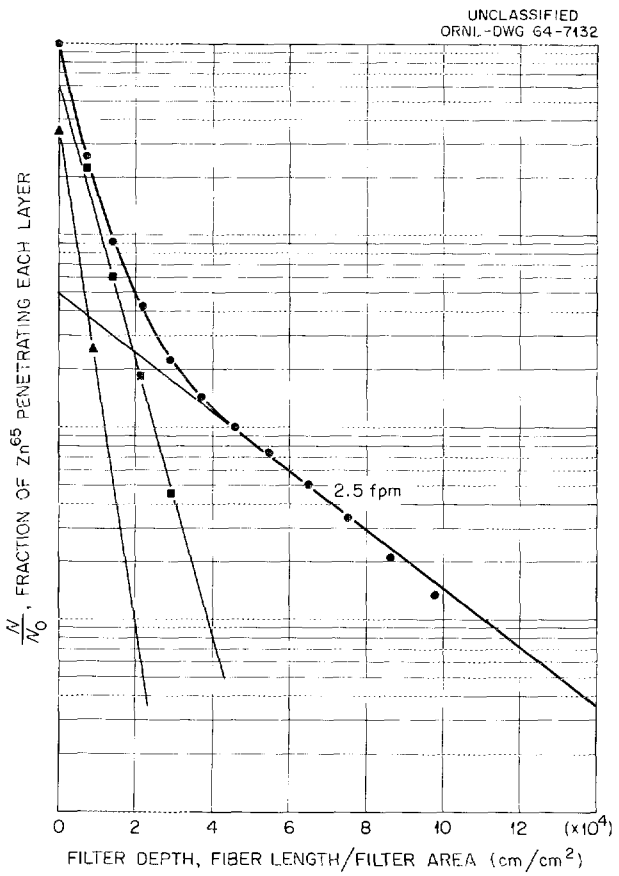


**Fig. 1.56. Filtration Efficiency at Various Depths Through Filter.**

Several series of experiments have been performed in which the porosity of the filter mats was raised from its original value (0.72) to 0.94. The data from a typical experiment are shown in Fig. 1.56 in which log $N/N_0$ for each layer is plotted as the ordinate against depth in the filter. Each layer contained approximately $10^4$ cm of fiber per square centimeter of filter area, evaluated from disk weights and the density of the fiber. It may be noted that the filtration curve has been resolved into three straight lines, evidencing three different particle-size groups. The effect of varying the filter porosity is shown in Figs. 1.57 and 1.58. The two sets of experiments plotted in Fig. 1.57 show that increasing the fraction of solids (or inversely, lowering the porosity) improves filtration, as expected. In this low-velocity range (2.5 and 10 fpm) the efficiency of filtration decreases with increasing velocity, indicating the

[21]On loan from Technischer Überwachungs-Verein, Essen e. V., Germany.

[22]W. E. Browning, Jr., and M. D. Silverman, *Nucl. Safety Program Semiann. Progr. Rept. Dec. 31, 1962*, ORNL-3401, pp. 50–55.

[23]M. D. Silverman and W. E. Browning, Jr., *Trans. Am. Nucl. Soc.* 6(2), 401 (1963).

[24]M. D. Silverman and W. E. Browning, Jr., *Science* 143, 572 (1964).

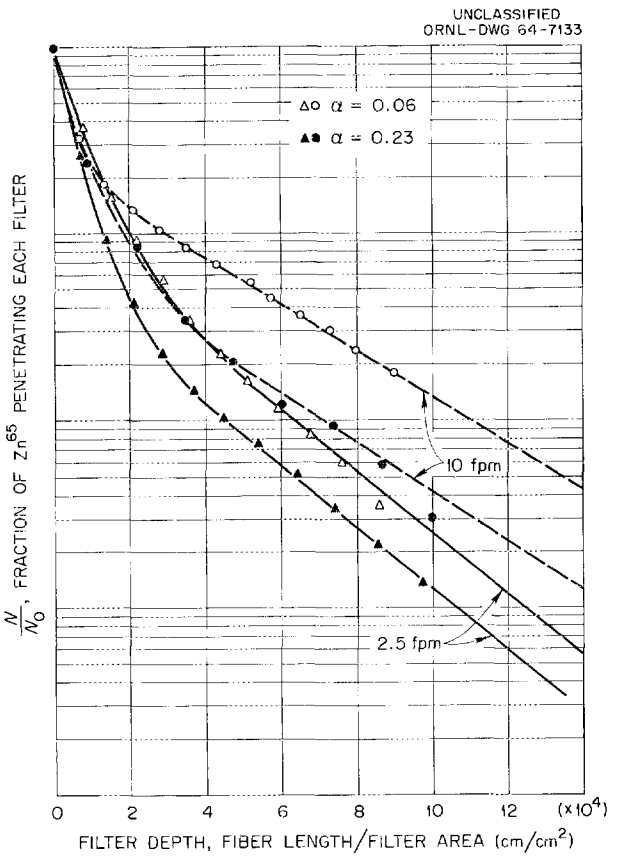


**Fig. 1.57. Effect of Porosity on Filtration Efficiency at Low Velocity.**

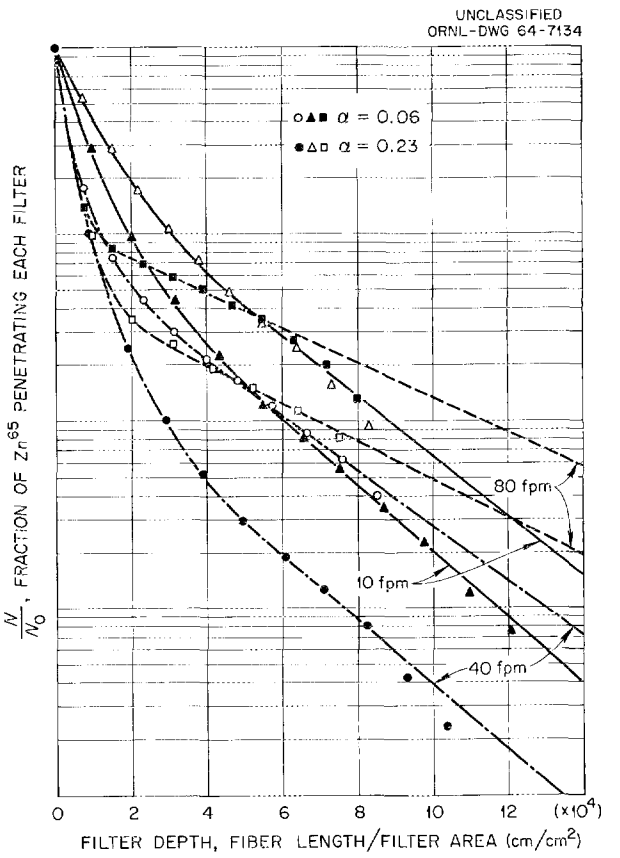


**Fig. 1.58. Effect of Porosity on Filtration Efficiency at High Velocity.**

diffusion regime. In Fig. 1.58, where the linear velocity is increased from 10 to 80 fpm, the effect of lowering the porosity is again shown by the improved filtration in each pair of experiments. Filtration efficiency apparently increases with increasing velocity over this range of flow, although the effect is greatest in going from 10 to 40 fpm and least from 40 to 80 fpm.

In summary, for each pair of experiments increasing $\alpha$ (the fraction of solids) or, inversely, lowering the porosity reduces the amount of the penetrating fraction. For the lower part of the curve, however, there is no change in slope, indicating that the same size-particle group continues to penetrate. Furthermore, filter efficiency seems to be improved by increasing $\alpha$ mainly at intermediate flow rates (40 fpm), less at lower and higher velocities (10 and 80 fpm), and insignificantly at very low flow rates (2.5 fpm).

Data previously obtained in the low-velocity range were treated by the simplified Stairmand[25] equation for particle diffusion. This equation, along with those of Langmuir,[26] Davies,[27] and Chen,[28] is based on a model of Lamb's original equations of flow around an isolated cylinder.[29] Fuks[30] has shown that filter efficiency calculated

[25] C. J. Stairmand, *Trans. Inst. Chem. Engrs. (London)* **28**, 130 (1950).

[26] I. Langmuir, OSRD Report No. 865, Office of Technical Services, Washington, D.C., 1942.

[27] C. N. Davies, *Proc. Inst. Mech. Engrs. (London)* **B1**, 185 (1952).

[28] C. Y. Chen, *Chem. Rev.* **55**, 595 (1955).

[29] H. Lamb, *Hydrodynamics*, 6th ed., p. 77, Cambridge, London, 1932.

[30] N. A. Fuks and I. B. Stechkina, *Proc. Acad. Sci. USSR, Chem. Technol. Sect.* (English Transl.) **147**, 230 (1962); *Ann. Occupational Hyg.* **6**, 27 (1963).

on the basis of a model of a system of parallel cylinders appears to conform better with experimental data than does the isolated cylinder model. Fuks argues that for the development of a more precise theory for fibrous filtration of aerosols a more realistic model should be employed, for example, a system of parallel cylinders of equal width. The detailed data now made available on behavior of aerosol particles in a fibrous bed are being used to test these various theories of filtration. The results, when completed, should make it possible to interpret the high-velocity filter deposition distributions in terms of the character of aerosols.

# Part 2
# Containment Engineering

Reactor Division

S. E. Beall, Division Director
W. B. Cottrell, Program Coordinator

Key Words[a]

accident analysis
aerosol
agglomerates
containment
containment analysis
containment design criteria
containment research and development
containment tests
codes and standards
deposition
energy sources
fallout
fission gas release
fission product release
fission product transport
meltdown
particulate
uranium oxide

[a]See Foreword.

# 2.1 Nuclear Safety Pilot Plant

C. J. Barton P. P. Holz
L. F. Franzen L. F. Parsly
T. H. Row

The purpose and design of the Nuclear Safety Pilot Plant (NSPP) were described in previous reports.[1,2] Briefly, its purpose is to evaluate the transport behavior of fission products in a simulated containment system of sufficient size to permit the extrapolation of the transport behavior of fission products as observed in laboratory-scale tests up to actual containment systems. It is not the intent of this facility to simulate the fission-product release spectrum of any one postulated accident, but rather to produce a known, and variable, spectrum whose behavior in the model containment vessel may be observed as a function of time in response to various stimuli, for example, deposition (on different materials) and condensation (from steam in the vessel).

The facility has been designed and constructed with a plasma torch for melting fuel materials, a stainless steel containment vessel into which fission products are released, various sampling devices for determining the time and spatial distribution of the various chemical and physical forms of the released fission products, and provision has been made to test the effectiveness of various fission-product removal devices (e.g., sprays and filters). Inasmuch as the facility is to be operated with up to 1000 curies of activity in the fuel to be melted, a significant feature is the capability for remote operation, semiremote removal of samples, disassembly of the major items of hardware, and decontamination of the equipment.

Construction of the facility as initially designed was completed during the report period, and all equipment was placed into operation. However, installation of some of the more recently developed sampling devices, such as May packs and diffusion tubes, and extension of the experimental capability of the facility (by generating a steam environment within the vessel, by mixing the air in the vessel, and by decreasing the inlet flow velocity to the vessel) were considered desirable, and these changes are being made.

There were, however, many developmental tests conducted upon the furnace uncoupled from the containment vessel and two tests of the entire facility employing unirradiated $UO_2$ in which the $UO_2$ particular behavior in the vessel was observed.

## BEHAVIOR OF PARTICLES FROM MOLTEN $UO_2$

Two runs were made in which unirradiated $UO_2$ was melted. The behavior of the aerosol generated was observed by:

1. measuring the condensation nuclei concentration by a condensation nuclei counter,
2. sampling the vessel atmosphere with paper tape air samplers using various filter media,
3. using deposition coupons in the model containment vessel,
4. using a paper tape fallout sampler, and
5. using fallout cups.

In the first run, no sweep gas was used, and the fan in the model containment vessel was not

[1] M. H. Fontana and C. G. Lawson, *Nucl. Safety Program Semiann. Progr. Rept. June 30, 1962*, ORNL-3319, pp. 51–62.

[2] L. F. Parsly, Jr., *Nuclear Safety Pilot Plant Hazards Summary Report*, ORNL-TM-683 (Oct. 4, 1963).

**Table 2.1. Experiment Conditions and Distribution of Uranium**

| | Run 1 | Run 2 |
|---|---|---|
| **Experimental Conditions** | | |
| Torch gas | Helium | Helium |
| Torch gas flow | 1.7 cfm | 1.7 cfm |
| Sweep gas | None | Helium |
| Sweep gas flow | | 3.0 cfm |
| Vessel fan | Not operated | Operated |
| **Uranium Distribution (%)** | | |
| Boat | 81.9 | 90.8 |
| Furnace | 7.8 | 4.5 |
| Transfer line | | 0.4 |
| Model containment vessel | 4.8 | 1.9 |
| Removed in purging | 0.4 | 0.2 |
| Unaccounted for | 5.1 | 2.2 |

operated. In the second, sweep gas was used and the fan in the model containment vessel was operated. Table 2.1 summarizes the experimental conditions and the uranium distribution. It is notable that approximately twice as much $UO_2$ was volatilized in run 1 as in run 2; this is partially accounted for because the first pellet (of four) in run 2 shattered in the plasma flame and did not melt. Figure 2.1 shows the furnace at the end of run 2. Fragments from the first pellet are visible near the left-hand end of the boat. At the right, the glassy residue left from complete melting of the $UO_2$ is visible. All furnace surfaces are covered with a film of $UO_2$; this is normally observed.

The condensation nuclei data are shown in Fig. 2.2. In run 1, the particle count increased by a factor of 2 and decayed gradually. In run 2, the particle count exceeded the instrument maximum of $10^7$ particles/cm$^3$ 1 min after the torch was ignited. Readings decreased rapidly after the torch was turned off, dropping to $10^5$ particles/cm$^3$ in about 1 hr and thereafter decreasing more gradually. The behavior observed is a result of

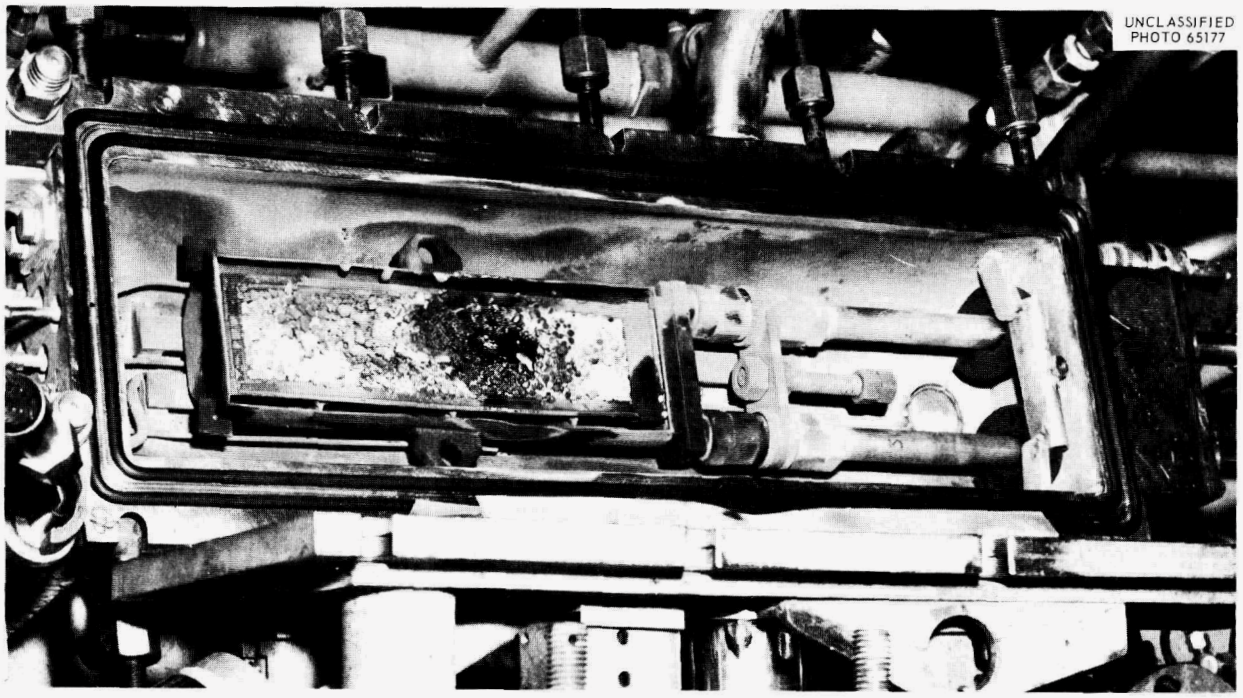


Fig. 2.1. Nuclear Safety Pilot Plant Furnace After Run 2.

the mixing effect of the fan. The particles do not originate from the fan; no significant increase in particle count is observed when the fan is operated in the model containment vessel without the torch being operated simultaneously.

The paper tape air sampler results are somewhat erratic, reflecting experimentation which was done with sampling rates and filter papers in these runs. Figures 2.3 and 2.4 present results obtained using 3.0-$\mu$ membrane filter at flows of 380 and 490 $cm^3$/min. These both show the rather stable behavior of the $UO_2$ aerosol after the concentration drops to approximately 10 $mg/m^3$.

Electron micrographs of a sample from run 1 are shown in Figs. 2.5 and 2.6. The sample was taken approximately $6\frac{1}{2}$ hr after meltdown. Figure 2.5 at 29,700X shows the agglomeration of the particles, and Fig. 2.6 at 165,000X shows the shape of the ultimate particles. Both spherical and cubic particles are present, of sizes from about 30 to 1500 A.

Figure 2.7 shows a sample from run 2 taken 3 min after the arc was extinguished. It illustrates the high degree of agglomeration present even in the early stage of a run.

Deposition coupons were used to investigate the spatial distribution of deposition in the vessel as well as the effect of material. The results of both runs show a definite spatial dependence; in run 2, the influence of the fan is clearly visible, with maximum deposition being found at the outer wall at the top level where the fan blowing across the end of the transfer line picks up the aerosol particles in a swirling flow pattern. In run 2, a basic adhesive surface (Scotch tape wrapped with the adhesive side out) was used to obtain data on the influence of position, and coupons of 14 other materials were placed in 8 of the 36 available

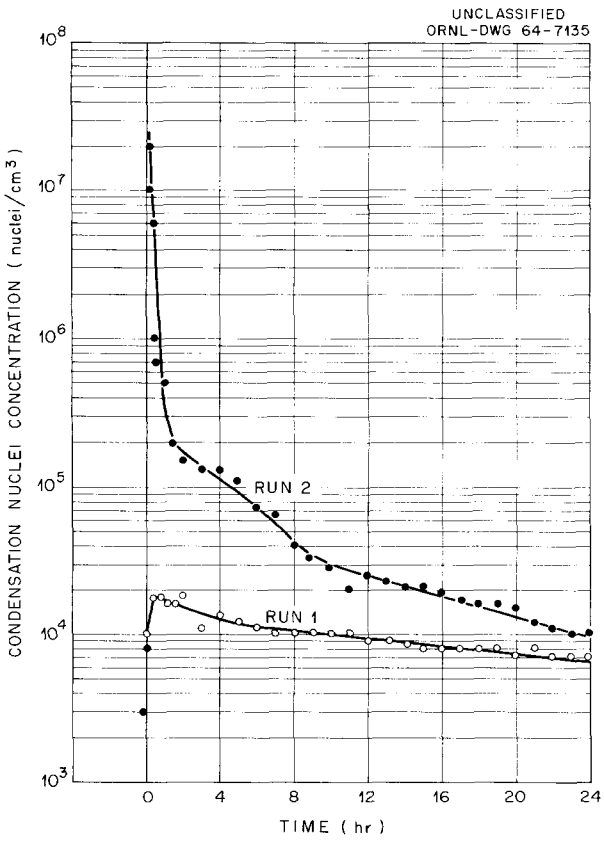


Fig. 2.2. Particle Count vs Time.

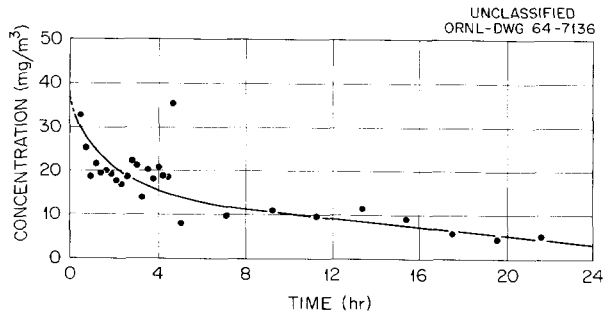


Fig. 2.3. Air Sampler Data, Top Level, Southwest Side of Vessel, Run 1.

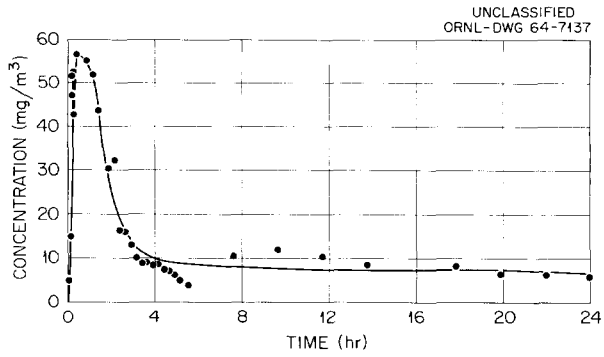


Fig. 2.4. Air Sampler Data, Bottom Level, Northeast Side of Vessel, Run 2.

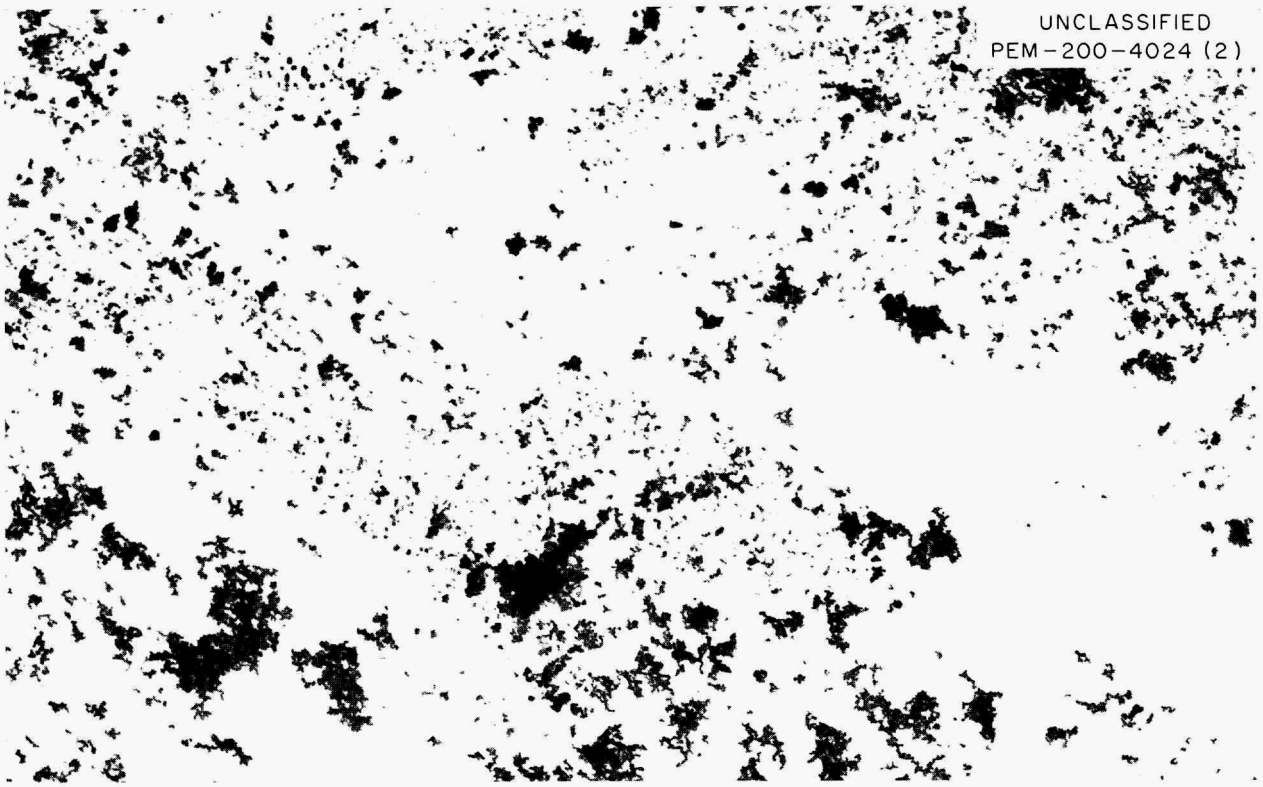


Fig. 2.5. Particles from Run 1. 29,700×.

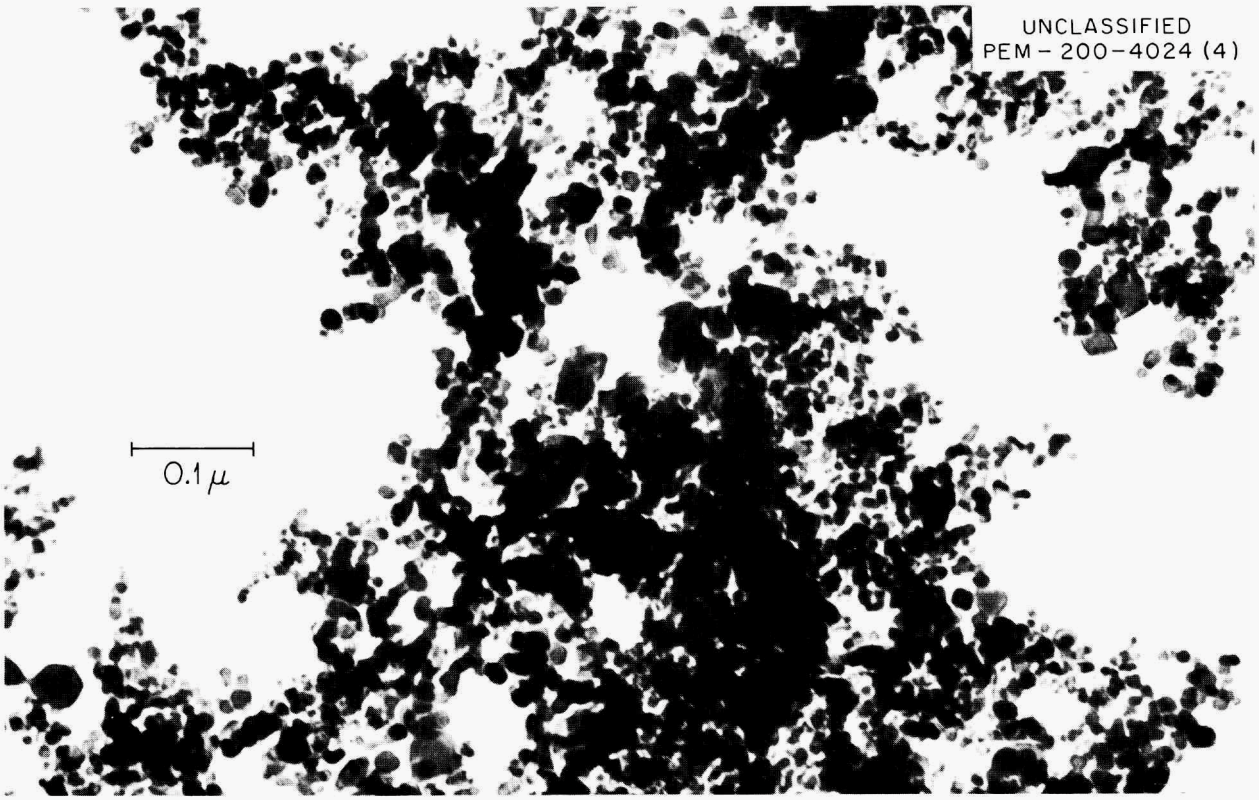


Fig. 2.6. Particles from Run 1. 165,000×.

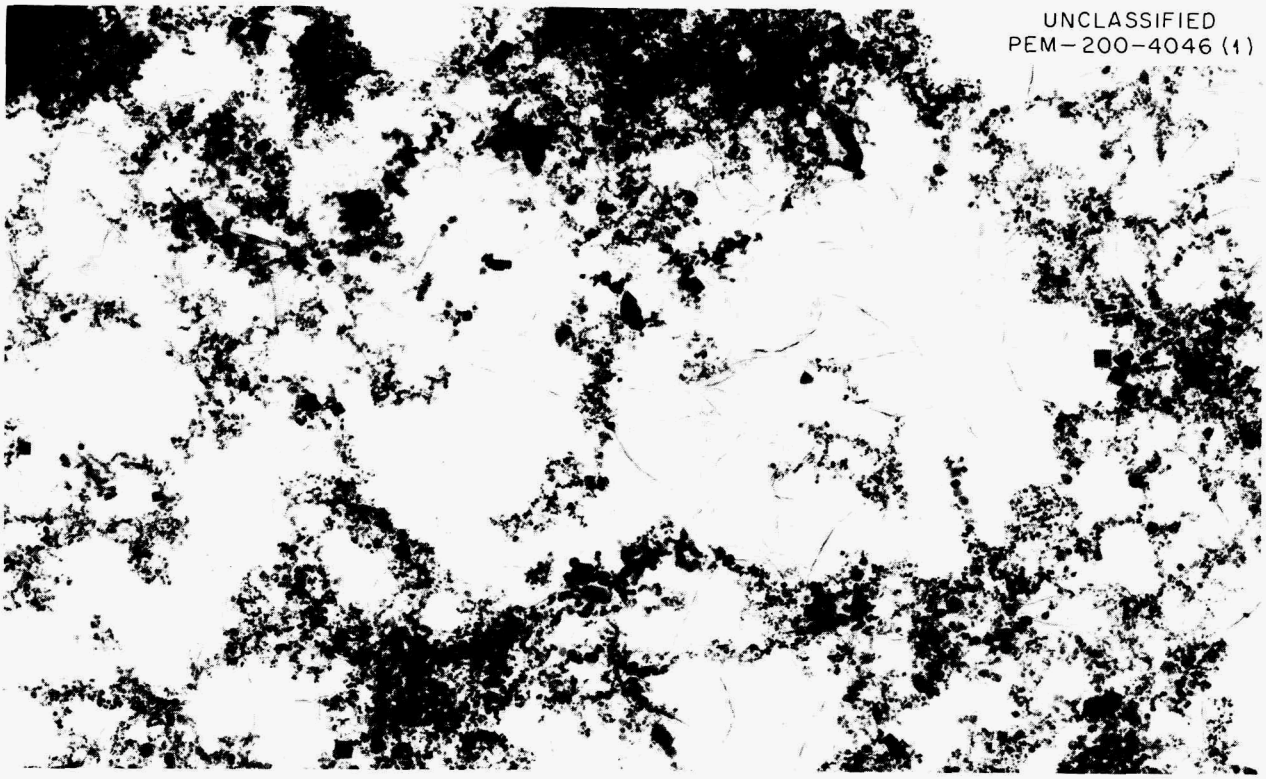


Fig. 2.7. Particles from Run 2. 29,700×.

locations to investigate the influence of material. The results indicate that greater deposition occurred on metals than on painted surfaces. Of the metals, copper and brass had the greatest accommodation coefficient, stainless steel the least. Deposition was very small in all instances, of the order of 0.001 to 0.01 $\mu g/cm^2$.

Fallout observations were disappointing in both runs. The amount of sample collected in the fallout cups was much lower than anticipated from vessel decontamination data. The paper tape fallout sampler showed significantly more fallout than the fallout cups in both runs, so that loss of material by reentrainment during purging of the vessel may be significant even though adhesive "fallout" paper is used in the cups.

## DEVELOPMENT OF SAMPLING DEVICES

Prototypes of three sampling devices have been designed and built during the report period. The first of these is the "May-pack cluster," a device designed to take a series of samples at a given location and to differentiate the chemical form of iodine associated with the samples. This device is shown in Fig. 2.8. The cluster contains 12 May-pack samplers, and vacuum can be applied to each in turn by means of a sequential valve. The valve used in the prototype limits its maximum operating temperature to 100°F; ultimately, valves suitable for 300°F will be installed. The May packs contain the following filter elements:

1. silver-plated copper screen to react with molecular iodine,
2. membrane filters to collect particles,
3. charcoal-impregnated glass fiber filters to collect readily adsorbed iodine compounds,
4. activated-charcoal beds to collect less readily adsorbed iodine compounds.

Space for additional filter elements is available.

The second device (Fig. 2.9) is a combined May-pack–diffusion-tube sampler. Its function is to look for possible unique constituents in the NSPP aerosol. It consists of five pairs of May-pack housings with 40-in. diffusion tubes inserted between the two housings in each pair. In each of the channels, part of the May pack would be loaded in the upstream housing and part in the downstream

UNCLASSIFIED
ORNL-DWG 64-1856

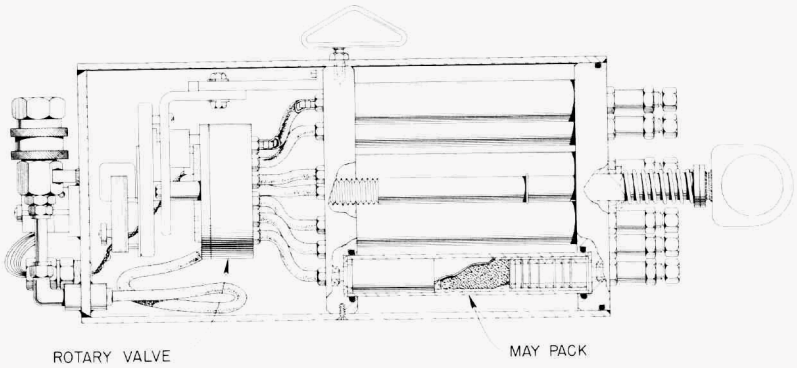


Fig. 2.8. May-Pack Cluster.

UNCLASSIFIED
ORNL-DWG 64-7138

Fig. 2.9. May-Pack–Diffusion-Tube Assembly.

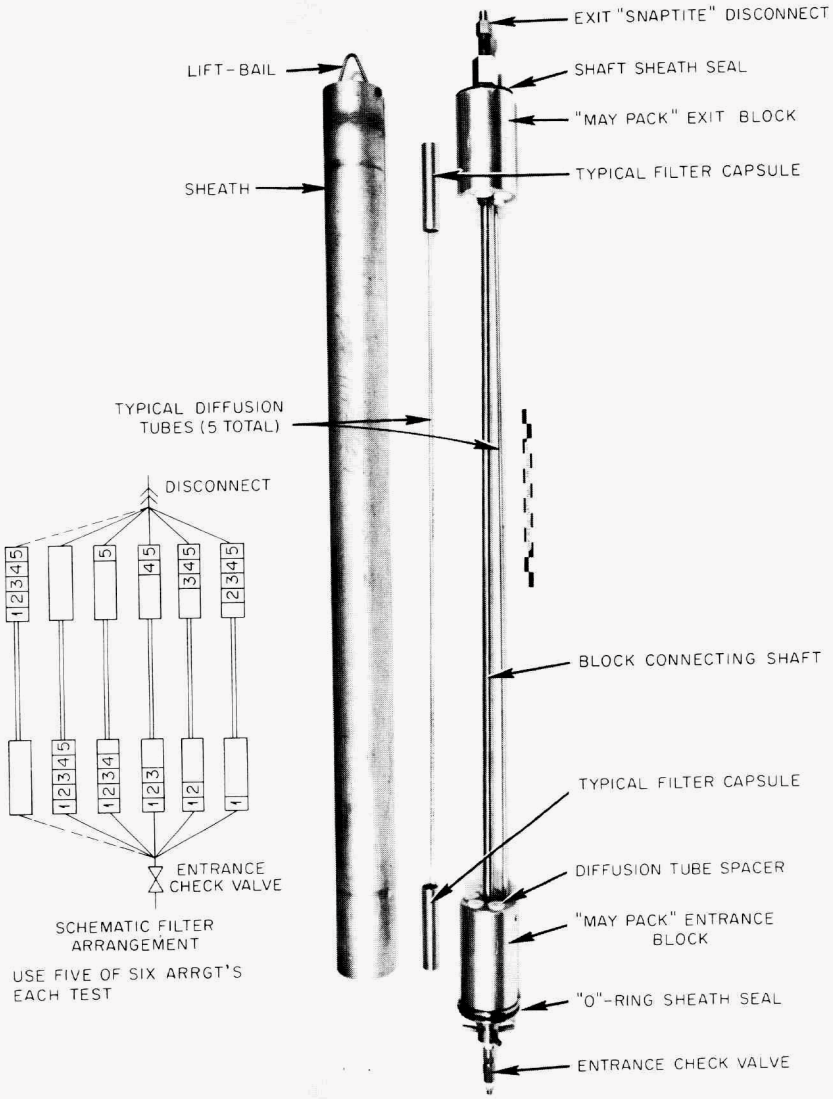

UNCLASSIFIED
PHOTO 66331

UNCLASSIFIED
PHOTO 65963

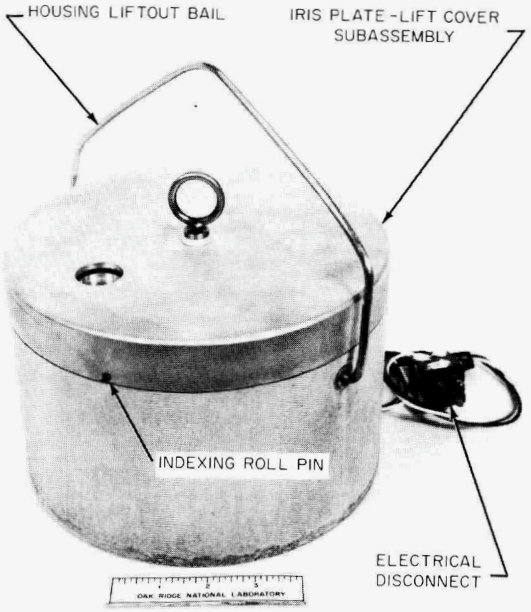


THE IRIS PLATE-LIFT COVER SUBASSEMBLY CONTAINS A RUBBER GASKET. TIGHTENING OF THE LIFT HOOK RESULTS IN CLAMPING THE IRIS TO THE LID PRIOR TO LIFTOUT PREPARATORY TO FALL-OUT SAMPLE ANALYSIS. HOUSING AND DRIVE COMPONENTS ARE DECONTAMINATED IN PLACE AND ARE NOT NORMALLY REMOVED FROM THEIR VESSEL STATION.

ASSEMBLED VIEW IN SAMPLING POSITION

UNCLASSIFIED
PHOTO 65961

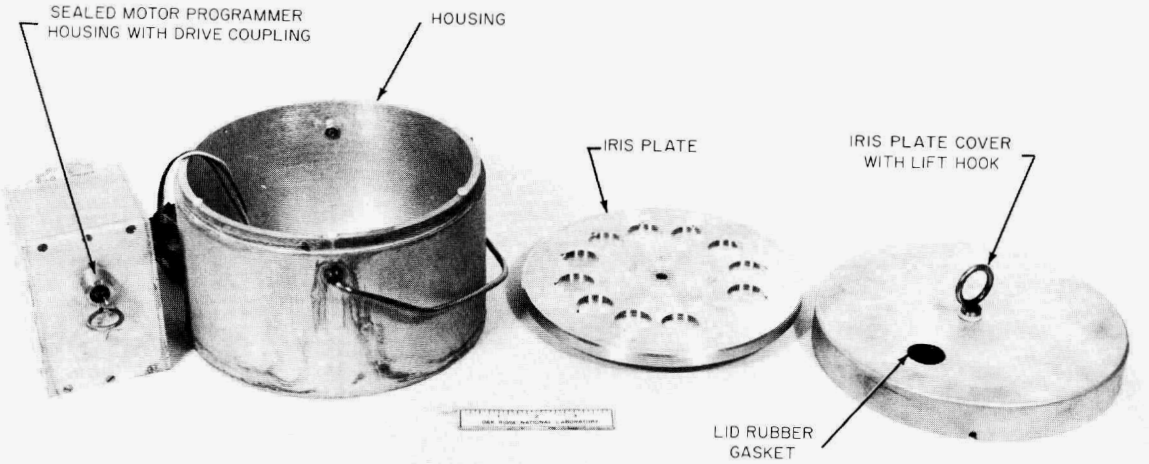


COMPONENTS

**Fig. 2.10. Fallout Sampler.**

housing so that the diffusion tube is at a different location in each channel. A typical loading might be:

1. diffusion tube upstream of entire May pack,
2. diffusion tube between silver bed and membrane filter,
3. diffusion tube between membrane filter and charcoal paper,
4. diffusion tube between charcoal paper and charcoal bed,
5. diffusion tube downstream of entire May pack.

It is expected that flow in the parallel channels will distribute evenly enough so that separate flow metering will not be required. Each device of this type will take one sample.

The third device (Fig. 2.10) is the NSPP fallout sampler. This device enables 11 time-dependent fallout samples to be taken and to be protected during purging and unloading operations. It uses a vibratory motor which allows precise indexing. The principle appears applicable not only to fallout sampling but also to collecting time-dependent deposition samples.

## PLASMA TORCH AND FURNACE DEVELOPMENT

Development work has been concentrated on making the torch operable at elevated pressure and in the presence of steam. Initial attempts to operate at pressure resulted in burnout of the anodes in a matter of seconds. It has been established that burnout occurs when the arc attaches to some point on the anode rather than moving continuously. Increasing the pressure constricts the plasma and increases the tendency for attachment. After several changes were made in the torch, satisfactory operation at 35 psig was achieved. The most significant change was that of reducing the arc chamber volume, thus increasing the intensity of the vortex induced in the arc chamber and its tendency to keep the arc moving. Polishing the anode and accurate centering of the cathode were found to be important in reducing the tendency for arc attachment. Improved anode cooling was achieved and may also have had some effect in improving operation at pressure.

Tests with steam in the furnace have not been satisfactory to date. To permit steam operation, two problems must be overcome. The first is to raise the furnace and boat temperatures so that condensation will not occur. This apparently has been solved by using a circulating-hot-water system for furnace and boat cooling; this permits cooling water temperatures up to 90°C to be used. An attempt was made to use steam as the coolant; this apparently did not provide sufficient cooling at the opening where the torch is mounted, since the furnace lid cracked in that area.

The second problem is to avoid chemical attack by steam on the electrodes. Significant erosion from the cathode of the plasma torch has been observed in the steam runs. In the runs made to date, the steam was introduced tangentially just downstream of the torch nozzle. It is suspected that some steam flowed or diffused along the anode wall countercurrent to the plasma and thus entered the arc chamber and reacted with the cathode. It is planned to try using an inert gas at the tangential inlet and to put steam into the furnace body to see if acceptable steam operation can be achieved.

Several runs were made to investigate aerosol generation by the plasma torch. In the first of these, the torch was mounted on a flange on the model containment vessel and operated for 5 min. One paper tape air sampler was used, and particle counts were taken using a Gardner Associates condensation nuclei counter. The air samples indicated that approximately 200 mg of copper was released into the model containment vessel; approximately twice as many particles were present as in the second $UO_2$ run. A sample was submitted for particle-size analysis; the results are not complete.

Additional runs have been made with the torch in the furnace. On taking the particle count sample from the bottom of the model containment vessel, which has been the normal sample point, one finds that no significant increase in the particle count is produced by operating the torch unless the fan is simultaneously operated or by operating the fan unless the torch is simultaneously operated. When both the torch and the fan are operated, the particle count goes off scale immediately. Results of chemical analyses taken during these runs are not yet available.

One run was made with the particle count sample point moved to the top of the model containment vessel. In this case, a significant increase in particle count was observed when the torch was operated, even though the fan was not operated. Operating the fan only had no significant effect on the particle count. In conjunction with the results of the other runs, this indicates that the fan is necessary to disperse the aerosol in the vessel.

# 2.2 Reactor Containment Handbook

H. B. Piper

Since the last reporting period,[3] final drafts of all chapters have been completed and distributed to carefully selected experts, both within ORNL and AEC, and throughout the nuclear community, for review. All chapters were critically reviewed.

Each chapter, along with its related comments, was placed in the hands of an individual or group of individuals who were responsible for final revision of that chapter in the light of comments received and current progress in that particular area of work. Revision of 9 of the 12 chapters has been completed, and completion of the remaining three chapters is expected in July or August, as may be seen in Table 2.2. Major revision was required in Chapters 2, 4, and 5.

In addition to the technical revision of the material, the revised drafts are being edited and the index is being prepared.

In view of the extensive revision, the draft will first be published in a completed form, with index, as a Technical Memorandum for further review before being released for general distribution as an ORNL-NSIC report. The Technical Memorandum will be issued in October 1964.

[3]H. B. Piper, *Nucl. Safety Semiann. Progr. Rept. Dec. 31, 1963*, ORNL-3547, p. 78.

**Table 2.2. Status of Reactor Containment Handbook**

| Chapter No. | Title | Final Draft Completed | Comments Received | Revision Complete | Index Complete | Final Editing Complete |
|---|---|---|---|---|---|---|
| 1 | Introduction | Mar. 16, 1964 | Apr. 20, 1964 | June 4, 1964 | June 8, 1964 | June 8, 1964 |
| 2 | Codes, Criteria, and Regulations | Apr. 26, 1963 | October 1963 | Apr. 6, 1964 | Apr. 14, 1964 | Apr. 2, 1964 |
| 3 | Radioactivity Generation, Release, and Transport | Jan. 23, 1964 | Mar. 15, 1964 | Apr. 17, 1964 | Apr. 24, 1964 | May 8, 1964 |
| 4 | Energy Sources | Mar. 19, 1963 | October 1963 | | | |
| 5 | Analytical Techniques | Mar. 6, 1964 | Apr. 10, 1964 | | | |
| 6 | Credible Accidents | Feb. 28, 1964 | Apr. 22, 1964 | June 30, 1964 | July 2, 1964 | |
| 7 | Containment Proof Testing | February 1964 | Mar. 15, 1964 | | | |
| 8 | Specific Containment Systems | Feb. 7, 1964 | Mar. 25, 1964 | July 2, 1964 | July 3, 1964 | |
| 9 | Design Details | February 1964 | Mar. 15, 1964 | June 9, 1964 | June 25, 1964 | |
| 10 | Containment Accessories | March 1964 | Apr. 22, 1964 | June 17, 1964 | June 29, 1964 | |
| 11 | Economics | February 1964 | Apr. 15, 1964 | May 29, 1964 | June 2, 1964 | June 8, 1964 |
| 12 | Research | Feb. 26, 1964 | Apr. 1, 1964 | May 14, 1964 | May 15, 1964 | May 19, 1964 |

# Part 3
# Physics

Neutron Physics Division

E. P. Blizard, Division Director
F. C. Maienschein, Coordinator

Key Words[a]

computer programs
criticality safety
perturbations
plate-type cores
reactivity effects

[a]See Foreword.

# 3.1 Reactivity Effects of Small Fuel Displacements for Plate-Type Reactors

E. G. Silver E. B. Johnson

As reported in previous issues of this report, an experimental-calculational program is under way to study the reactivity effects of small fuel displacements in water-moderated plate-type reactors fueled with highly enriched material.[1–5] In particular, interest is focused on the adequacy of available reactor codes for calculating the effects of such perturbations.

The results presented in this report are preliminary since the project is not yet completed.

## EXPERIMENT

The gross features of the slab reactor used for the experiments were described previously.[4,5] Briefly, the core consisted of unclad uranium-aluminum alloy plates 60.96 cm long, 7.49 cm wide, and 0.147 cm thick. Eight of these plates placed edge to edge constituted a fuel element 60.96 by 59.94 cm and 0.147 cm thick. These elements were spaced with centers 0.51 cm apart by support grooves cut into the side walls of an aluminum tank, and the spacing was maintained across the width of the core by four sets of plastic (Plexiglas) strips of the proper thickness. Pressure was applied to the core by Plexiglas structural members bearing against a 1.3-cm-thick Plexiglas slab placed against each outside element to keep the desired spacing. The arrangement is shown in Figs. 3.1 and 3.2. The core is water moderated and has an effectively infinite water reflector on two sides. The four surfaces formed of the element edges were unreflected, and the tank bottom and side walls were cadmium lined to minimize the return of neutrons from the room. Rigid fuel support was mandatory because of the extreme sensitivity of the core to element spacing.

A critical experiment with an unperturbed core was performed to find a suitable reference configuration. A core with 26 full elements and a half element (four fuel plates and four aluminum plates) at each outside position was found to have multiplication, $k$, of 0.9965 and was chosen as the reference core. All perturbed configurations were then made critical by modifying the partial elements at the outside positions and by adding small increments of water above the core, thereby providing some reflection to the upper edge. The thickness of the top reflector was never allowed to exceed 1.5 cm, and in this range the reactivity was found to be essentially linear with thickness. Figure 3.3 shows the change of reactivity with water height for two core configurations. No water heights lower than the top of the fuel plates were used, since meniscus and irregular-wetting effects introduced irreproducible changes in reactivity.

To date six perturbed configurations have been assembled, and at least preliminary values of the reactivity change have been deduced from the

[1] E. G. Silver *et al.*, *Nucl. Safety Program Semiann. Progr. Rept. June 30, 1962*, ORNL-3319, pp. 5–10.

[2] E. G. Silver *et al.*, *Neutron Phys. Div. Ann. Progr. Rept. Sept. 1, 1962*, ORNL-3360, pp. 12–16.

[3] E. G. Silver, *Nucl. Safety Program Semiann. Progr. Rept. Dec. 31, 1962*, ORNL-3401, pp. 3–4.

[4] E. G. Silver, *Nucl. Safety Program Semiann. Progr. Rept. June 30, 1963*, ORNL-3482, pp. 3–6.

[5] E. G. Silver and E. B. Johnson, *Neutron Phys. Div. Ann. Progr. Rept. Aug. 1, 1963*, ORNL-3499, vol. I, pp. 69–76.

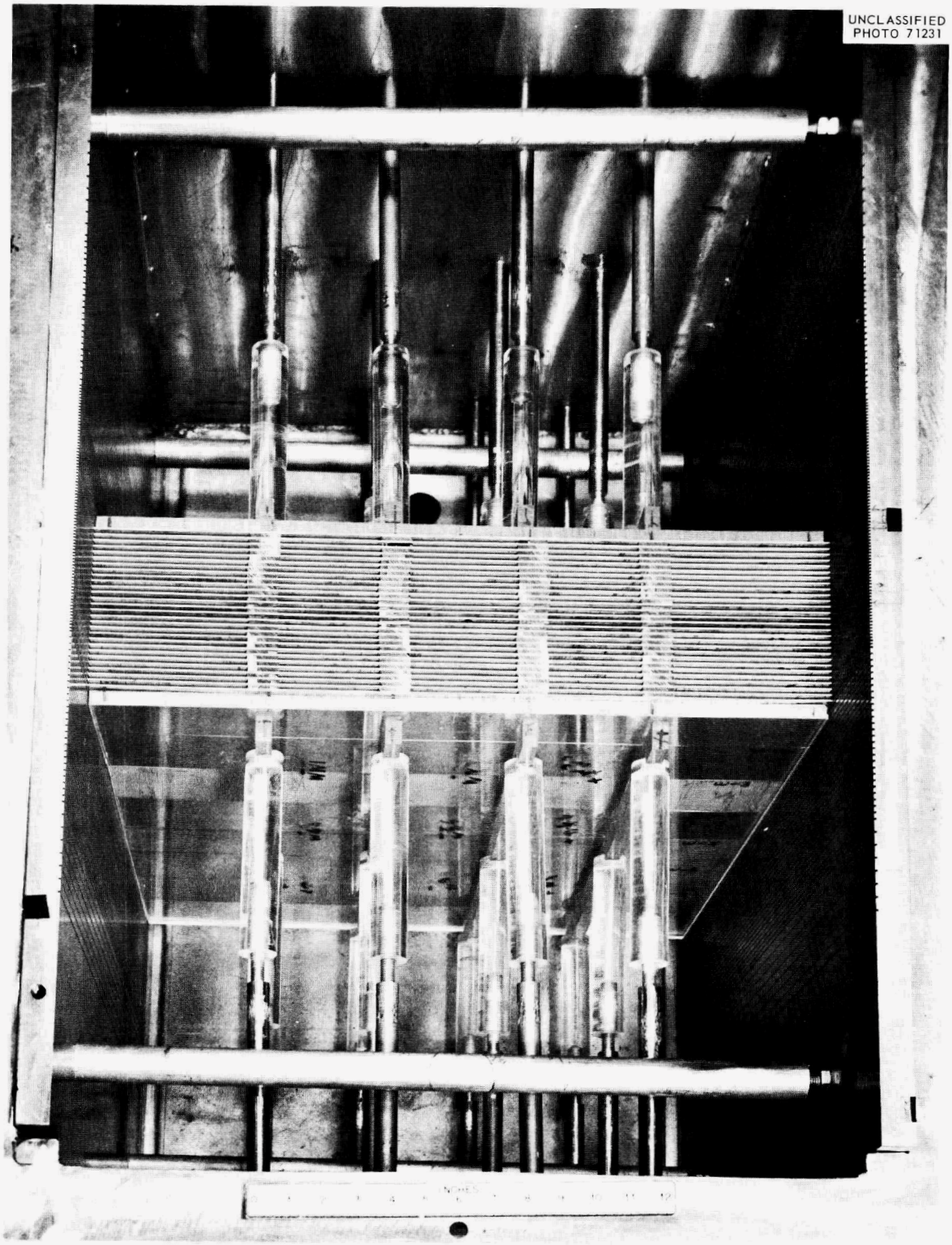


Fig. 3.1. View of 1DCA Experiment.

Fig. 3.2. View of 1DCA Experiment.

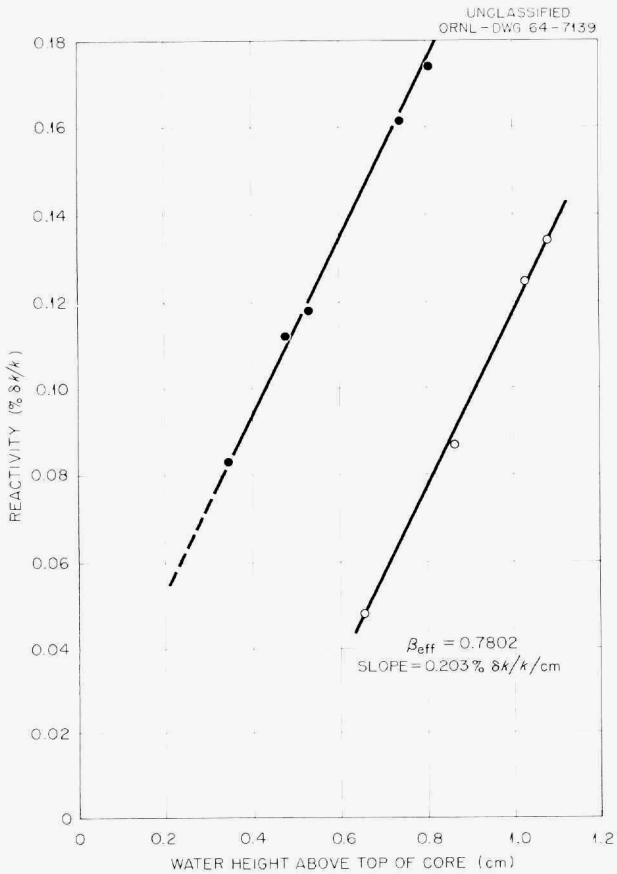


Fig. 3.3. Reactivity of 1DCA as Function of Water Height Above Core Top.

data. Figure 3.4 shows the configurations for which reactivity effects have been measured. A series of measurements is planned to measure reactivity effects due to perturbing a core containing a central water gap 1 in. wide. This mocks up control-rod wells or similar water spaces.

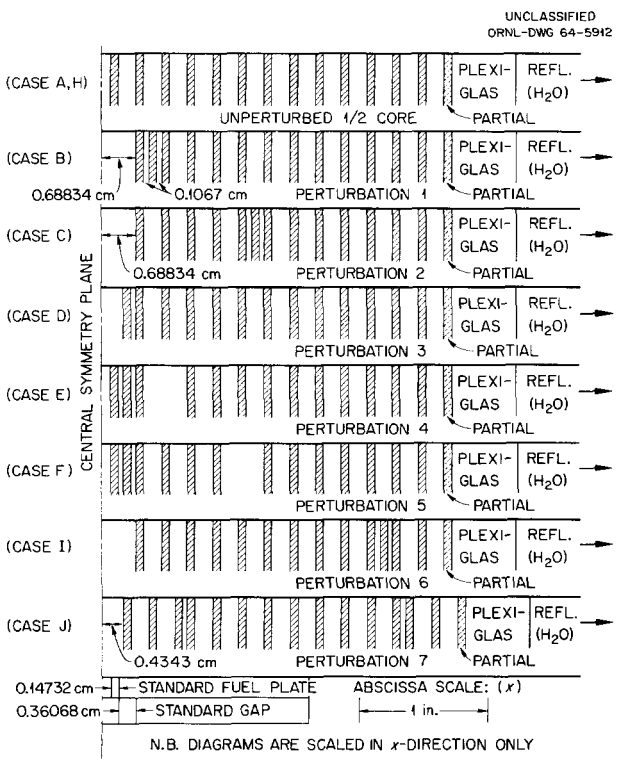


**Fig. 3.4. 1DCA Configurations Which Have Been Assembled and Reactivity Measured.**

## DIFFUSION-THEORY CALCULATIONS

After extensive initial calculations to determine the best parameters for the design of the experiment, the final calculations were undertaken on the model actually used in the experiments. In order to avoid the possibility that a grossly different group structure would make comparison of diffusion and transport calculations difficult, the GAM-MOD code[6] was used to obtain flux-weighted 16-group cross sections from a 99-group elementary cross-section library, which is incorporated in GAM-II code,[7] in P-2 approximation. The GAM-MOD calculation provided cross sections for groups 1 to 14 (down to energy $E$ = 0.4 ev). Group 15 cross sections were calculated by hand from the earlier 34-group MODRIC cross sections, flux weighting by use of the relation:

$$\sigma_{15} = \frac{\sum_{i'=20}^{32} \Phi_{i'} \sigma_{i'} (\Delta u)_{i'}}{\sum_{i'=20}^{32} \Phi_{i'} (\Delta u)_{i'}} ,$$

where $i'$ represents the group numbers from the 34-group cross sections, and $\Phi_{i'}$ was obtained from a MODRIC calculation. The thermal-group (group 16) cross sections were the same as those used in the thermal group of the 34-group model. In this group the hydrogen transport cross section was modified to take care of binding effects by using the results obtained by Bracci and Coceva,[8] Dio,[9] and Küchle[10] with a pulsed-neutron method for measuring the diffusion coefficient, $D$, in water. Their average value of $D$ was 35,400 $cm^2$/sec, which corresponds to $\lambda_{tr}$ = 0.4811 cm or $\Sigma_{tr}$ = 2.0786 $cm^{-1}$. Then, using the relation

$$\Sigma_{tr} = N_H \sigma_{tr}(H) + N_O \sigma_{tr}(O) ,$$

and substituting the known atomic densities of the two constituents and the value of $\sigma_{tr}$ for oxygen used in the cross-section library, there results the value $\sigma_{tr}(H)$ = 29.076 barns, which was used in all the calculations. Also used in the final calculations was a recent version of MODRIC which employs transfer coefficients from any group to the ten groups next below it, rather than the continuous slowing down from group to group used by earlier versions of the code.

There are two inadequacies inherent in the calculational model. One arises from the choice of the transverse leakage and the other from the limitation of the present MODRIC code to no more than 25 regions, which requires that at least some

[6] J. L. Lucius, *GAM-MOD-2, an IBM 7090 Neutron Cross Section Program*, KDP-168 (1963).

[7] G. D. Joanou and J. S. Dudek, *GAM-II, a $B_3$ Code for the Calculation of Fast-Neutron Spectra and Associated Multigroup Constants*, GA-4265 (1963).

[8] A. Bracci and C. Coceva, *Nuovo Cimento* **4**, 59 (1956).

[9] W. H. Dio, *Nukleonik* **1**, 13 (1958).

[10] M. Küchle, *Nukleonik* **2**, 131 (1960).

of the core be homogenized. Any one of three possible parameters specifying the transverse leakage can be varied to minimize the former inadequacy, and the uranium density in the homogenized region can be modified to counter the latter.

The transverse leakage, which is determined by the transverse buckling, can be modified in three ways. The code can calculate a transverse buckling for each group, $i$, and region, $j$, by use of the equation

$$B_{ij}^2 = \frac{\pi^2}{(X + \Gamma D_{ij})^2} + \frac{\pi^2}{(Y + \Gamma D_{ij})^2}$$

by adjusting the extrapolation parameter $\Gamma$ in one case or, in another, one of the transverse dimensions, such as $Y$. In the third case, a value can be chosen directly for the transverse buckling, equal for all groups and regions.

Attempts to minimize both inadequacies in the code, based on the experimentally determined reference core, were carried out in the following manner (one-half of the reference core consisted of 13 full fuel elements plus a one-half element at the extremity). First, a series of criticality search calculations was made with either 0, 3, 7, or 10 full fuel elements, the maximum possible with the MODRIC code, explicitly specified out of the 13 actually required for criticality. The outer half-element was explicitly included in each configuration. In each case the thickness of the homogenized region that would make the reactor critical was found. The results were then extrapolated to zero thickness of the homogenized region to find the critical thickness of a core with all elements explicitly included. This was done for several values of each of the three possible transverse leakage parameters to find that value of the parameter which would give the critical thickness of the reference core. Figure 3.5 shows the extrapolations to zero thickness of the homogenized region and the value of the parameter $\Gamma$ of 8.15 obtained by interpolating between the extrapolated end points to find the correct thickness. A similar extrapolation and interpolation with the transverse dimension $Y$ as the variable parameter resulted in a value of $Y$ of 76.1 cm, as shown in Fig. 3.6.

The extrapolation to find the best value of the transverse buckling was simpler since this parameter could be determined directly by a criticality search calculation. In this case, four reactor configurations of the correct experimental thickness were calculated with 0, 3, 7, and 10 explicit elements and the transverse buckling for criticality was found in each case. Figure 3.7 shows how these data were extrapolated to the reference core of 13 explicit full elements to produce a value of $B^2$ of $3.391 \times 10^{-3}$ cm$^{-2}$.

Calculations of fully homogenized cores were then made using each of these transverse leakage parameters, obtained as described, to find in each case the uranium concentration that would make the reactor critical. In the final MODRIC calculations this concentration was used in the homogenized region with the corresponding value of the transverse leakage parameter. Thus each perturbation was calculated by three models using $\Gamma = 8.15$, $Y = 76.1$ cm, or $B^2 = 3.391 \times 10^{-3}$ cm$^{-2}$ respectively.

In a fourth method, the perturbations were also calculated with the "physical" (i.e., unadjusted)

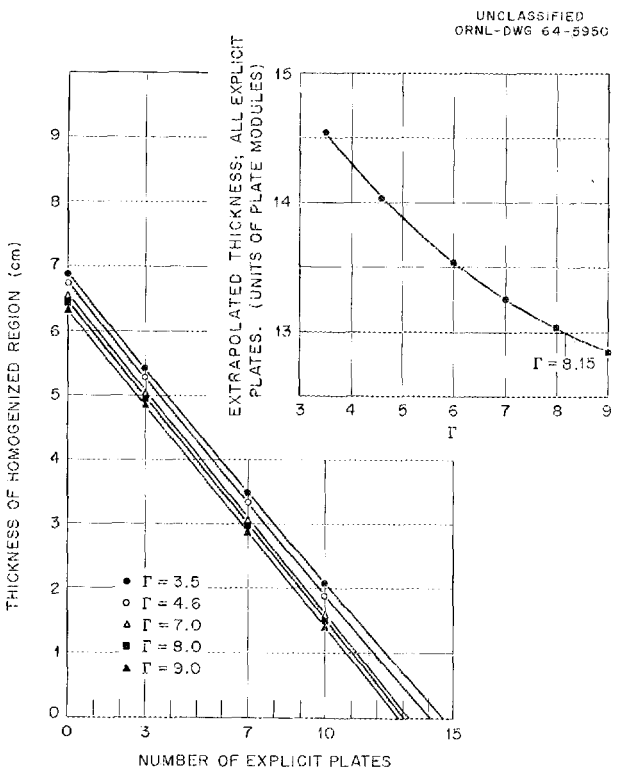


**Fig. 3.5. Thickness of Homogenized Region as Function of Number of Explicit Plates for Various Values of $\Gamma$, the Buckling Correction Parameter; and Critical Thickness as Function of $\Gamma$ Derived from Extrapolated Values of Critical Thickness with All Plates Explicit.**

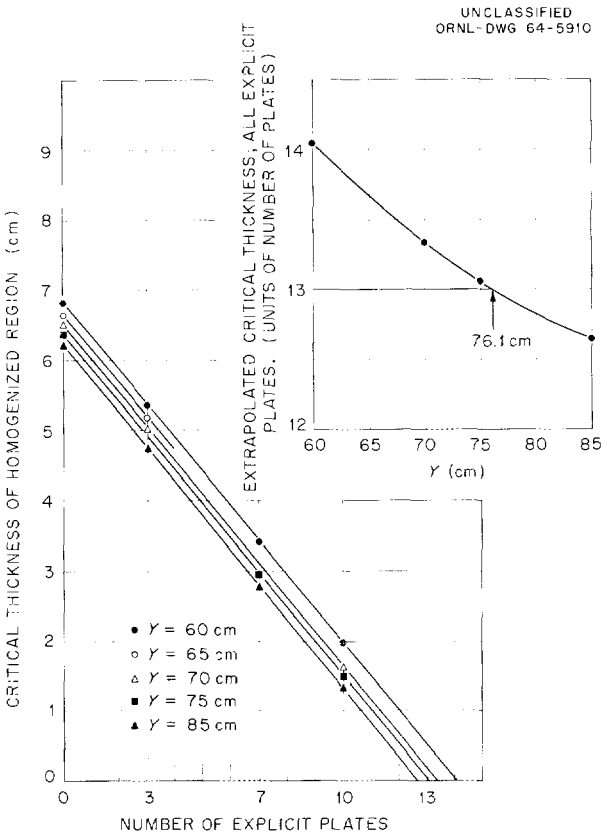


Fig. 3.6. Thickness of Homogenized Region as Function of Number of Explicit Plates for Various Values of Transverse $Y$ Dimension; and Critical Thickness as Function of $Y$ from Extrapolated Values of Critical Thickness with All Plates Explicit.

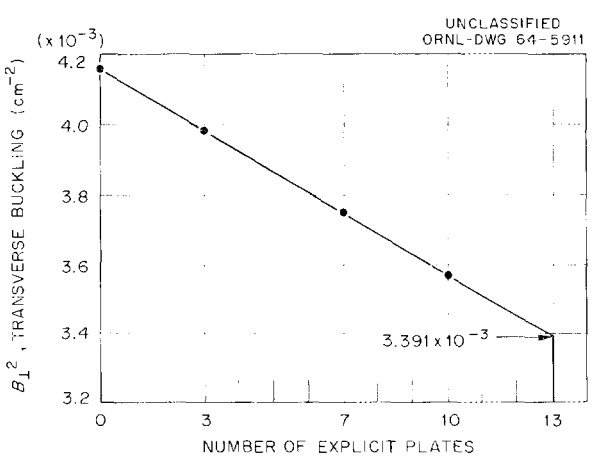


Fig. 3.7. Transverse Buckling, $B_\perp^2$, as Function of Number of Explicit Plates Extrapolated to 13 Explicit Plates.

values of the transverse dimensions and the "correct" value of $\Gamma(3 \times 2 \times 0.71 = 4.26)$.

The reason for using four different methods of selecting the input parameters and for calculating each perturbation by each set of parameters was to ascertain that the values obtained for $\delta k/k$ do not depend substantially on the choice of method. The preliminary determinations of the core dimensions had shown that in some cases the results might depend quite strongly on the transverse leakage model. Table 3.1 gives the reactivity difference, in units of $\delta k/k$, obtained for the cases that have been compared with the experiment for each of the four transverse leakage models. It is clear from the table that the calculated effect of the perturbation is not sensitive to the choice of the transverse leakage model. The four models are:

1. unmodified transverse dimensions but $\Gamma$ taken to be 8.15 (the best value found by extrapolative procedure) and $B_\perp^2$ calculated for each group and region,
2. $\Gamma = 4.26$, but transverse dimensions modified to best value found by extrapolation (i.e., $59.94 \times 76.10$ cm) and $B_\perp^2$ calculated for each group and region,
3. transverse buckling using best value found by extrapolation (i.e., $B_\perp^2 = 3.391 \times 10^{-3}$ cm$^{-2}$ for all groups and regions),
4. unmodified (i.e., transverse dimensions are $59.94 \times 60.96$ cm), $\Gamma = 4.26$ and $B_\perp^2$ calculated for each group and region.

The results of the experiment were obtained in reactivity units (dollars), whereas the calculation results are expressed in percent $\delta k/k$. In order to compare these, the value of $\beta_{eff}$ must be known. This value was obtained by calculating the multiplication for the unperturbed core with a modified fission spectrum from which the delayed-neutron contribution has been subtracted. The values for the fission spectrum used are shown in Table 3.2. In order to assess the effect of the transverse leakage on this parameter, it was calculated for each of the four models, as well as for a core with a transverse buckling one-tenth as large as the best value. The results are shown in Table 3.3. It is seen that the value of $\beta_{eff}$ does not depend on the model to a significant extent. Even increasing the transverse dimensions so as to multiply the element area tenfold made only a 4% change in $\beta_{eff}$. A mean value of

Table 3.1. Calculated Multiplication Differences in Units of Percent $\delta k/k$ for Experimentally Measured Perturbations as Obtained by Four Different MODRIC Transverse Leakage Models

| Case | Multiplication Difference (% $\delta k/k$) for Model — | | | |
|---|---|---|---|---|
| | 1, $\Gamma = 8.15$ | 2, $Y = 76.1$ cm | 3, $B^2 = 3.39 \times 10^{-3}$ cm$^{-2}$ | 4, Unmodified |
| A-B | −0.278 | −0.274 | −0.269 | −0.267 |
| A-C | −0.634 | −0.616 | −0.581 | −0.601 |
| A-D | −0.056 | −0.055 | −0.053 | −0.053 |
| A-E | −0.231 | −0.235 | −0.234 | −0.227 |
| A-F | −0.569 | −0.579 | −0.605 | −0.566 |
| H-J | +1.510 | +1.521 | +1.545 | +1.506 |
| H-I | +0.012 | +0.030 | +0.132 | +0.059 |

Table 3.2. Fission Neutron Spectra Used to Calculate $\beta_{eff}$

| Group No. | Lethargy Interval | Fission Spectra | | |
|---|---|---|---|---|
| | | Total | Delayed | Prompt |
| 1 | 0–1.6 | 0.20672 | 0 | 0.20672 |
| 2 | 1.6–2.4 | 0.36662 | 0 | 0.36662 |
| 3 | 2.4–2.8 | 0.14984 | 0.000709 | 0.14913 |
| 4 | 2.8–3.6 | 0.17624 | 0.002738 | 0.17350 |
| 5 | 3.6–4.9 | 0.08522 | 0.002431 | 0.08279 |
| 6 | 4.9–6.9 | 0.01537 | 0.000622 | 0.01475 |
| | Total | 1.00001 | 0.006500 | 0.99351 |

Table 3.3. Values of $\beta_{eff}$ Obtained by MODRIC Calculations with Various Transverse Leakage Assumptions

| Model | $\beta_{eff} = \frac{k_{tot} - k_{prompt}}{k_{tot}}$ (%) |
|---|---|
| A | 0.7853 |
| B | 0.7775 |
| C | 0.7791 |
| D | 0.7789 |
| $(B_\perp^2) = 0.1 \times [B_\perp^2 \text{ (model D)}]$ | 0.07491 |

$\beta_{eff} = 0.7802\%$ (a relative effectiveness for delayed neutrons equal to 1.200) was used to convert the experimental data to percent $\delta k/k$ units for comparison with the calculations.

## TRANSPORT-THEORY CALCULATIONS

The transport-theory calculations were carried out with a code called DTK, which is an updated version of DSN. These codes are one-dimension multigroup transport-theory codes which use the $S_n$ method of Carlson[11] for approximating the angular fluxes. In the present instance $n = 4$ was used, and a set of 18-group cross sections developed by Mills[12] was employed. This cross-section group structure is like that of the 16-group set used in the diffusion calculations, except that two groups are each split. Since the code has no set limit on the number of regions, it was possible to perform the transport calculations with all elements explicitly described. However, the transport calculations were also made utilizing the same structure used in the corresponding MODRIC cases to assess the

[11] B. Carlson, C. Lee, and J. Worlton, *The DSN and TDC Neutron Transport Codes*, LAMS-2346 (1959).

[12] C. B. Mills, *Neutron Cross Sections for Fast and Intermediate Nuclear Reactors*, LAMS-2255 (1959).

effect of a homogenized region far from the perturbation. The calculations including homogenized regions were performed using a less-rigid convergence criterion than that used in the calculation with all elements explicit. Hence the uncertainties associated with the results are relatively large for this series.

By the procedure described in the previous section, the value of $\beta_{eff}$ was calculated by transport theory also. Within the limits of accuracy so far obtained, the result agrees with that obtained by diffusion theory.

## RESULTS AND COMPARISONS

A set of 13 configurations, representing 10 pairs for determination of perturbations was set up and calculated as described above. Figure 3.8 shows the configurations. In each case the homogenized region was removed as far as possible from the perturbed region in order to minimize this possible source of error. Table 3.4 lists the results of both methods of transport calculation as well as the average value of the three adjusted MODRIC models and the experimental results, all expressed in units of percent $\delta k/k$.

All the diffusion-theory results have an associated uncertainty of 0.007% $\delta k/k$ due solely to the convergence uncertainty. No allowance has been made for cross-section or dimension errors, since these should introduce only negligible errors in the change of multiplication between two calculations using the same dimensions, cross sections, and densities exactly. For the transport calculations the errors, due to the same source, are given in Table 3.4 in each instance. The experimental errors are yet to be established.

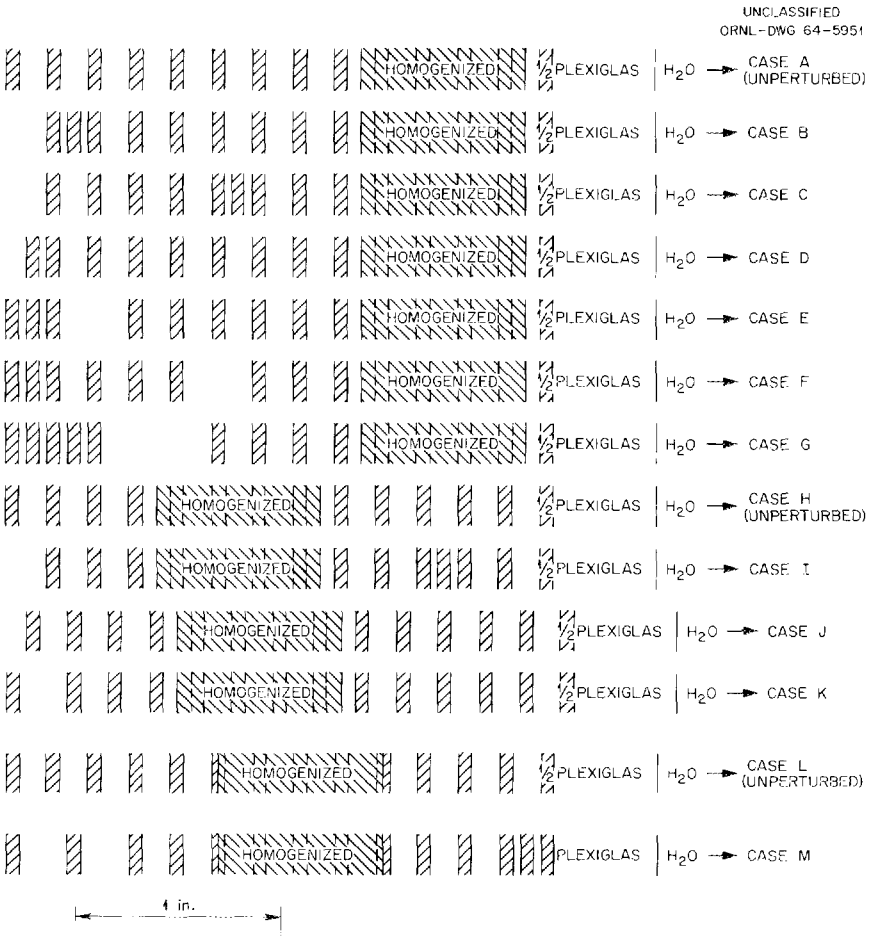


Fig. 3.8. Calculated Configurations, Showing Homogenized Regions.

It is clearly observable that the transport-code results are superior to those obtained by diffusion theory. This is not surprising, since diffusion theory systematically underestimates the flux peaks and drops associated with water gaps and fuel plates. Figure 3.9 shows the thermal flux, as calculated by both methods in one instance, and this effect is clearly seen. In this figure the flux is given in absolute units, as obtained from the calculations.

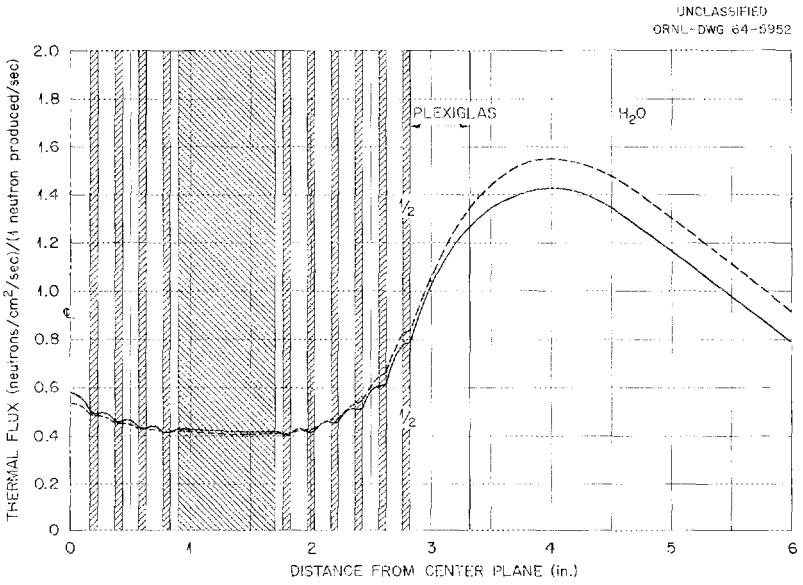


Fig. 3.9. Transport-Theory and Diffusion-Theory Thermal Flux in Configuration C of 1DCA.

Table 3.4. Calculated and Measured Values of the Multiplication Change in Units of % $\delta k/k$ Resulting from Seven Perturbations of the Reactor

The average value of the results from the three adjusted MODRIC models is given, as are the results obtained by the DTK transport code

| Case | Multiplication Change (% $\delta k/k$) | | | |
|---|---|---|---|---|
| | MODRIC, Average | Transport | | Experiment |
| | | Homogenized | All Explicit | |
| A-B | −0.272 | −0.458 ±0.017 | −0.414 ±0.004 | −0.496 |
| A-C | −0.608 | −0.831 ±0.035 | −0.836 ±0.004 | −1.004 |
| A-D | −0.054 | −0.123 ±0.01 | −0.129 ±0.004 | −0.141 |
| A-E | −0.231 | −0.330 ±0.012 | −0.329 ±0.004 | −0.342 |
| A-F | −0.580 | −0.680 ±0.01 | −0.672 ±0.004 | −0.663 |
| H-I | +0.058 | −0.250 ±0.010 | −0.230 ±0.004[a] | −0.477 |
| H-J | +1.520 | +1.365 ±0.008 | +1.316 ±0.004[b] | +1.367 |

[a]A-I; since all elements are explicitly included in this series, only one unperturbed configuration was necessary.
[b]A-J; since all elements are explicitly included in this series, only one unperturbed configuration was necessary.

## CONCLUSION

The conclusion which may be tentatively drawn, from the incomplete results so far, is that the diffusion theory is indeed, as was surmised as a result of the earlier experimental work with the BSR-I, unable to calculate correctly such localized perturbations as are represented by moving single fuel plates. On the other hand, transport-code methods in the $S_4$ approximation are very much better and, within the limits of accuracy so far obtained, appear to give substantially correct results in most cases. The assistance of G. E. Whitesides in preparing the calculations on the IBM 7090 is gratefully acknowledged, as is the help of R. K. Reedy and E. R. Rohrer in performing the experiments.

# Part 4
# Radiochemical Plant

Chemical Technology Division

F. L. Culler, Division Director
C. E. Guthrie, Coordinator

**Key Words**[a]

accident analysis
aerosol
explosion
filter
fire
fuel reprocessing facilities
maximum credible accident
plutonium
uranium

[a]See Foreword.

# 4.1 Radiochemical-Plant Safety Studies

C. E. Guthrie H. W. Godbee

The hazards associated with a large radiochemical plant for either fuel processing or radioisotope source production may exceed those of a reactor. There are large amounts of fission products and/or nuclear materials in storage in such plants in readily dispersible form. Uncontrolled chemical reactions, fires, and nuclear accidents provide possible means for dispersal. It is imperative, therefore, that the hazards and means of combating them be assessed and understood before such a plant is built. In order to accomplish this, three general areas must be covered: (1) assessing the credible radiochemical-plant accidents and their consequences and determining which variables have a major effect on the hazards; (2) studying in detail the significant variables (e.g., the properties of aerosols produced in an accident, the mechanisms leading to a criticality accident, and the maximum criticality accident possible); and (3) developing means for combating or ameliorating the consequences of radiochemical-plant accidents.

## CREDIBILITY OF RADIOCHEMICAL-PLANT ACCIDENTS

Final editing was completed on the report *Theoretical Possibilities and Consequences of Major Accidents in $U^{233}$ and $Pu^{239}$ Fuel Fabrication and Radioisotope Processing Plants,* and it was issued as ORNL-3441[1] with a foreword by Harold L. Price, AEC Director of Regulation. This work has been reported previously in a semiannual report.[2] One of the most significant assumptions in the above study was the fraction of radioactivity that would be released from radiochemical-plant fires and explosions and the properties of the aerosols (e.g., the fraction which would escape through absolute filters) produced in such accidents. A laboratory study has been initiated to investigate these questions.

## CHARACTERIZATION OF AEROSOLS FORMED IN CHEMICAL PLANTS PROCESSING RADIOACTIVE MATERIALS

Aerosols that could be formed by fires or explosions in plants processing radioactive material have received surprisingly little experimental work. Characterization of such aerosols is important to a full understanding of the performance of available safety equipment (such as off-gas lines, filters, and stacks) under all conditions of use. The purpose of this program is to generate and to characterize aerosols that could be expected to be produced by radiochemical-plant accidents. The results of these studies are necessary for the development of devices, such as filters, to prevent the escape of these aerosols to the atmosphere.

Fires involving organic solvents that contain radioactive elements such as uranium, strontium, and plutonium are generally considered the most likely sources of such aerosols. Thus, the burning of organic solvents (with and without incorporated radioactive elements) is being studied first. The apparatus (Fig. 4.1) assembled for these studies consists basically of an aerosol generation chamber (made of Lucite) equipped with a pump for moving air through the chamber and instruments for

[1] C. E. Guthrie and J. P. Nichols, *Theoretical Possibilities and Consequences of Major Accidents in $U^{233}$ and $Pu^{239}$ Fuel Fabrication and Radioisotope Processing Plants,* ORNL-3441 (April 1964).

[2] C. E. Guthrie and J. P. Nichols, *Nuclear Safety Program Semiann. Progr. Rept. June 30, 1963,* ORNL-3483, pp. 57–61.

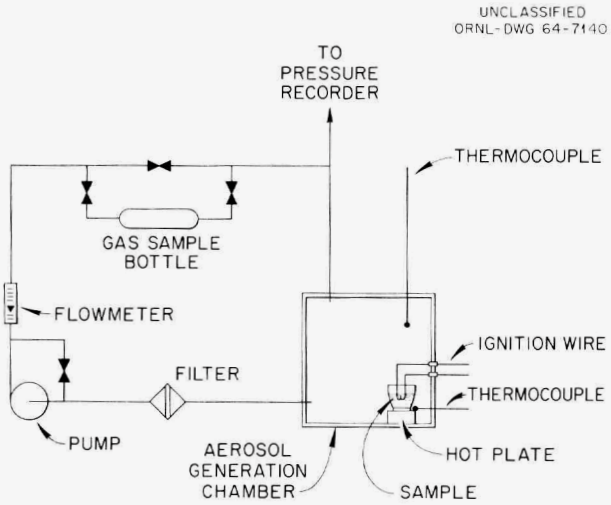


**Fig. 4.1. Schematic Diagram of Apparatus to Generate Aerosols by Burning Flammable Liquids.**

measuring the air flow rate, pressure, and temperature. The nominal volume of the chamber is about 28 liters. A glass fiber filter in the air-circulation line (Fig. 4.1) was used to estimate the total mass concentration (mass of material per unit volume of air) or loading of the stable aerosol formed. However, in future experiments this filter is to be replaced by suitable instruments to determine not only loading but also particle size and particle-size distribution of the aerosol. An aerosol is generated in the chamber by heating the sample with the hot plate to such a temperature that it ignites when current is passed through the ignition wire (Fig. 4.1).

In an experiment without radioactive materials to check the apparatus, 1 ml of a 70 vol % *n*-dodecane–30 vol % tributyl phosphate mixture was heated to 100°C. When current was supplied to the

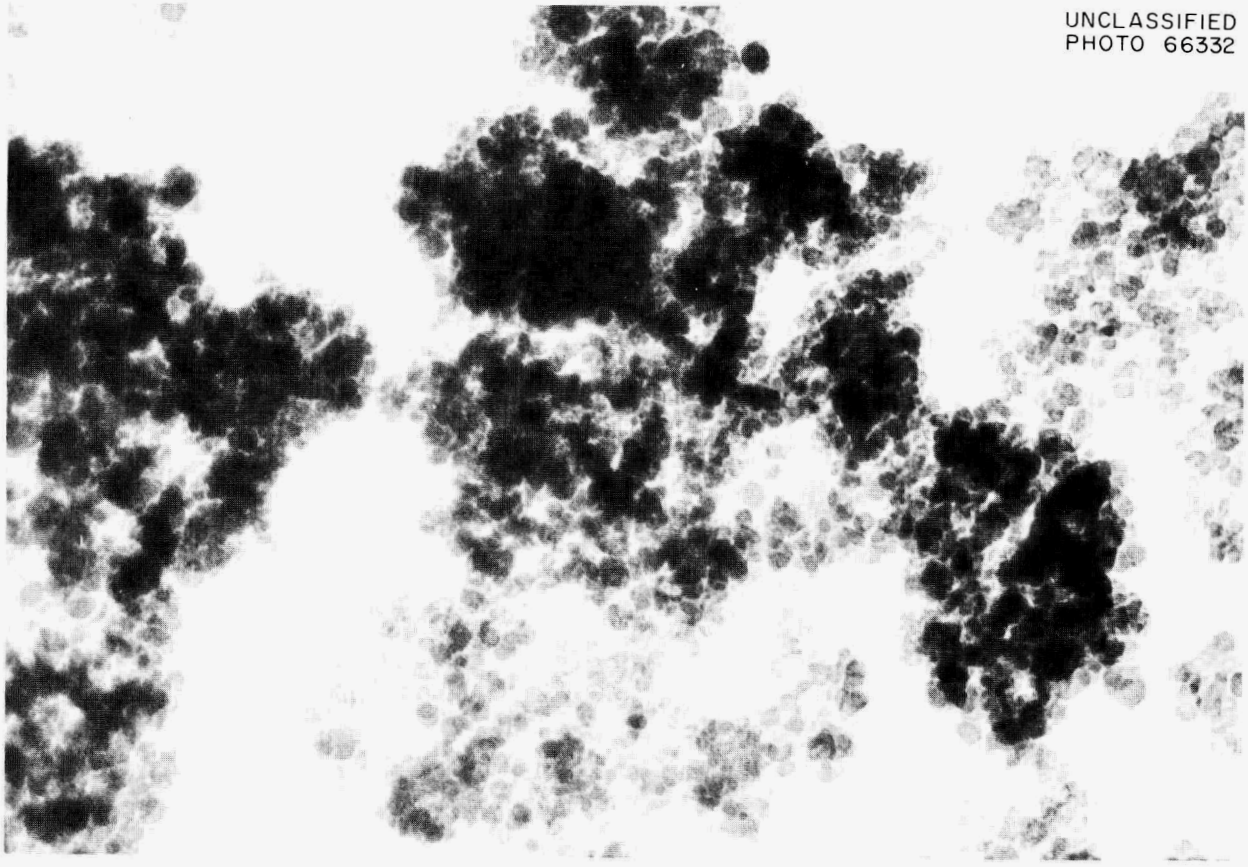


**Fig. 4.2. Soot Particles from Burning 70 vol % *n*-Dodecane–30 vol % Tributyl Phosphate in Limited Air. 122,000×.**

ignition wire, the mixture burst into flame and continued to burn for about 2 min. The pump was turned on after 30 min settling time, and air was circulated through the chamber at 8 liters/min for 75 min. A typical micrograph of the soot that collected on the floor of the chamber is shown in Fig. 4.2. The median size of the particles making up these agglomerates is about 0.02 $\mu$ (Fig. 4.3). The stable aerosol loading as determined from the mass of material retained on the glass fiber filter was 0.11 mg/liter.

The next stage of this investigation is to study the above system under the same conditions but with uranium incorporated into the sample.

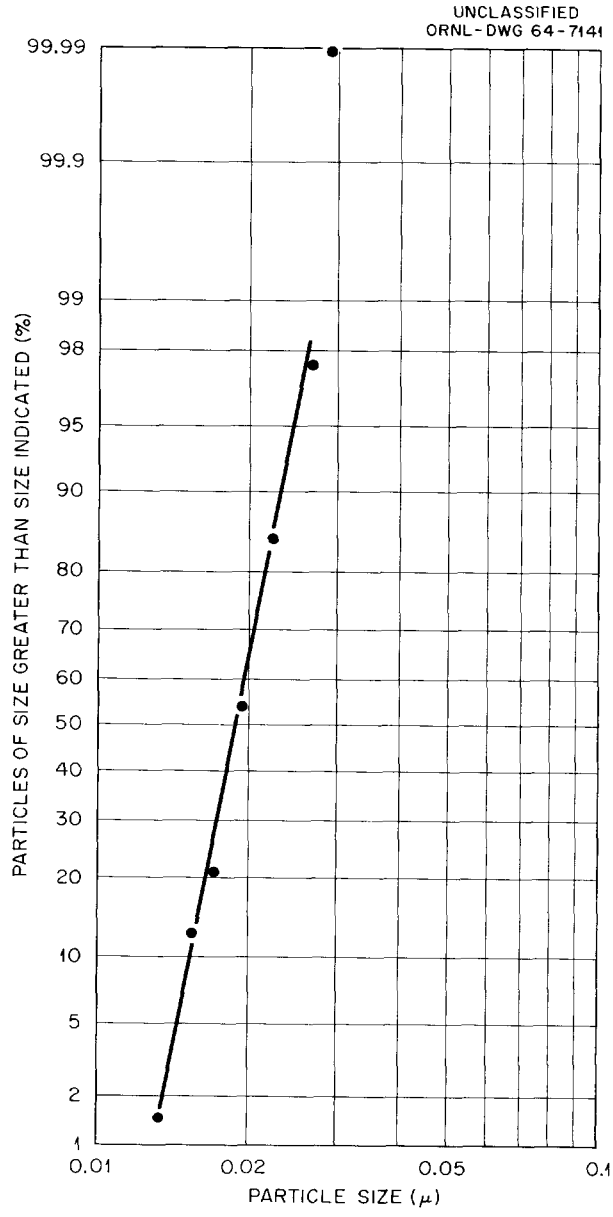


**Fig. 4.3. Size Distribution of Soot Particles from Burning 70 vol % *n*-Dodecane–30 vol % Tributyl Phosphate in Limited Air.**

# Part 5
# Nuclear Safety Information

Reactor Division

S. E. Beall, Division Director
W. B. Cottrell, Coordinator

Key Words[a]

containment
fast reactors
filters
information retrieval
iodine
large reactors
monitor, general practice
reactivity effects
reactor kinetics
reliability analysis
safety reviews
safety systems

[a]See Foreword.

# 5.1 Nuclear Safety Information Center

J. R. Buchanan W. B. Cottrell S. P. Hendrix

The Nuclear Safety Information Center (NSIC) has now been in operation for one year. During this time, it has made genuine progress in its prime task of serving the nuclear community by collecting, evaluating, storing, and disseminating nuclear safety information from every available source. Over 2500 sources of information have been collected, evaluated, and stored.

Beginning in fiscal year 1965 the scope of the "Radioactive Effluent Control, Monitoring, Movement, and Dosage" subject area is being broadened to include aspects of waste disposal concerned with the terrestrial and ocean disposal of solid, liquid, or gaseous effluents. Waste treatment, except as it is an integral part of a waste disposal scheme, would be excluded. In order to handle the additional work load, the staff has been augmented by a professional member from the ORNL Health Physics Division who will devote one-half of his time to NSIC. With this exception, the organization and scope of the Center is unchanged from that reported in previous issues of this progress report.[1,2]

## COMPUTER CAPABILITY FOR INFORMATION RETRIEVAL

In order to expand the services it can offer, the NSIC has been exploring the possible use of computers for the preparation of routine bulletins of the Center's accessions and for making retrospective searches of the Center's files. Information would continue to be collected, evaluated, and indexed into the manual storage system of 5- by 8-in. cards for use by NSIC's staff specialists and visitors.

Information to be stored on magnetic tape would include bibliographic data, descriptors or subject words, and a short abstract of 50 to 100 words. Utilizing the IBM 7090-1401 computer facilities at the ORGDP, it is planned that NSIC would initially issue a quarterly categorized bulletin of all its accessions. Computer programs would be developed that would enable the Center to make routine retrospective searches of its files and also give it the capability of selectively disseminating information to match the requirements of a particular customer.

Data was obtained on several information systems that use computer services in a fashion similar to that envisioned by NSIC. This data gathered by visits, telephone conversations, and from the literature indicate that the Center's plans are well founded and economically feasible. Information was also obtained that will aid the ORGDP group in developing detailed programs for NSIC.

## GENEVA EXHIBIT

More than 1300 sources of information relating to the containment of nuclear facilities have been selected by NSIC to form a miniature information center that will be a part of the USAEC Division of Technical Information's exhibit at the Third International Conference on the Peaceful Uses of Atomic Energy at Geneva, Switzerland, August 31 through September 9, 1964. In addition to the usual 5- by 8-in. extract cards used by NSIC, microfiche copies of the original documents will be on file.

Microfiche readers and reader-printers will be provided so that the documents may be perused. In addition, microfiche duplicates may be made for visitors to the exhibit if they wish.

[1] W. B. Cottrell and J. R. Buchanan, *Nucl. Safety Program Semiann. Progr. Rept. June 30, 1963*, ORNL-3483, pp. 53–55.

[2] J. R. Buchanan and W. B. Cottrell, *Nucl. Safety Program Semiann. Progr. Rept. December 31, 1963*, ORNL-3547, pp. 79–80.

## INSTALLATIONS VISITED AND MEETINGS ATTENDED

NSIC staff representatives either attended meetings or visited at the following installations since the last report period.

American Public Health Association 91st annual meeting, Kansas City, Missouri, November 11–15, 1963.

Contamination Analysis and Control Seminar held by Millipore Filter Corporation, Atlanta, Georgia, February 24, 1964.

Meeting on Indexing Words Used by Physics Information Centers, National Academy of Sciences–National Research Council, Washington, D.C., March 20–21, 1964.

Informal conference with personnel at Aerospace Research Applications Center, University of Indiana, April 9, 1964.

Informal conference with personnel at General Electric Technical Information Center, Evendale, Ohio, April 10, 1964.

Symposium on Engineering with Nuclear Explosives (3d Plowshare Symposium), University of California, Davis, California, April 21–23, 1964.

Conference on AEC Meteorological Activities, Brookhaven National Laboratory, May 19–21, 1964.

International Symposium on Surface Contamination, Gatlinburg, Tennessee, June 8–12, 1964.

American Nuclear Society 10th annual meeting, Philadelphia, Pennsylvania, June 14–18, 1964.

Health Physics Society 9th annual meeting, Cincinnati, Ohio, June 15–18, 1964.

## CENTER STUDIES

Several special studies have been assigned to the Center for consideration. The current status of these assignments is as follows:

### Evaluation of Iodine Effluent Monitoring and Area Monitoring Programs at Savannah River, Hanford, Idaho Falls, and Oak Ridge

The survey has been completed and a final report issued.[3]

### Behavior of Iodine in Reactor Containment Systems

An initial draft of a comprehensive survey of radioiodine release, transport, and removal within containment structures has been completed. It is undergoing review and revision. The final report will be issued in the latter half of 1964.

### Secondary Shutdown Systems

Information on the design, cost, and operating experience of secondary, or emergency, poison-injection systems for power reactors is being collected. Questionnaires were sent to all United States and selected foreign reactors having power ratings in excess of 10 Mw. An initial draft of this report will be completed in the summer of 1964. This study replaces one planned on the "Effectiveness of Safety Injection Systems for Emergency Reactivity Control."

### Reliability of Safety Systems

A report on this study will be prepared late in 1964.

### Reactivity Effects of Fuel Element Bowing

W. K. Ergen of the NSIC staff presented a paper entitled "Thermal Bowing of Fuel Rods During Transients" at the June 1964 American Nuclear Society meeting in Philadelphia. No further studies are planned in this field at present.

### Kinetics of Large Reactor Cores

A report will be prepared and issued in the latter part of 1964.

---

[3] K. E. Cowser, *Current Practices in the Release and Monitoring of $I^{131}$ at NRTS, Hanford, Savannah River, and ORNL*, ORNL-NSIC-3 (July 1964).

### Safety of Fast Gas-Cooled Reactors

The study is under way and will be issued in 1964.

### Review of Safety Analysis Procedures and Methods

No initiating date for this study has been set.

### Nuclear Safety Contract File

Work on the second issue of an active file of nuclear safety contracts will be undertaken in the fall of 1964.

### Fundamentals of Filter Testing

A study on the fundamentals of filter testing is planned. It will be concerned with research concerned with filter design and performance as well as preliminary and in-place testing of filters. The study will be undertaken in the latter half of 1964.

### OTHER ACTIVITIES

In this report period the Center received and answered 31 specific requests for nuclear safety information from private companies, government groups, and private individuals. In addition, staff specialists consulted with 16 visitors to the Center. During the period, 53 requests to be added to the distribution of reports prepared by NSIC were received and filled.

On March 18, 1964, NSIC moved into its newly remodeled quarters in the southeast corner of Building 9711-1. The rooms, which occupy about 1500 $ft^2$ of floor space, are adjacent to the Document Reference Section of the Y-12 Technical Library.

---

## 5.2 Technical Progress Review

W. B. Cottrell J. R. Buchanan

Two issues of *Nuclear Safety*, a quarterly technical progress review prepared by Oak Ridge National Laboratory for the USAEC, were issued during the report period. *Nuclear Safety* may be purchased from the Superintendent of Documents, U.S. Government Printing Office, Washington 25, D.C., for $2.50 per year for each subscription or for 70¢ per issue.

ORNL-3691
UC-80–Reactor Technology
TID-4500 (34th ed.)

*INTERNAL DISTRIBUTION*

1. Biology Library
2-4. Central Research Library
5. Reactor Division Library
6-7. ORNL–Y-12 Technical Library
Document Reference Section
8-42. Laboratory Records Department
43. Laboratory Records, ORNL R.C.
44. Laboratory Shift Supervisor
45. R. D. Ackley
46. R. E. Adams
47. R. G. Affel
48. T. A. Arehart
49. E. D. Arnold
50. S. I. Auerbach
51. J. A. Auxier
52. C. J. Barton
53. S. E. Beall
54. S. R. Bernard
55. D. S. Billington
56. F. T. Binford
57. E. P. Blizard
58. C. J. Borkowski
59. G. E. Boyd
60. J. C. Bresee
61. R. B. Briggs
62. W. E. Browning
63. F. R. Bruce
64. J. R. Buchanan
65. T. J. Burnett
66. A. D. Callihan
67-71. W. B. Cottrell
72. K. E. Cowser
73. J. A. Cox
74. G. E. Creek
75. G. A. Cristy
76. F. L. Culler
77. M. E. Davis
78. Wallace de Laguna
79. J. S. Eldridge
80. L. C. Emerson
81. W. K. Ergen
82. R. B. Evans
83. M. F. Fair
84. B. R. Fish
85. J. L. Fowler
86. A. P. Fraas
87. J. H. Frye
88. J. H. Gillette
89. W. R. Grimes
90. E. E. Gross
91. C. E. Guthrie
92. Fred Haywood
93. R. L. Heestand
94. K. M. Henry
95. P. P. Holz
96. T. W. Hungerford
97. G. S. Hurst
98. E. B. Johnson
99. W. H. Jordan
100. G. W. Keilholtz
101. M. T. Kelley
102. F. Kertesz
103. O. H. Klepper
104. J. O. Kolb
105. D. M. Lang
106. C. E. Larson
107. C. G. Lawson
108. R. A. Lorenz
109. H. G. MacPherson
110. F. C. Maienschein
111. W. J. Martin
112. H. C. McCurdy
113. A. B. Meservey
114. A. J. Miller
115. C. E. Miller
116. E. C. Miller
117. W. H. Montgomery
118. J. G. Morgan
119. K. Z. Morgan
120. M. T. Morgan
121. F. H. Neill
122. M. L. Nelson
123. J. P. Nichols
124. G. W. Parker
125-126. R. B. Parker
127. L. F. Parsly
128. H. B. Piper
129. P. H. Pitkanen
130. S. A. Reynolds
131. J. M. Robbins
132. B. F. Roberts
133. T. H. Row
134. G. W. Royster
135. A. F. Rupp

136. J. L. Scott
137. H. E. Seagren
138. R. P. Shields
139. E. G. Silver
140. M. D. Silverman
141. O. Sisman
142. M. J. Skinner
143. W. S. Snyder
144. W. M. Stanley
145. W. G. Stockdale
146. E. G. Struxness
147. J. A. Swartout
148. A. J. Taylor
149. E. H. Taylor
150. D. F. Toner
151. P. R. Vanstrum
152. F. C. VonderLage
153. C. S. Walker
154. G. M. Watson
155. A. M. Weinberg
156. M. E. Whatley
157. G. C. Williams
158. J. W. Youngblood
159. Gale Young

*EXTERNAL DISTRIBUTION*

160. A. L. Baietti, Tracerlab, Richmond, California
161. R. W. McNamee, Union Carbide Corporation, New York
162. W. D. Manly, Union Carbide Corporation, New York
163. F. A. Gifford, USAEC Weather Bureau Office, Oak Ridge Operations Office
164. H. N. Culver, TVA-EGCR Site
165. Morton I. Goldman, Nuclear Utility Services, Inc., 1025 Connecticut Ave., N.W., Washington 6, D.C.
166. Howard Kraig, Westinghouse Electric Corporation, Astronuclear Laboratory, Post Office Box 10864, Pittsburgh 36, Pennsylvania
167. E. R. Irish, HAPO, GE-Richland, Washington
168. C. E. Thomas, Atomic Energy Division, Babcock and Wilcox Company, Lynchburg, Virginia
169. Robert Wascher, Babcock and Wilcox Company, Lynchburg, Virginia
170. H. W. Behrman, USAEC, Oak Ridge Operations Office
171. D. F. Cope, USAEC, Oak Ridge Operations Office
172. F. C. Huffman, USAEC, Oak Ridge Operations Office
173. Wayne Smalley, USAEC, Oak Ridge Operations Office
174. Research and Development Division, USAEC, Oak Ridge Operations Office
175. David B. Hall, Los Alamos Scientific Laboratory, Post Office Box 1663, Los Alamos, New Mexico
176. C. R. Williams, Liberty Mutual Insurance Company, 175 Berkeley Street, Boston 17, Massachusetts
177. John C. Geyer, Department of Sanitary Engineering and Water Resources, Johns Hopkins University, Baltimore 18, Maryland
178. John P. Howe, Cornell University, Ithaca, New York
179. Herbert J. C. Kouts, Brookhaven National Laboratory, Upton, L.I., New York
180. A. W. Castleman, Jr., Brookhaven National Laboratory, Upton, L.I., New York
181. H. W. Newson, Department of Physics, Duke University, Durham, N.C.
182. K. R. Osborn, Manager, Industrial Development, General Chemical Division, Allied Chemical & Dye Corporation, 40 Rector Street, New York 6, New York
183. D. A. Rogers, 11 Lingerwood Place, Morristown, New Jersey
184. Leslie Silverman, School of Public Health, Harvard University, 665 Huntington Ave., Boston 15, Massachusetts
185. R. C. Stratton, Apt. 5-J, 98 Garden Street, Hartford 5, Connecticut
186. Theos J. Thompson, Department of Nuclear Engineering, Massachusetts Institute of Technology, Cambridge 38, Massachusetts

187. Dick Duffey, Professor of Nuclear Engineering, Department of Chemical Engineering, University of Maryland, College Park, Maryland
188. Thomas L. Flynn, Ebasco Services, Inc., 2 Rector Street, New York, New York
189-191. Advisory Committee on Reactor Safeguards, Atomic Energy Commission, Washington 25, D.C., Attn: R. F. Fraley
192. George P. Dix, USAEC, Division of Reactor Development, Space Nuclear Propulsion Office, Washington 25, D.C.
193. Merson Booth, USAEC, Division of Reactor Development, Analysis and Evaluation Branch, Washington 25, D.C.
194. Howard G. Hembree, USAEC, Division of Reactor Development, Engineering and Testing Branch, Washington 25, D.C.
195. Walter G. Belter, USAEC, Division of Reactor Development, Environmental and Sanitary Engineering Branch, Washington 25, D.C.
196-198. J. A. Lieberman, Assistant Director for Nuclear Safety, Division of Reactor Development, USAEC, Washington 25, D.C.
199. L. Kornblith, Assistant Director for Reactors, Division of Compliance, USAEC, Washington 25, D.C.
200. C. K. Beck, Deputy Director of Regulation, USAEC, Washington 25, D.C.
201-202. Argonne National Laboratory, 9700 South Cass Avenue, Argonne, Illinois, Attn: R. C. Vogel
203. Atomic Energy Commission, Army Reactors, Division of Reactor Development, Washington 25, D.C.
204. Atomic Energy Commission, Civilian Reactors, Division of Reactor Development, Washington 25, D.C., Attn: A. Giambusso
205. Atomic Energy Commission, Division of Compliance, Region IV, Post Office Box 15266, Denver 15, Colorado, Attn: John W. Flora
206-208. Atomic Energy Commission, Division of Reactor Licensing, Washington 25, D.C., Attn: Edson G. Case
209-212. Atomic Energy Commission, Division of Safety Standards, Washington 25, D.C., Attn: J. J. DiNunno
213. Atomic Energy Commission, Maritime Reactors Branch, Division of Reactor Development, Washington 25, D.C.
214-215. Atomic Energy Commission, Naval Reactors Branch, Division of Reactor Development, Washington 25, D.C., Attn: T. Rockwell, R. S. Brodsky
216-222. Atomic Energy Commission, Research and Development Branch, Division of Reactor Development, Washington 25, D.C., Attn: S. A. Szawlewicz
223-224. Atomics International, Post Office Box 309, Canoga Park, California, Attn: A. A. Jarrett
225. Canoga Park Area Office, Post Office Box 591, Canoga Park, California, Attn: C. W. Richards
226. Chicago Operations Office, Atomic Energy Commission, 9800 South Cass Ave., Argonne, Illinois, Attn: D. M. Gardiner
227-228. IIT Research Institute, 10 W. 35th Street, Chicago 16, Illinois, Attn: T. A. Zaker, M. A. Salmon
229-230. Idaho Operations Office, Atomic Energy Commission, Post Office Box 2108, Idaho Falls, Idaho, Attn: George Wehmann, D. Williams
231. National Bureau of Standards, Washington 25, D.C., Attn: C. Muelhause
232-239. Phillips Petroleum Company, Post Office Box 1259, Idaho Falls, Idaho, Attn: Glenn O. Bright, Warren E. Nyer, Frank Schroeder, T. R. Wilson
240. San Francisco Operations Office, Atomic Energy Commission, 2111 Brancroft Way, Berkeley 4, California, Attn: Lt. Col. John B. Radcliffe
241-242. Space Technology Laboratories, Inc., One Space Park, Redondo Beach, California, Attn: D. B. Langmuir, S. M. Zivi
243. United Nuclear Corporation, Development Division, 5 New Street, White Plains, New York, Attn: C. Graves

244-245. University of California, Institute of Engineering Research, Berkeley 4, California, Attn: Prof. H. A. Johnson, Dr. V. E. Schrock
246. Dr. David Okrent, Argonne National Laboratory, 9700 South Cass Avenue, Argonne, Illinois
247. Dr. David L. Morrison, Battelle Memorial Institute, 505 King Avenue, Columbus 1, Ohio
248. University of Minnesota, Department of Chemical Engineering, Minneapolis, Minnesota, Attn: Prof. H. Isbin
249. USAEC Liaison Office, Post Office Box 985, Toronto 18, Ontario, Canada, Attn: Glen B. Boyer
250. M. M. Mann, Assistant Director of Regulation, USAEC, Washington 25, D.C.
251. USAEC, Division of Compliance, Washington 25, D.C.
252. G. F. Stone, TVA-EGCR Site
253. Division of Technical Information, AEC, Washington, Attn: R. E. Bowman
254. Division of Reactor Development, USAEC, Washington, Attn: I. E. Jackson
255-871. Given distribution as shown in TID-4500 (34th ed.) under Reactor Technology category (75 copies – CFSTI)